AN INVESTIGATION OF THE COMPLEXES OF ZINC AND GERMANIUM WITH 8-HYDROXYQUINOLINE

by

VANITHA MAHARAJ

Submitted in partial fulfillment of the
requirements for the degree of
Masters of Science,
in the
Department of Chemistry and Applied Chemistry,
University of Natal
Durban
1991

DURBAN
1991

TO MY PARENTS

PREFACE

The experimental work described in this thesis was carried out in the Department of Chemistry and Applied Chemistry, University of Natal, Durban, from January 1990 to September 1991 under the supervision of Dr. B.S. Martincigh and Professor L.F Salter.

These studies present original work by the author and have not been submitted in any form to another University. Where use has been made of the work of others it has been duly acknowledged.

ACKNOWLEDGEMENTS

I am indebted to the Foundation for Research and Development for financial assistance provided during the course of this work.

I am grateful to my supervisors, Dr. B.S. Martincigh and Professor L.F. Salter for their assistance, enthusiasm and interest in the progress of this work.

I also thank Professor J.W. Bayles for his concern, guidance and friendly approachable manner during the course of this work.

I wish to thank my parents, my brother and my sister for all their help, support and encouragement over the years.

I also wish to thank my laboratory colleagues, Sion Edwards, Kim Bolton and Simon Aliwell for providing assistance, thought-provoking discussions and a convivial working environment.

My thanks go to the technical staff of the Department for all their help and co-operation.

ABSTRACT

The experimental work described in this thesis is aimed at the elucidation of the speciation of the zinc and germanium 8-hydroxyquinoline systems. A knowledge of this speciation could aid in modelling the kinetics of solvent extraction of zinc and germanium with 7-alkyl derivatives of 8-hydroxyquinoline.

In this study the stability constants of the ligand 8-hydroxyquinoline with the ions H^+, Zn^{2+} and Ge^{4+} have been investigated by potentiometry at 25°C in a partially aqueous medium. A titration technique was used in which the hydrogen ion concentration was monitored using a glass indicating electrode. The partially aqueous medium comprised of 0.1 mol dm^{-3} $NaClO_4$ in 60% (v/v) dioxane and the concentration levels of the reagents were at least millimolar. The analysis of the potentiometric data was carried out with the aid of the computer programs HALTAFALL, ESTA and STATGRAPHICS.

The results obtained for the systems involving the H^+ and Zn^{2+} ions compare with those reported in the literature. The stability constant of a protonated species in the zinc-8-hydroxyquinoline system (ZnLH) was established for the first time. Precipitates obtained from the Zn^{2+} titrations were identified as zinc 8-hydroxyquinolate dihydrate.

The germanium 8-hydroxyquinoline system has not been

studied previously via potentiometry techniques. The complex hydrolysed species of germanium in aqueous solutions and the unusual features displayed in the formation curves increased the complexity of species selection. Although a suitable model of the species present could not be determined some evidence suggests the presence of protonated species. Hence, a prerequisite for resolving the germanium-8-hydroxyquinoline system could be a more complete understanding of the hydrolysis of germanium in the partially aqueous medium used.

CONTENTS

CHAPTER 1

INTRODUCTION

In this study the complexes of zinc and germanium with 8-hydroxyquinoline were investigated. This chapter describes the significance of this work, a literature survey of previous work reported on the systems and the theory of the method employed, i.e. glass electrode potentiometry.

The ligand investigated in this study, viz. 8-hydroxyquinoline (also referred to as oxine) forms chelates with forty three metal-ions [1]. Hence it is an important chelating agent with applications in gravimetric, titrimetric, spectrophotometric, fluorimetric, polarographic and amperometric analysis, and, *inter alia*, in solvent extraction and chromatography [2]. Oxine also has outstanding antibacterial properties when complexed to iron or copper [3,4]. (The origin of the bacteriostatic action of oxine lies in its ability to inactivate an essential trace element through complex formation.) Figure 1.1 shows the structure of 8-hydroxyquinoline in two dimensions and as a space-filled diagram. From Figure 1.1 it can be seen that oxine is bidentate with nitrogen and oxygen as donor atoms.

In our laboratories, the kinetics of solvent extraction of germanium with 7-alkyl derivatives of oxine, viz. Kelex and Lix (commercially available extractants) has been studied extensively [5,6].

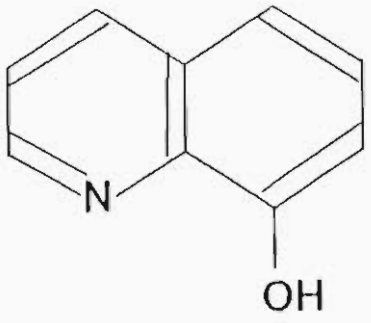

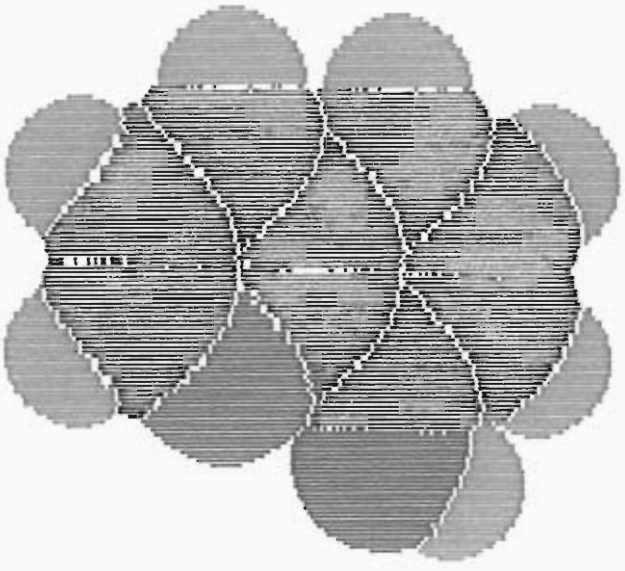

Figure 1.1 Structure of 8-hydroxyquinoline represented two dimensionally and as a space-filled diagram.

The hydrophobic group (the alkyl chain) was introduced to make the oxine less soluble in the aqueous phase - a property of major importance for hydrometallurgical purposes [7]. The hydrophobicity of the alkyl chain forces the germanium extraction reactions to occur at the interface when the aqueous phase containing germanium(IV) and the organic phase containing the 7-alkylated oxine derivative are mixed.

8-Hydroxyquinoline is the parent molecule of the extractants discussed above and it was therefore chosen as the ligand in this study. The metals zinc and germanium were chosen since they both occur in the fourth row of the periodic table and are found together in the ore. Germanium is mainly produced from the zinc ore, sphalerite [8]. The electrolysis of zinc, in zinc production, can be achieved with a good yield only when germanium has been completely eliminated from the electrolyte. This separation is therefore a preliminary operation to the recovery of the metal from solution. Moreover, the recovery of germanium from such solutions constitutes the main available source of this metal [9]. This shows the interdependence between zinc and germanium.

The aim of this project was to determine the protonation constants of 8-hydroxyquinoline and use these results to determine the stability constants of the complexes formed in the zinc-8-hydroxyquinoline system, and thereafter to extend the acquired technique to the complicated germanium-8-hydroxyquinoline system. Knowledge of the predominant

species at particular pH values and their stability constants could aid in modelling the kinetics of metal recovery in processes such as the zinc-germanium extraction discussed above.

1.1 SURVEY OF PREVIOUS WORK

A literature survey revealed that the protonation constants of 8-hydroxyquinoline had been determined as early as 1910. Hence the importance of oxine was realised almost a century ago. The chronological development of the methods and conditions used to measure the protonation constants of 8-hydroxyquinoline are shown in Table 1.1.

An increase in pK_{101} (negative logarithm of the dissociation constant of the proton from the -OH group) and concomitant decrease in pK_{102} (negative logarithm of the dissociation constant of the proton from the $-NH^+$ group) with increasing organic content of a mixed solvent has been reported previously for 8-hydroxyquinoline [10]. Inspection of Table 1.1 shows that this trend is observed up to 70% dioxane, but 75% dioxane does not follow the predicted trend. This could be due to the large proportion of dioxane in the solvent which perhaps excessively diminishes the dielectric constant of the medium thereby changing its properties to such an extent that it could no longer follow the predicted trend.

The solubility of 8-hydroxyquinoline appears to be reduced on metal complexation. Hence many metal

TABLE 1.1

Previous work reported on the protonation of 8-hydroxyquinoline.

DATE	pK_{102}	pK_{101}	METHOD & CONDITIONS	REF
1910	4.8	10.36	Salt hydrolysis and partition measurements in an aqueous medium.	12
1927	4.5	9.7	Colourimetry at 18°C in an aqueous medium.	13
1947	5.07	9.84	Potentiometry at 20°C in an aqueous medium.	14
1947	-	10.38	Solubility measurements in alkaline buffers at 25°C.	15
1947	-	10.3	Spectrophotometry at room temperature.	15
1949	5.00	9.85	Spectrophotometry and solubility measurements in aqueous buffer at 20°C and μ = 0.1 mol dm^{-3}.	16
1949	4.92	-	Potentiometry at 25°C and 0.073 mol dm^{-3} $NaClO_4$.	17
1949	3.18	12.33	Potentiometry at 25°C and 70% dioxane.	4
1952	3.97	11.54	Potentiometry at 25°C and 50% dioxane.	18
1954	5.13	9.89	Potentiometry at 20°C and μ = 0.01 mol dm^{-3}.	3

1954	4.48	10.80	Potentiometry at 20°C in 0.3 mol dm^{-3} $NaClO_4$ and 50% dioxane.	19
1954	3.6	14.1	Potentiometry in 75% dioxane.	20
1958	3.14	11.22	Potentiometry at 25°C in 0.3 mol dm^{-3} $NaClO_4$ and 75% dioxane.	21
1958	4.08	10.82	Potentiometry at 25°C in 0.3 mol dm^{-3} $NaClO_4$ and 50% dioxane.	22
1963	3.97	11.48	Potentiometry at 25°C in 0.1 mol dm^{-3} $NaClO_4$ and 60% dioxane.	23

chelates, e.g. zinc-oxinate, are sparingly soluble in aqueous media. Owing to this property zinc-oxinate is precipitated for the gravimetric determination of zinc [11]. Previously reported stability constants for the zinc-8-hydroxyquinoline system are given in Table 1.2.

The extraction of zinc(II) as the species $ZnL_2 2HL$ (where L represents completely deprotonated oxine), with a stability constant of 27.65, was reported [24] using distribution measurements. Hence it can be seen that the conditions of measurement strongly influence the type of species formed.

In the case of germanium it is known to exist as complicated species in aqueous solution, viz. GeO_5^{2-} [24], $H_2Ge_7O_{16}^{2-}$ [26], $HGe_8O_{18}^{3-}$ [7], $GeO(OH)_3^-$, $GeO_2(OH)_2^{2-}$ and $(Ge(OH)_4)_8(OH)_3^{3-}$ [27]. V.A. Nazarenko [28] reported the existence of germanium(IV) as the germanic acid species, $Ge(OH)_4$, at pH $\leq$ 2.4 and at a germanium dioxide concentration greater than or equal to 0.01 mol dm^{-3}. According to C.F. Baes and R.E. Mesmer [29] this $Ge(OH)_4$ species hydrolyses in dilute solution, i.e. 1 x 10^{-5} mol dm^{-3} Ge(IV), to form the monogermanates $GeO(OH)_3^-$ and $GeO_2(OH)_2^{2-}$ or $Ge(OH)_6^{2-}$; and at concentrations in excess of 0.005 mol dm^{-3} they suggest the presence of the polynuclear species $Ge_8O_{16}(H_2O)_5(OH)_3^{3-}$ in solution.

In relation to the systems of interest in this work only one value for a germanium-8-hydroxyquinoline complex has been reported, i.e. $GeL_2(OH)_2$ with a

TABLE 1.2

Stability constants for the zinc-8-hydroxyquinoline complexes reported in the literature.

$\log K_{ML}$	$\log K_{ML_2}$	*CONDITIONS AND MEDIA*	*REF*
9.34	8.22	Potentiometry at 20°C and 0.3 mol dm^{-3} $NaClO_4$ in 50% dioxane.	19
9.96	8.90	Potentiometry at 25°C and 50% dioxane.	18
9.96	9.02	Potentiometry at 25°C and 0.1 mol dm^{-3} in 60% dioxane.	23
10.91	9.90	Potentiometry at 25°C and 70% dioxane.	4

stability constant of 6.61 at an ionic strength of 0.5 mol dm^{-3} NaCl [30]. This complex and its corresponding stability constant was determined via distribution measurements. These differ from potentiometric measurements dramatically (as shown for the zinc-8-hydroxyquinoline system). An extensive literature survey revealed that the germanium-8-hydroxyquinoline system has been investigated to a limited extent and never previously by potentiometry.

1.2 METHOD OF INVESTIGATION

Various techniques, such as potentiometry, polarography, spectrophotometry, ion exchange and others have been employed in the study of chemical equilibria and for the determination of stability constants.

The ideal method of studying equilibria in solution should be one which gives accurate and precise values of the concentrations of all species present in any conceivable system without disturbing the position of the equilibrium; and it should be quick. No such technique has been devised but "of the methods available, potentiometry is the most versatile and precise" [31].

The principles involved in solution equilibria and the potentiometric determination of the related equilibrium constants will be outlined here. The complete theory of these determinations can be found in the literature [32-38].

An equilibrium constant characterises the formation of an equilibrium in solution. This constant is termed protonation when it refers to the protonation of a ligand, and a stability constant when it refers to the the formation of a metal complex.

Consider a system consisting of three components, represented by L(ligand), M(metal), H(proton), where the following generalised equilibrium is established:

$$pL + qM + rH \rightleftharpoons L_pM_qH_r \qquad 1.1$$

The cumulative thermodynamic stability constant is defined as:

$$B_{pqr} = \frac{\{L_pM_qH_r\}}{\{L\}^p \{M\}^q \{H\}^r} \qquad 1.2$$

where { } denotes activity.

In aqueous solutions, both the metal ion and the proton will be hydrated. Therefore the activity of the water should also appear in the formulation of the thermodynamic stability constant. However, in very dilute solutions, the water is effectively in its standard state [32] and its activity is thus negligibly different from unity. Hence the above formulation is acceptable.

The equilibria are conventionally written as the formation of a complex from its components. The subscripts of β (p,q,r) represent the coefficients of the components present in the complex, and the order

in which these appear are ligand, metal, proton. When the proton subscript is negative, this refers to a proton removed from a water molecule or a hydroxide species.

Complex equilibria are generally expressed in terms of concentrations. This preference over activities is due to the problems involved in measuring activity [39]. The cumulative stoichiometric stability constant of the above equilibrium is thus defined as:

$$\beta_{pqr} = \frac{[L_p M_q H_r]}{[L]^p [M]^q [H]^r} \qquad 1.3$$

where [ ] denotes concentration in mol dm^{-3}.

This expression is only constant if the associated activity coefficient quotient, Q_γ shown below, is constant.

$$Q_\gamma = \frac{\gamma_{LMH}}{\gamma_L^p \gamma_M^q \gamma_H^r} \qquad 1.4$$

where γ denotes activity coefficient. This is accomplished by performing the measurement in the presence of a relatively high concentration of background electrolyte which maintains a constant ionic strength. The activity coefficients and hence the activity coefficient quotient remain constant if it is assumed that the activity coefficients are functions of ionic strength [40,41]. The stability constants thus determined are only applicable at the specific ionic strength for the specific medium in

which they are measured.

Equilibria can also be characterised by stepwise equilibrium constants. A set of stoichiometric protonation constants could thus be represented as follows:

$$K_{101}=\frac{[LH]}{[L]\,[H]} \qquad 1.5$$

$$K_{102}=\frac{[LH_2]}{[LH]\,[H]} \qquad 1.6$$

$$K_{103}=\frac{[LH_3]}{[LH_2]\,[H]} \qquad 1.7$$

In general, these stepwise constants are related to the cumulative constant in the following way:

$$\beta_n=\prod_{i=1}^{n} K_i \qquad 1.8$$

The determination of stability constants is based on equations known as the mass balance equations. Thus, at any point in the titration the total concentration of the components can be expressed in terms of the free component concentrations and the stability constants of the complexes as follows:

$$T_L = [L] + \sum_{r=-R}^{R} \sum_{q=0}^{Q} \sum_{p=1}^{P} p\beta_{pqr} [L]^p [M]^q [H]^r \qquad 1.9$$

$$T_M = [M] + \sum_{r=-R}^{R} \sum_{q=1}^{Q} \sum_{p=1}^{P} q\beta_{pqr} [L]^p [M]^q [H]^r \qquad 1.10$$

$$T_H = \sum_{r=-R}^{R} \sum_{q=1}^{Q} \sum_{p=1}^{P} r\beta_{pqr} [L]^p [M]^q [H]^r . \qquad 1.11$$

The determination of the equilibrium concentrations of all the species present in a solution in which complexes are formed, is seldom possible. However, a particularly useful technique for measuring the concentration of one species and relating it to the reactions occurring and the associated stability constants (see Section 4.2) is potentiometry, where the concentration changes caused by the complex formation are reflected in the potential of a sensing electrode.

In this work a potentiometric titration method was used, in which a glass-membrane electrode was used to follow the concentration of free (uncomplexed) hydrogen ion. This was possible because the reactions being studied involved competition between the hydrogen ion and the metal ion for the ligand.

The cell used to follow the hydrogen ion concentration was:

reference electrode	test solution	glass electrode

The details of this cell and the method used to calibrate it are described in Chapter 3.

The relatively low solubility of oxine and especially the metal-oxinates in aqueous media dictated that a partially aqueous medium should be used for this study, viz. 0.1 mol dm^{-3} $NaClO_4$ in 60% (v/v) dioxane. A preliminary step in using an aqueous-organic mixed solvent system entailed the determination of the contraction factor for the exact mixture, since volumes are not additive on mixing aqueous and organic solvents. The partially aqueous medium also required conditioning of the glass electrode, in the appropriate solvent for at least 24 hours before a titration, to ensure reliable results.

A good choice of background electrolyte is imperative in order to maintain a constant medium composition, thereby affecting the measurements minimally. Beck [42] lists the qualities of a good background electrolye. The salt used in this study ($NaClO_4$) is one of the few salts that possesses these qualities.

The ionic strength of all solutions used in this study gave a final concentration of 0.1 mol dm^{-3}, with $NaClO_4$ as inert background electrolyte, in 60% (v/v) dioxane, taking into account the contraction factor of 0.9803. In this mixed solvent the rate of change of activity coefficients with ionic strength should be

small at the concentration of 0.1 mol dm^{-3} $NaClO_4$ [43]. These conditions for the medium and the constant temperature of 25°C allowed comparison of the measured quantities with those reported in the literature [23].

Steger [23,44] calculated the ionisation constant of water (K_w) in 60% (v/v) dioxane-water to be 16.34. However this value was not in keeping with those reported over a range of mass % dioxane reported in the 'IUPAC Stability Constants of Metal-Ion Complexes' [45]. K_w in aqueous dioxane was reported to be 15.94 for 56.3 wt% dioxane [46]. This is equivalent to 54.5% (v/v) dioxane and is the closest to 60% (v/v) dioxane. Since this latter value of 15.94 for K_w appeared to be a more reliable one, it was employed throughout this study.

Once the potentiometric data have been collected a graphical representation of this numerical data in the form of formation curves is obtained. These plots allow the detection of outlying experimental points and give an indication of the types of species present in solution. Once an acceptable model of the species present has been deduced the corresponding stability constants are calculated. In this study the stability constants were calculated from the potentiometric data by using the computer program ESTA (see Section 4.3.2).

CHAPTER 2

MATERIALS AND APPARATUS

Only A-grade volumetric glassware, Milli-Q water, i.e. water that has been passed through the Milli-Q apparatus (a series of ion-exchange and organic removal resins) and purified 1,4-dioxane were used. Unless otherwise stated the solutions used for the measurements were prepared by dilution of the appropriate standardised stock solutions and were made up to an ionic strength of 0.245 mol dm^{-3} by using calculated amounts of the $NaClO_4$ stock solution.

2.1 PURIFICATION OF 1,4-DIOXANE

The procedure used to purify 1,4-dioxane was essentially that of Vogel [47] and is outlined below. A volume of 1 dm^3 MERCK ANALAR diethylene dioxide, henceforth called dioxane (min. 99% pure, sp. gr. 1.03, with 25 ppm 2,6-di-tert-butyl-4-methylphenol as the stabiliser), 14 cm^3 of MERCK ANALAR HCl (min. 37%, sp. gr. 1.19) and 100 cm^3 of water were refluxed for ±10 hours whilst a slow stream of high purity nitrogen was bubbled through the solution to remove the volatile acetaldehyde formed. MERCK ANALAR KOH pellets (min. 85% pure) were added to the solution once it had been cooled. Stirring was continued until some pellets remained undissolved. The solution separated into two layers, and the aqueous layer was removed. Most of the water remaining in the organic layer was removed by keeping the dioxane over fresh KOH pellets for 24

hours with stirring. The organic solution was then refluxed over an excess of BDH ANALAR sodium metal, for ±9 hours, i.e. until the vigorous bubbling ceased and the Na remained bright. Finally, the dioxane was distilled from Na and stored out of contact with air. Molecular sieve (SAARCHEM) with a bead size of 4Å was used to absorb any water during storage. Such sieves are crystalline synthetic zeolites whose crystal lattice contains numerous cavities connected with one another by pores having exactly defined diameters.

A Karl Fischer titration [48], revealed that the water content in both purified and unpurified dioxane was approximately 0.15 ± 0.01%. The Karl Fischer titration was modified in that dioxane was used as the solvent rather than methanol, thereby minimising the interference of atmospheric moisture and any error in the method since the water levels were relatively low for accurate Karl Fischer reagent determination.

^{13}C nmr spectra for both the unpurified and purified dioxane was recorded on a VARIAN GEMINI 200 mHz SPECTROMETER. The spectra obtained were similar with a single peak at δ = 3.62 ppm, accounting for all the carbon atoms since they are considered to be equivalent in the dioxane structure. A representative nmr spectrum is shown in Figure 2.1.

2.2 PREPARATION AND STANDARDISATION OF STOCK SOLUTIONS OF BACKGROUND ELECTROLYTE

Sodium perchlorate, $NaClO_4$, was used as the background

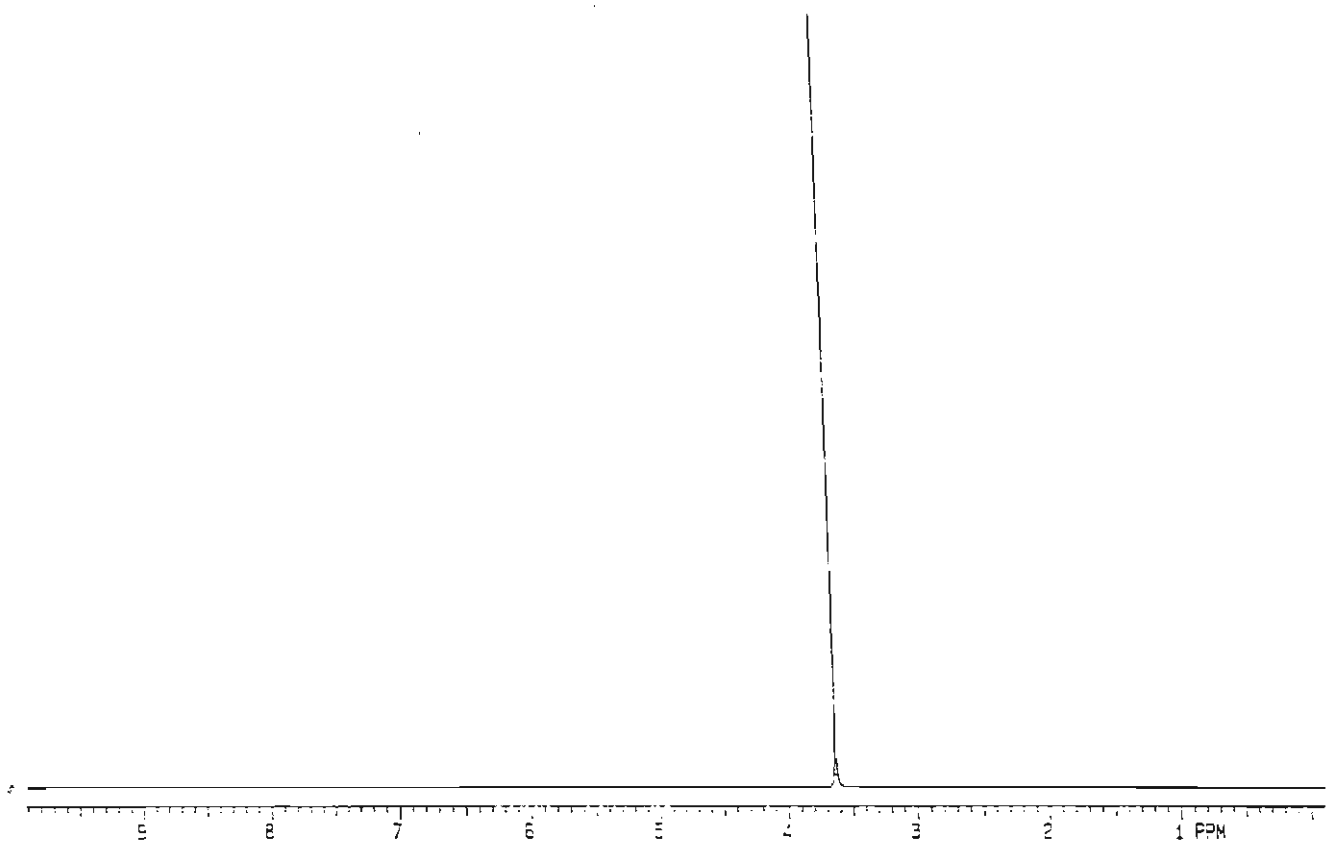

Figure 2.1 The carbon-13 nmr spectrum of dioxane.

electrolyte in these measurements. A stock solution (ca. 2 mol dm^{-3}) was prepared by mass from MERCK ANALAR $NaClO_4$ (min. 99% pure) and standardised by passing a 5.00 cm^3 aliquot through a cation exchange resin. A column (32.5 cm x 3.0 cm) was packed with BDH AMBERLITE IR-120(H), which is an analytical grade ion-exchange resin supplied in the protonated form with a strongly acidic active group, viz. $-SO_3H$. Prior to use the resin was converted to the Na^+ form (by eluting with a 10% solution of NaCl) and then converted back to the H^+ form (by treating it with a 10% solution of HCl) [49]. This was done to ensure that the resin was completely in the H^+ form, and also to clean, and improve the effective capacity of the resin. After each treatment the column was washed with water until a neutral eluate was obtained. The aliquot of $NaClO_4$ was then passed through the column and the $HClO_4$ collected was titrated against a freshly prepared and standardised NaOH solution, by using methyl red as the indicator.

The above standardisations compared to within 0.3% of the concentrations obtained by mass. This difference could be attributed to the requisite filtering of the $NaClO_4$ solutions, hence the above standardisation procedure was used throughout this work.

2.3 PREPARATION AND STANDARDISATION OF STOCK SOLUTIONS OF STRONG ACID

Stock solutions of perchloric acid (ca. 1 mol dm^{-3})

were prepared by diluting MERCK ANALAR $HClO_4$ (min. 70% pure, sp. gr. 1.67) to the required concentration and standardised by titration against freshly recrystallised BDH ANALAR borax [50].

2.4 PREPARATION AND STANDARDISATION OF STOCK SOLUTIONS OF STRONG BASE

Stock solutions of sodium hydroxide (ca. 1 mol dm^{-3}) were prepared from MERCK TITRISOL concentrated volumetric solutions and were made up with water which had been freshly boiled, and purged with high purity nitrogen, to expel CO_2. These stock solutions were standardised by titration against a primary standard, viz. BDH ANALAR potassium hydrogen phthalate (KHP), with phenolphthalein as the indicator [51].

The solutions prepared from these stock solutions were standardised by potentiometric titration against a standard $HClO_4$ solution, and application of the Gran method of end-point detection (see Section 4.1). The carbonate content determined from the Gran plots (see Section 4.1) was checked by the titration method described in Vogel [52] and compared favourably, e.g. $[CO_3^{2-}]$ = 3.908 $x10^{-3}$ mol dm^{-3} from the Gran plot and 3.839 x 10^{-3} mol dm^{-3} from the titration.

2.5 PREPARATION AND STANDARDISATION OF STOCK SOLUTIONS OF 8-HYDROXYQUINOLINE

Stock solutions of 8-hydroxyquinoline, also referred

to as oxine, (ca. 0.5 mol dm^{-3} and 1 mol dm^{-3}) were prepared by mass from ALDRICH ANALAR 8-HYDROXYQUINOLINE (99+% pure) and were made up to volume with purified dioxane. These solutions were standardised by a potentiometric titration against a standard $HClO_4$ solution. The reaction was monitored with a combination glass electrode and a PW9409 Philips digital pH meter. A typical titration curve for the 0.5 mol dm^{-3} stock 8-hydroxyquinoline solution is shown in Figure 2.2. Representative data is given in Table 2.1.

At first an attempt was made to purify 8-hydroxyquinoline by recrystallisation as follows. Oxine was dissolved in a minimal amount of hot 95% ethanol and water; the crystals obtained were then dried to constant mass under high vacuum in a drying pistol by using acetone (which boils at 56.2°C) as the heating medium and phosphorus pentoxide, P_2O_5, as the drying agent [53]. Elemental analysis, recorded on a PERKIN ELMER CHN ANALYSER, gave the following results for recrystallised oxine - C: 73.80%, H: 4.92%, N: 9.78% and O: 11.50%; while the following results were obtained for a sample of oxine taken directly from the bought reagent - C: 73.93%, H: 4.92%, N: 9.78% and O: 11.37%. The corresponding results calculated from the molecular formula for oxine are as follows - C: 74.46%, H: 4.87%, N: 9.65% and O: 11.02%. Hence it can be seen that recrystallisation of 8-hydroxyquinoline did not improve the purity. Stock solutions were therefore prepared directly from the bought reagent by mass.

TABLE 2.1

Data obtained for the titration of a 25.00 cm^3 aliquot of an approximately 0.1 mol dm^{-3} 8-hydroxyquinoline solution with a standard 0.10 mol dm^{-3} $HClO_4$ solution.

Volume $HClO_4/cm^3$	EMF1/mV	EMF2/mV	EMF3/mV
7.00	213.0	217.0	220.0
7.50	210.0	-	-
8.00	209.0	215.0	218.0
8.50	208.0	-	-
9.00	207.0	213.0	216.0
9.50	206.0	212.0	216.0
10.00	206.0	212.0	215.0
10.50	205.0	211.0	215.0
11.00	205.0	211.0	215.0
11.50	204.0	211.0	215.0
12.00	204.0	211.0	214.0
12.50	204.0	210.0	214.0
13.00	204.0	210.0	215.0
13.50	204.0	210.0	215.0
14.00	205.0	210.0	215.0
14.50	205.0	211.0	215.0
15.00	205.0	211.0	216.0
15.50	206.0	212.0	216.0
16.00	207.0	212.0	217.0
16.50	207.0	213.0	218.0
17.00	208.0	214.0	219.0
17.50	209.0	214.0	220.0
18.00	210.0	215.0	221.0
18.50	211.0	217.0	222.0
19.00	213.0	218.0	224.0
19.50	215.0	220.0	225.0
20.00	217.0	222.0	227.0
20.20	218.0	223.0	228.0
20.50	219.0	224.0	229.0
20.70	220.0	225.0	230.0
21.00	221.0	226.0	232.0
21.20	223.0	227.0	232.0
21.50	225.0	228.0	234.0
21.70	225.0	229.0	235.0
22.00	226.0	231.0	237.0
22.20	228.0	233.0	238.0
22.50	229.0	235.0	240.0
22.70	231.0	236.0	242.0
23.00	233.0	238.0	245.0

23.20	236.0	240.0	246.0
23.50	238.0	244.0	249.0
23.70	241.0	246.0	251.0
24.00	244.0	249.0	254.0
24.20	247.0	251.0	256.0
24.50	250.0	255.0	258.0
24.70	252.0	257.0	261.0
25.00	256.0	260.0	264.0
25.20	257.0	262.0	266.0
25.50	260.0	265.0	269.0
25.70	263.0	267.0	271.0
26.00	266.0	270.0	273.0
26.20	267.0	271.0	275.0
26.50	269.0	274.0	277.0
26.70	271.0	275.0	279.0
27.00	273.0	278.0	281.0
27.20	274.0	279.0	282.0
27.50	277.0	280.0	284.0
27.70	278.0	281.0	285.0
28.00	279.0	283.0	286.0
28.20	280.0	284.0	288.0
28.50	281.0	285.0	289.0
28.70	283.0	286.0	290.0
29.00	284.0	288.0	291.0
29.20	285.0	289.0	292.0
29.50	286.0	290.0	293.0
29.70	287.0	291.0	294.0
30.00	288.0	292.0	295.0
30.50	290.0	293.0	296.0
31.00	291.0	295.0	297.0
31.50	292.0	297.0	299.0
32.00	294.0	298.0	300.0
32.50	295.0	299.0	302.0
33.00	297.0	300.0	303.0
33.50	298.0	301.0	304.0
34.00	299.0	302.0	305.0
34.50	300.0	303.0	306.0
35.00	301.0	304.0	307.0
36.00	302.0	305.0	308.0
37.00	304.0	306.0	309.0
38.00	305.0	308.0	310.0
39.00	306.0	309.0	311.0
40.00	307.0	310.0	312.0
41.00	308.0	311.0	313.0
42.00	309.0	312.0	314.0
43.00	310.0	313.0	315.0
44.00	311.0	314.0	316.0
45.00	312.0	315.0	317.0

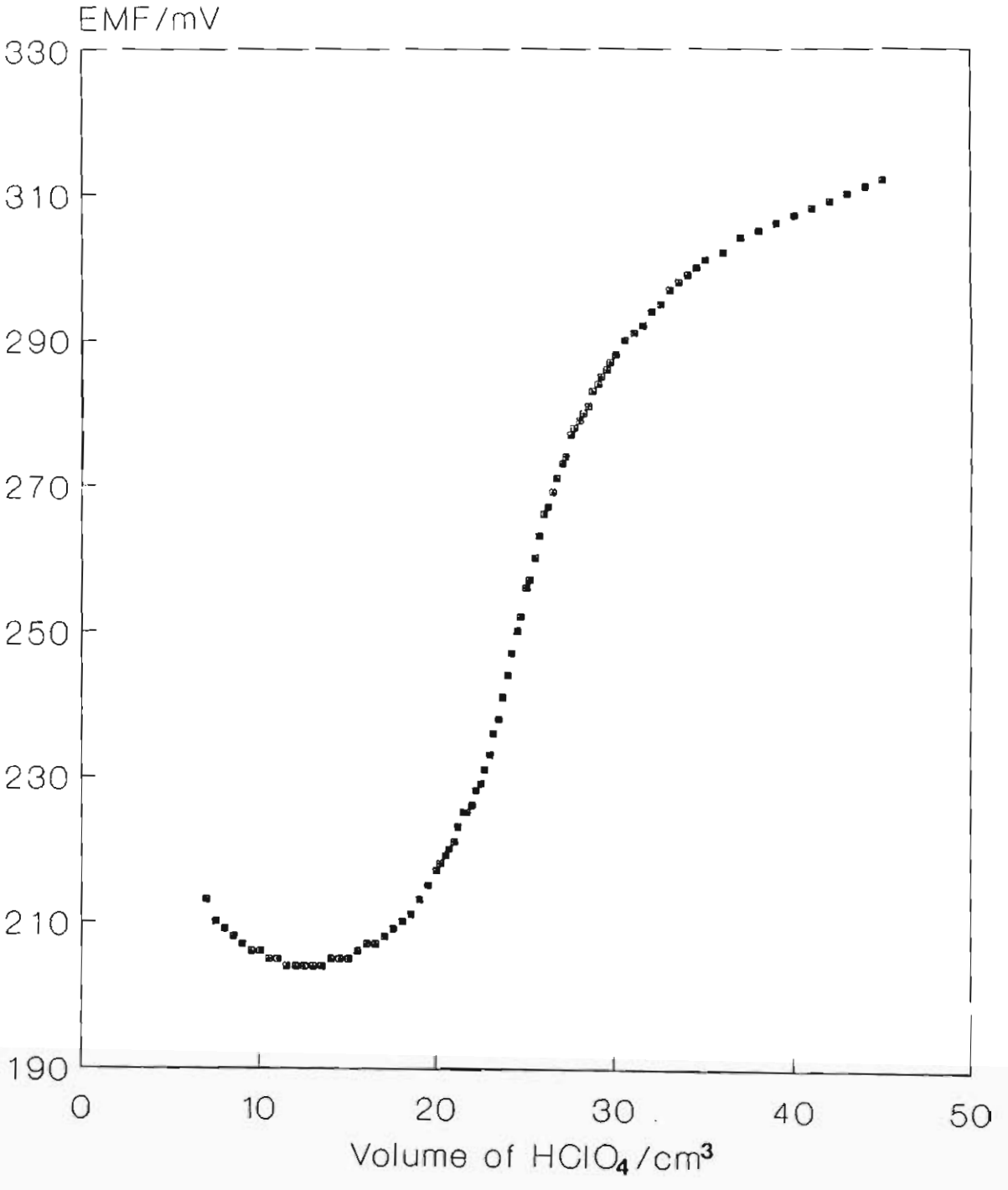

Figure 2.2 A typical titration curve for the standardisation of 8-hydroxyquinoline, a weak base, with a strong acid.

The ir spectrum of 8-hydroxyquinoline used in this study was recorded on a PYE UNICAM SP3-300 INFRARED SPECTROPHOTOMETER. This ir spectrum (shown in Figure 2.3(a)) is similar to the spectrum reported in the literature [54] (shown in Figure 2.3(b)). These ir spectra showed the following major absorption/cm^{-1}: 1580, 1510 (s, Ar-vibrations), 1410 (s, -O-H bending) and 1100 (s, C-O-H vibration).

The proton nmr spectrum of 8-hydroxyquinoline in deuterated methanol (CD_3OD) was recorded on a VARIAN GEMINI 200 mHz SPECTROMETER. This nmr spectrum (shown in Figure 2.4(a)) is comparable to the proton nmr spectrum for 8-hydroxyquinoline in dimethylsulfoxide (DMSO) reported in the literature [55] (shown in Figure 2.4(b)). The $^1H_{nmr}$ spectrum of oxine used in this study showed the following δ/ppm: 8.77 (1H, dd, 2-H), 8.18 (1H, dd, 4-H), 7.47-7.29 (3H, m, 3-,6-, and 5-H) and 7.12 (1H, dd, 7-H), which account for the six ring protons of 8-hydroxyquinoline. These assignments are similar to those reported in the literature [55]. However, the δ values are reported to be further downfield - probably an effect of the solvent.

The uv spectrum of 8-hydroxyquinoline dissolved in dioxane (shown in Figure 2.5) was recorded on a VARIAN DMS 300 UV VISIBLE SPECTROPHOTOMETER. This spectrum showed λ_{max}/nm at 304.4 and 321.2, which are attributable to conjugated systems.

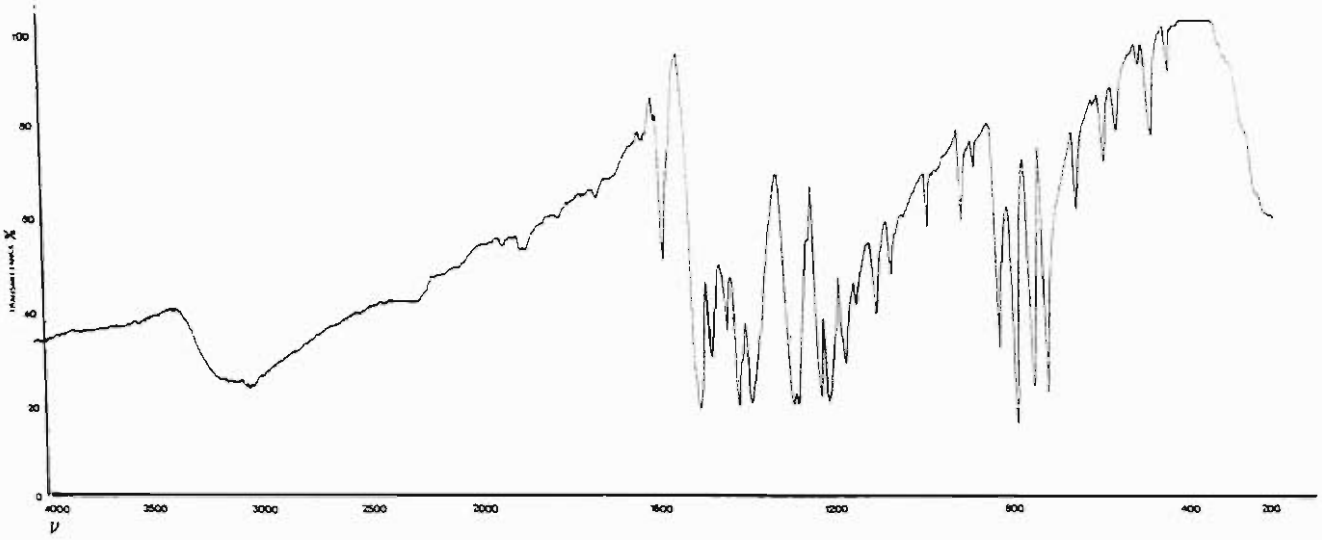

Figure 2.3(a) The infrared spectrum of 8-hydroxyquinoline used in this study.

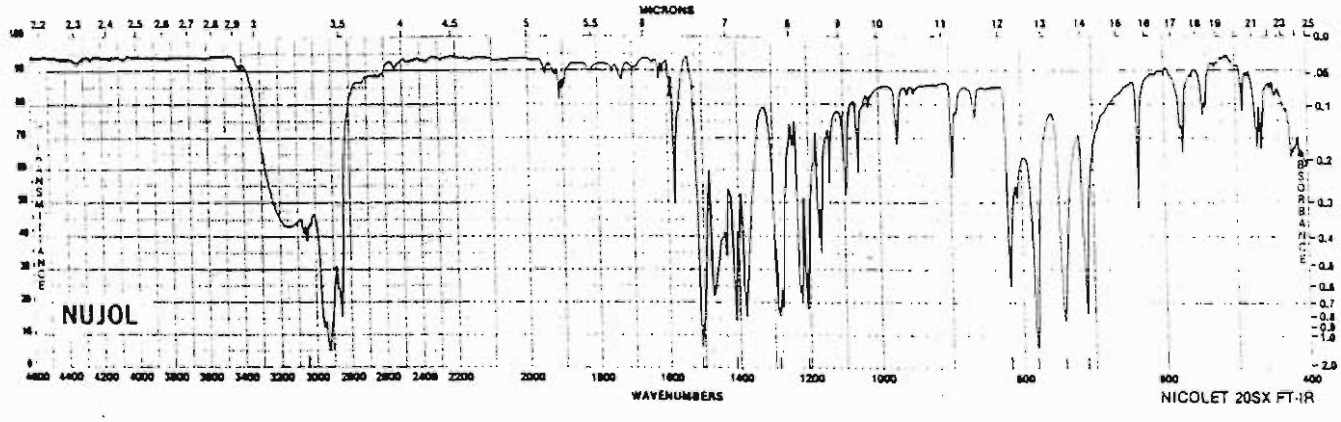

Figure 2.3(b) The infrared spectrum of 8-hydroxyquinoline reported in [54].

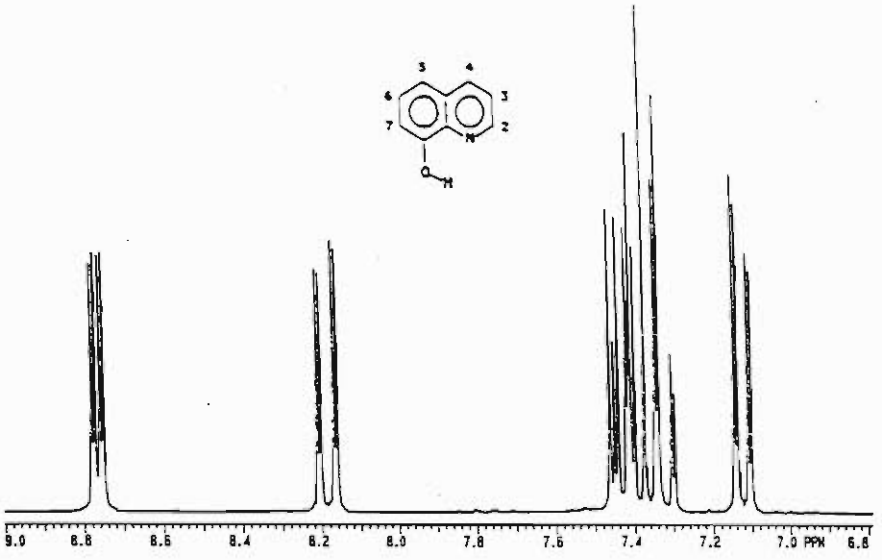

Figure 2.4(a) The proton nmr spectrum of 8-hydroxyquinoline (in CD_3OD) used in this study.

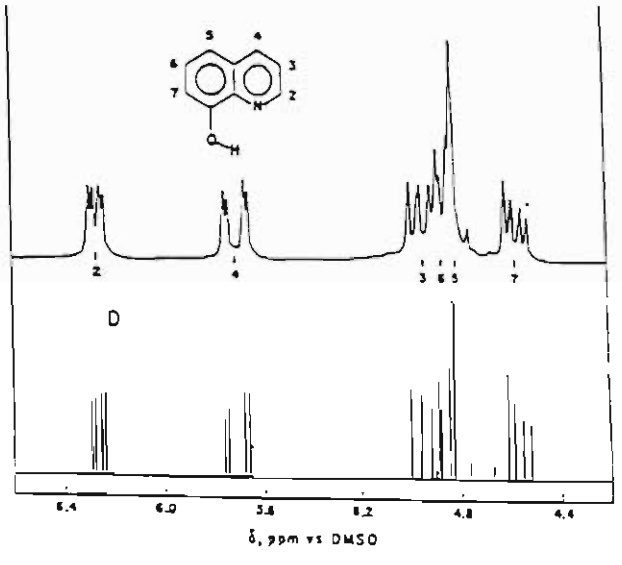

Figure 2.4(b) The proton nmr spectrum of 8-hydroxyquinoline (in DMSO) reported in [55].

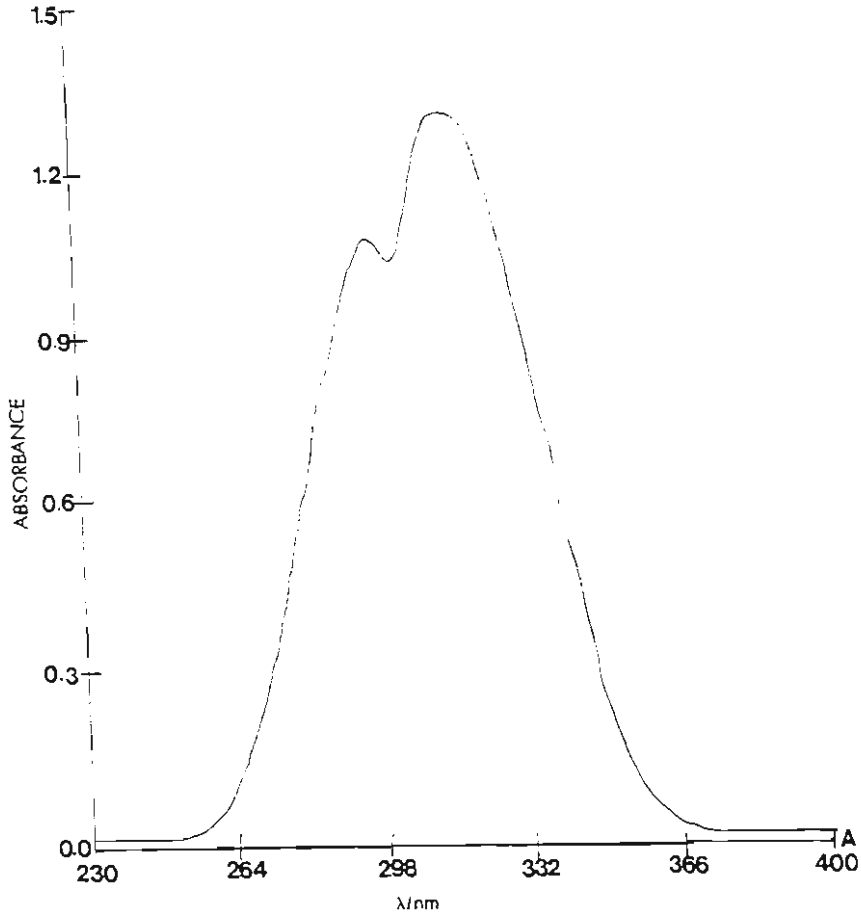

Figure 2.5 The ultraviolet - visible spectrum of 8-hydroxyquinoline in dioxane used in this study.

2.6 PREPARATION AND STANDARDISATION OF STOCK SOLUTIONS OF METAL PERCHLORATES

2.6.1 ZINC PERCHLORATE

Stock solutions of zinc perchlorate, $Zn(ClO_4)_2$, of ca. 0.5 mol dm^{-3} were prepared by mass from BDH ANALAR ZnO (min. 99.7%). Approximately 20.34 g of ZnO was dissolved in approximately 43 cm^3 of 16.62 mol dm^{-3} $HClO_4$; the resulting solution was then filtered to remove solid impurities and made up to 500 cm^3 with water. The stock solution was diluted to 0.1 mol dm^{-3} and standardised by direct titration against a standard 0.1 mol dm^{-3} solution of EDTA (MERCK Titriplex III ANALAR, min 99% pure) by using Eriochrome Black T as the indicator [56]. The excess acid in the $Zn(ClO_4)_2$ stock solution was determined by potentiometric titration. In these titrations a 20.00 cm^3 aliquot of standard 0.10 mol dm^{-3} $HClO_4$ was added to a 20.00 cm^3 aliquot of 0.10 mol dm^{-3} $Zn(ClO_4)_2$ solution and this was titrated against a freshly prepared and standardised NaOH solution.

2.6.2 GERMANIUM PERCHLORATE

The germanium perchlorate, $Ge(ClO_4)_4$, stock solution (ca. 0.023 mol dm^{-3}) was prepared by mass from ALDRICH ELECTRONIC GRADE GeO_2 (min. 99.999% pure).

In the literature, much controversy exists regarding the allotropic forms and the solubility of germanium

dioxide (GeO_2).

J.W. Mellor [57] and A. Navrotsky [58] report the existence of at least two allotropic forms of GeO_2 while J.H. Müller and H.R. Blank [59] suggest that three forms exist and V.A. Nazarenko [60] reports the existence of four allotropic forms, viz. the hexagonal 'soluble' form (α-GeO_2), the tetragonal 'insoluble' form (β-GeO_2), the cubic form (β-cristobalite) and the amorphous vitreous form.

There are also discrepencies in the reported densities of these various forms. H.P. Klug and R.G. Brasted [61] gave a density of 3.61 g cm^{-3} for the soluble form of GeO_2 (m.p. 1116 ± 4°C) and a density of 6.00 g cm^{-3} for the insoluble (tetragonal) form of GeO_2 (m.p. 1086 ± 5°C). A.W. Laubengayer and D.S. Morton [62], on the other hand, give a density of 6.239 g cm^{-3} at 25°C for the soluble form of GeO_2 (m.p. 1116 ± 4°C) and a density of 4.228 g cm^{-3} at 25°C for the insoluble (tetragonal) form of GeO_2 (m.p. 1086 ± 4°C).

Turning to the solubility of GeO_2, C. Winkler [57] reported that 100 parts of H_2O at 20°C dissolves 0.405 parts of GeO_2 and at 100°C, 1.05 parts of GeO_2. J.H. Müller and M.S. Iszard [63] mentioned that 10.9 g of GeO_2 dissolved per litre of H_2O at 100°C. According to W. Pugh [64], the solubility of α-GeO_2 in H_2O at 25°C is 447 mg per 100 cm^3, and the equilibrium saturation is reached after six days. V.A. Nazarenko [60]

suggested that 100 g of H_2O at 0°C dissolved 270 mg of α-GeO_2 and at 100°C, 1190 mg. The solubility curves of α-GeO_2 (hexagonal) and β-GeO_2 (tetragonal) with increasing temperature are reported by A.J. de la Cuadra Blanco and A. de la Cuadra Herrera [65]. These curves indicate that 1 dm^3 of H_2O can dissolve 0.004 g of β-GeO_2 and 5.2 g of α-GeO_2 at 25°C; while at 100°C, 0.09 g of β-GeO_2 and 14 g of α-GeO_2 can be dissolved.

A. Navrotsky [58] reported that the transformation from the rutile to the quartz form occurs at 1033°C at atmospheric pressure, but the reverse transformation is very sluggish in the absence of the appropriate mineralising agents. Nils Ingri [66] also reported transformation of GeO_2 to the soluble form by heating to 1130°C and then cooling it quickly.

W. Pugh [64] suggested that the solubility of GeO_2, as an acid oxide, was repressed by HCl reaching a minimum at an acid concentration of 5.3 mol dm^{-3}.
A. de la Cuadra [67] and W. Pugh [64] reported an increased solubility of GeO_2 with increasing NaOH concentration.

The first and slowest stage of the dissolution of GeO_2 in water is the formation of H_2GeO_3 [68]:

$$GeO_2 + aq \rightarrow [GeO_2.aq] \rightarrow GeO(OH)_2 + aq$$

In the presence of H^+ or OH^- ions, parallel reactions are possible:

$$GeO_2 + H_3O^+ \rightarrow Ge(OH)_3^+$$

$$GeO_2 + OH^- \rightarrow HGeO_3^-$$

Initial attempts to prepare a 0.025 mol dm^{-3} solution of $Ge(ClO_4)_4$ were unsuccessful when the following solvents were used to dissolve GeO_2:

a) H_2O at room temperature,
b) boiling H_2O,
c) concentrated $HClO_4$,
d) boiling H_2O + ~1 mol dm^{-3} NaOH, and
e) boiling H_2O + ~1 mol dm^{-3} NaOH + concentrated $HClO_4$.

Hence it was necessary to establish the crystallographic form of the GeO_2 used in this study. This was achieved by x-ray powder diffraction using a Philips PW1710 X-Ray-Diffractometer. The spectrum (shown in Figure 2.6) revealed the presence of the pure hexagonal, quartz type structure contaminated with less than 0.1% of the tetragonal, rutile type structure. This implied that a high purity soluble form of GeO_2 was present. The energy dispersive spectrum of a similar sample of GeO_2 was recorded on a JOEL JSM 35 Scanning electron microscope fitted with a KEVEX 7000/77 energy dispersive x-ray analysis system. This spectrum (shown in Figure 2.7) confirmed the high purity of GeO_2, viz. 100.00% germanium was

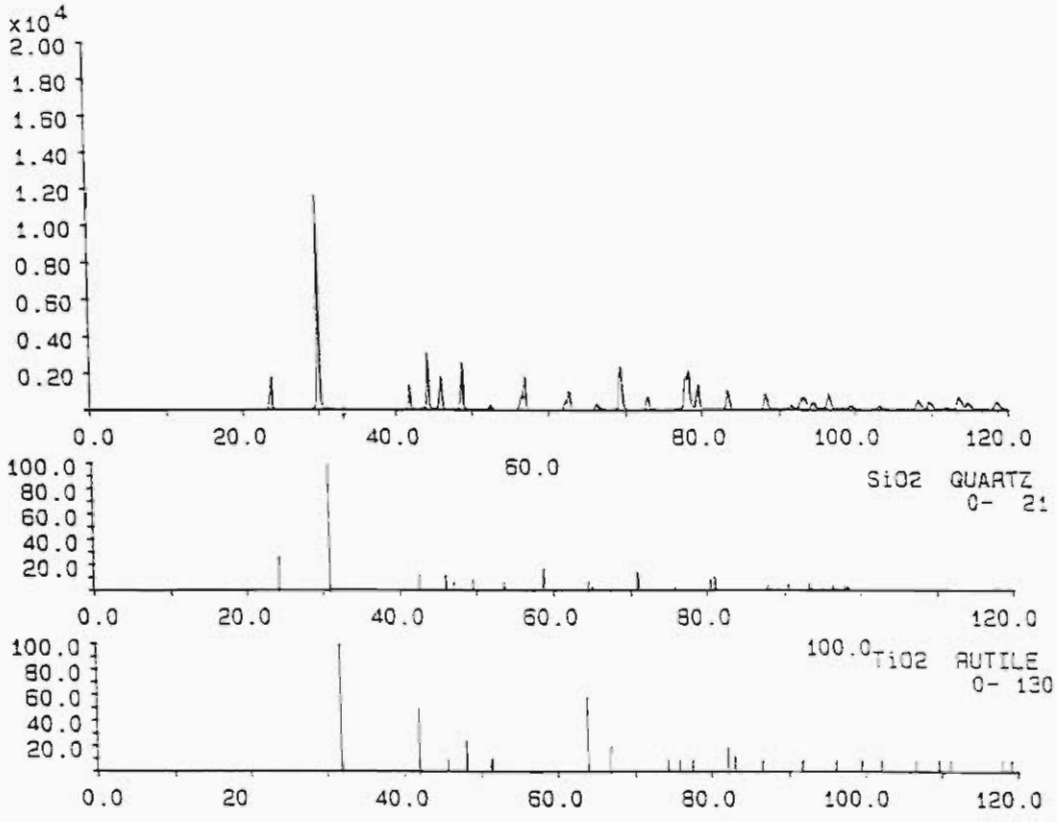

Figure 2.6 The x-ray powder diffraction spectrum of germanium dioxide.

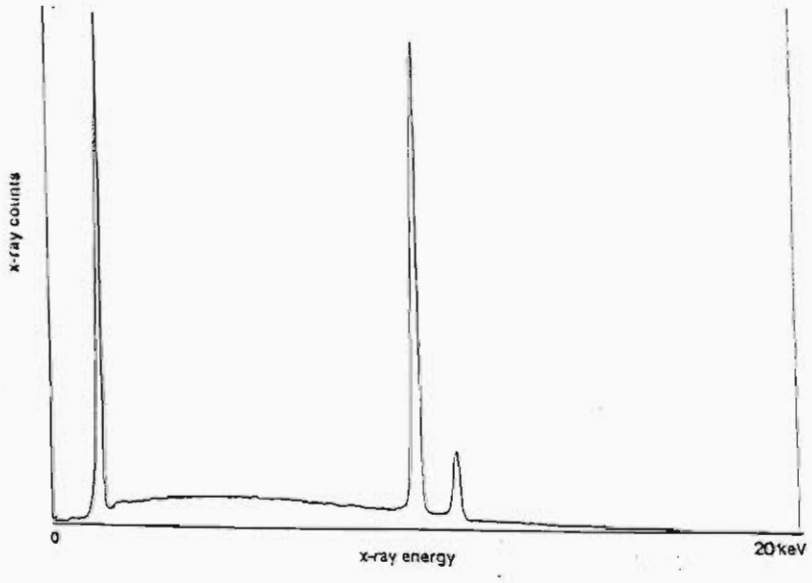

Figure 2.7 The energy dispersive spectrum of germanium dioxide.

detected with absolutely no contamination.

Dissolution of GeO_2 was attained by adding small quantities of GeO_2 to a hot 1 mol dm^{-3} NaOH solution (±150 cm^3); this was followed by the addition of hot, boiled-out water (±700 cm^3) with stirring. When the solution cooled to room temperature, concentrated $HClO_4$ was added dropwise until the solution was acidic. This solution was allowed to reach equilibrium overnight, thereafter it was filtered using 542 Whatman filter paper and made up to 1 dm^3 with water. The final $Ge(ClO_4)_4$ solution had a pH of approximately 3.

The stock solution was standardised by a back-titration method [69]. This procedure entailed acidifying a 20.00 cm^3 aliquot of $Ge(ClO_4)_4$, with approximately 2.5 cm^3 of a 1 mol dm^{-3} HCl solution. The solution was then diluted with water to 50 cm^3 and a 25.00 cm^3 aliquot of a standard (ca.0.05 mol dm^{-3}) EDTA solution was added. The mixture was cautiously heated to boiling and then boiled for 10 min. At this stage the EDTA had complexed all the Ge^{4+} ions in the solution. The excess EDTA was back-titrated against a freshly prepared standard (ca. 0.05 mol dm^{-3}) BDH ANALAR $ZnSO_4.7H_2O$ (min.99.5%) solution, using Eriochrome Black T as the indicator. The zinc solution was standardised against a standard EDTA solution as described in Section 2.6.1.

The excess acid in the $Ge(ClO_4)_4$ stock solution was determined by potentiometric titration. In these titrations a 20.00 cm^3 aliquot of standard 0.10 mol dm^{-3} $HClO_4$ solution was added to a 20.00 cm^3 aliquot of 0.02362 mol dm^{-3} $Ge(ClO_4)_4$ solution and this was titrated against a freshly prepared and standardised NaOH solution. Plots for these titration curves (EMF versus volume) are shown in Figure 2.8. Representative data is given in Table 2.2.

Two end-points are observed in this titration curve, viz. a sharp end-point and a shallow one. This feature is characteristic of a solution that contains a weak acid in the presence of a strong acid. According to the literature [28] germanium is expected to be in the form of germanic acids in the original solution, i.e. at a pH of approximately 3. Germanic acids are also reported to be weak acids [70], thus it is reasonable to assume that the second end-point (the shallow one) is due to the neutralisation of the germanic acids. This assumption can be verified by comparing the concentration of the germanium obtained by the back-titration method to that obtained from the calculation using values from this excess acid determination (see Figure 2.8), i.e. the concentration of germanium determined by dividing the product of the volume of NaOH required to neutralise the germanic acid (viz. the difference between the two end-points) and the concentration of the NaOH, by the aliquot of the germanium solution used in this excess acid determination. The results are comparable to within four decimal places. Hence the assumption that the

TABLE 2.2

Data for the potentiometric titration of 20.00 cm^3 of 0.1000 mol dm^{-3} $HClO_4$ and 20.00 cm^3 of a 0.02362 mol dm^{-3} $Ge(ClO_4)_4$ solution with 0.0999 mol dm^{-3} NaOH.

Volume NaOH/cm^3	EMF1/mV	EMF2/mV
0.00	322.0	322.0
2.00	319.0	320.0
4.00	316.0	317.0
6.00	312.0	314.0
8.00	308.0	309.0
10.00	303.0	304.0
12.00	297.0	299.0
14.00	290.0	291.0
16.00	280.0	281.0
17.00	273.0	274.0
18.00	264.0	265.0
18.50	257.0	258.0
19.00	249.0	250.0
19.30	242.0	243.0
19.50	237.0	238.0
19.80	224.0	225.0
20.00	213.0	212.0
20.30	106.0	104.0
20.50	-44.50	-46.90
20.70	-66.00	-68.30
21.00	-82.60	-85.60
21.30	-94.40	-96.90
21.50	-100.5	-102.3
21.80	-108.2	-110.7
22.00	-113.1	-115.4
22.30	-	-122.1
22.50	-123.9	126.3
22.80	-	-133.1
23.00	-133.8	-136.6
23.50	-144.6	-147.6
24.00	-155.6	-159.6
24.50	-167.8	-173.6
25.00	-186.4	-193.6
25.50	-	-214.0
26.00	-225.0	-231.0
26.50	-	-242.0
27.00	-244.0	-249.0
28.00	-255.0	-259.0
29.00	-263.0	-266.0
30.00	-268.0	-271.0
32.00	-276.0	-278.0
34.00	-281.0	-283.0
36.00	-286.0	-287.0
38.00	-289.0	-290.0
40.00	-291.0	-293.0
44.00	-296.0	-297.0
48.00	-299.0	-300.0

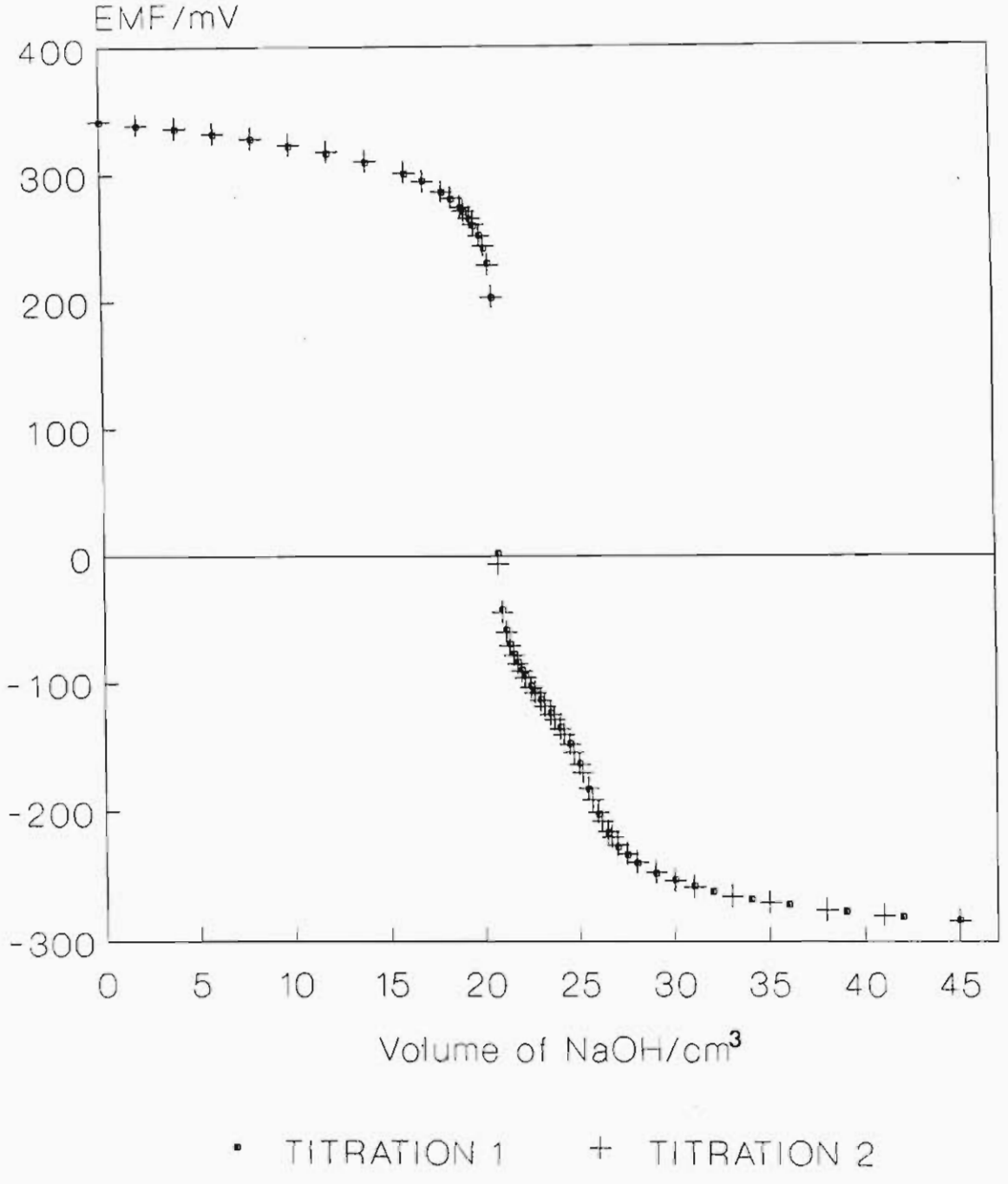

Figure 2.8 Determination of excess acid in germanium perchlorate, by titrating a mixture of germanium perchlorate and $HClO_4$ with a strong base.

second end-point is attributable to germanic acids is justified.

2.7 PREPARATION OF THE SILVER-SILVER CHLORIDE REFERENCE ELECTRODE

The silver-silver chloride reference electrodes used in this study were prepared from previously used silver-silver chloride reference electrodes. Hence the old silver-silver chloride coatings had to be removed from the platinum foil. This was achieved by following the method described by D.T. Sawyer and J.L. Roberts [71]. The procedure entailed immersion in potassium cyanide solutions, followed by thorough rinsing with water. The electrode was then treated with concentrated nitric acid (HNO_3), followed by a brief immersion (approximately 3 min.) in 50% aqua regia consisting of HCl, HNO_3 and H_2O in the ratio 3:1:4 respectively. Further treatment entailed washing with 16 mol dm^{-3} HNO_3 and rinsing in H_2O. The surface oxides were removed by cathodising the electrode in 0.01 mol dm^{-3} sulphuric acid. The current density was set at 10 mA cm^{-2} with a platinum wire as the anode. This was followed by rinsing with H_2O.

The electrode was ready for plating at this stage and the procedure used for the plating was essentially that of D.P. Shoemaker and C.W. Garland [72], and is outlined below. The electrode was cathodised with a silver wire as the anode, in a plating bath containing a solution of 10 g of silver cyanide, 10 g of

potassium cyanide, 3 g of potassium hydroxide and 15.5 g of potassium carbonate made up to a volume of 250 cm^3 with H_2O. The current density was again set at 10 mA cm^{-2} and plating continued for approximately 3 hours. All traces of cyanide were removed by washing with H_2O.

The silver plated electrode was then 'aged' for two days in an acidified silver nitrate solution. The final stage required anodising the silver plated electrode in 0.1 mol dm^{-3} HCl. The current density was set at 10 mA cm^{-2} with a platinum wire as the cathode. The silver-silver chloride electrode was then stored in H_2O which had been purged with acidified nitrogen to remove oxygen. The electrode was never allowed to dry out [72].

2.8 THE POTENTIOMETRIC CELL

In this work stability constants were determined potentiometrically by measuring hydrogen ion concentration with a glass electrode. The potentiometric cell was assembled as follows:

The test solution was placed in a METROHM No. EA 876-50 jacketed glass reaction vessel thermostatted at 25.0 ± 0.1°C by water circulating from a LAUDA cooling bath type MGW fitted with a COLORA heating unit type K-5131. The plastic lid of the reaction vessel was fitted with a glass electrode, nitrogen bubbler, thermometer and the reference electrode/ salt bridge

assembly. The remaining hole in the lid was covered with a teflon stopper and was used for the introduction of titrant solution via a burette. The glass electrodes employed were of the RADIOMETER G202B and METROHM 6.0102.100 (low sodium error) type. These electrodes were always conditioned before use (see Section 3.2.1). The reference electrode and salt bridge were assembled by using two INGOLD liquid junction tubes, type 303/95/T/NS, with water jackets on the upper halves. This enabled the reference electrode/salt bridge assembly to be thermostatted at the same temperature as the reaction vessel. The solution in the reference electrode was 0.01 mol dm^{-3} NaCl + 0.09 mol dm^{-3} $NaClO_4$ in 60% (v/v) dioxane, and that in the salt bridge was 0.1 mol dm^{-3} $NaClO_4$ in 60% (v/v) dioxane. A drop of $AgClO_4$ solution was added to the reference electrode solution before inserting the Ag/AgCl electrode, to ensure that the solution was saturated with AgCl and thus prevent dissolution of the AgCl coating on the reference electrode. The EMF of the cell was measured to ± 0.1 mV with a RADIOMETER PHM 84 research pH meter.

The titrant solutions were dispensed from grade 'A' burettes. If they were sodium hydroxide solutions, a drying-tube containing an absorbent (BDH soda-lime, self-indicating, 5-10 mesh) for CO_2 was attached to the top of the burette, thereby preventing the absorption of CO_2 by the solution.

A stream of high-purity nitrogen, which had been freed

from O_2 and CO_2, as well as acid and alkaline impurities (by passage through Feiser's [73], 10% NaOH and 10% H_2SO_4 solutions respectively), and then presaturated with 0.1 mol dm^{-3} $NaClO_4$ in 60% (v/v) dioxane, was bubbled through the test solution during the entire duration of the experiment. The solution in the cell was stirred by a magnetic bar stirrer at all times. The cell assembly is shown in Figure 2.9.

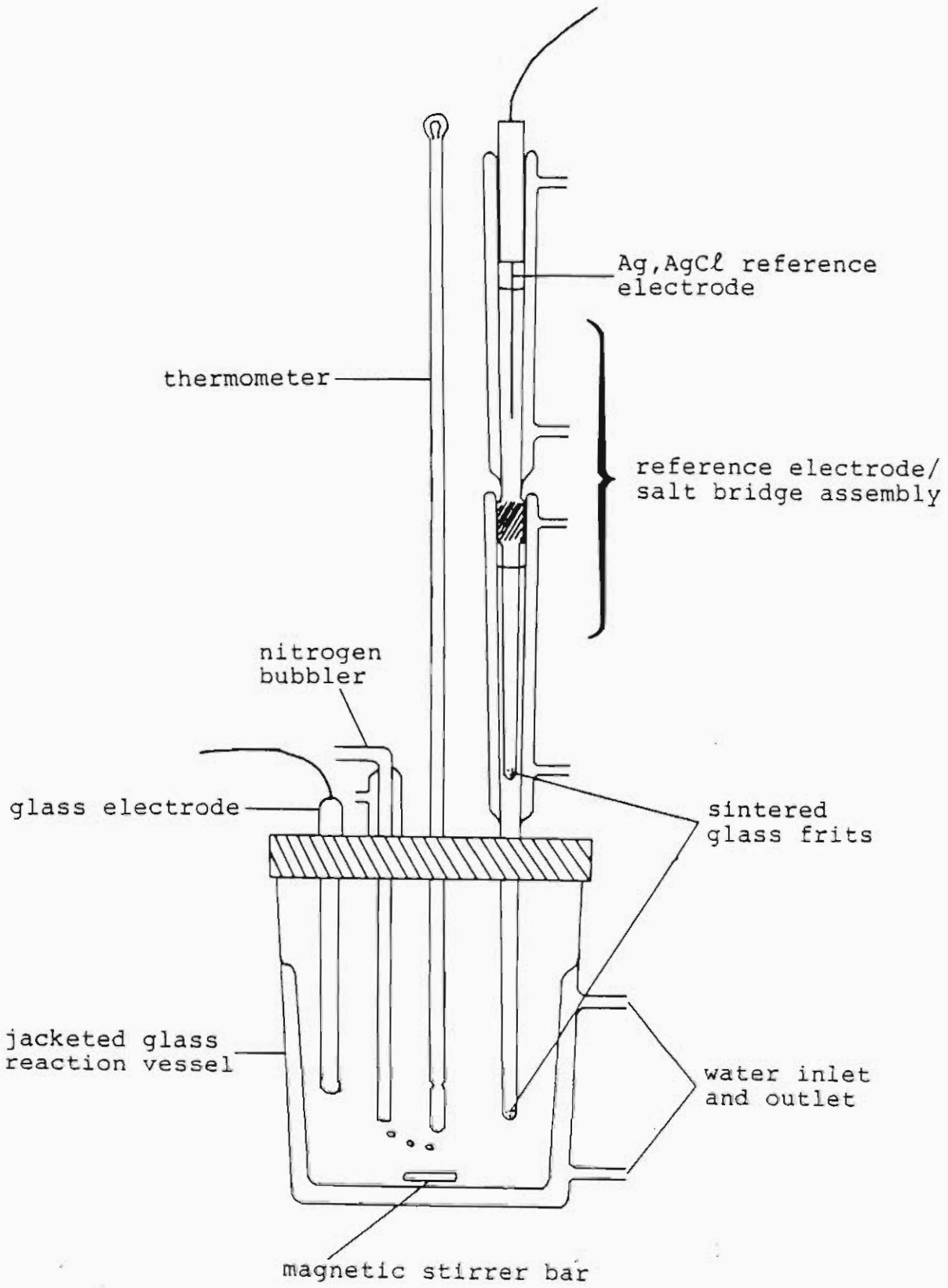

Figure 2.9 The potentiometric cell assembly.

CHAPTER 3

EXPERIMENTAL PROCEDURE

This chapter describes the density measurements used to determine the contraction factor for a partially aqueous medium, viz. 60% (v/v) dioxane in 0.1 mol dm^{-3} $NaClO_4$; the experimental technique used in this study, i.e. glass electrode potentiometry; and the calibration of the potentiometric cell. This is followed by a description of a series of potentiometric titrations carried out in order to obtain the stability constants of the complexes formed for each system studied. Numerical data obtained from these experiments are included. The synthesis and analysis of the zinc 8-hydroxyquinolate precipitate is also outlined.

3.1 DETERMINATION OF THE CONTRACTION FACTOR

Volumes are not additive when aqueous and organic solvents are mixed. Hence it was necessary to determine the contraction factor for the partially aqueous medium, viz. 0.1 mol dm^{-3} $NaClO_4$ in 60% (v/v) dioxane, used in this study. The change in volume on mixing $NaClO_4$ and dioxane was determined by measuring the densities of the pure liquids and the mixtures, using a Sonic Digital Densimeter (Paar Precision Density Meter-DMA 10). This instrument works on a principle of determining the number of oscillations produced by the solution in a set time.

The instrument was allowed to attain a constant temperature of 25.0 ± 0.1°C over a period of at least 40 min. Thorough rinsing of the instrument with acetone followed by drying after each measurement was essential in order to ensure accurate measurements for the different mixtures. The numerical data for the density measurement experiments are listed in Tables 3.1 and 3.2.

Various dioxane-$NaClO_4$ mixtures were made up to an additive total volume, V_{tot}, of 5.00 cm^3 . These mixtures comprised of 40 to 80% (v/v) dioxane, $V_{dioxane}$, in 5% increments; appropriate volumes of 2.0 mol dm^{-3} $NaClO_4$, V_{NaClO_4}, to give a final ionic strength of 0.1 mol dm^{-3}, and water, V_{H_2O}, constituted the rest of V_{tot}. The volumes of dioxane, $NaClO_4$ and H_2O required to make the various mixtures are given in Table 3.1.

An example of the calculation of the various volumes required, for the mixture containing 60% (v/v) dioxane follows:

$$V_{tot} = 5.00\ cm^3$$

$$V_{dioxane} = \frac{5.00\ cm^3 \times 60}{100} = 3.00\ cm^3$$

TABLE 3.1

Volumes of pure dioxane, 2.0 mol dm^{-3} $NaClO_4$ and H_2O required to make the various dioxane-$NaClO_4$ mixtures used for the density measurements.

% *dioxane*	$V_{dioxane}$ /cm^3	V_{NaClO_4} /cm^3	V_{H_2O} /cm^3
40	2.00	0.25	2.75
45	2.25	0.25	2.50
50	2.50	0.25	2.25
55	2.75	0.25	2.00
60	3.00	0.25	1.75
65	3.25	0.25	1.50
70	3.50	0.25	1.25
75	3.75	0.25	1.00
80	4.00	0.25	0.75

$$V_{NaClO_4} = \frac{5.00\ cm^3 \times 0.1\ mol\ dm^{-3}}{2.0\ mol\ dm^{-3}} = 0.25\ cm^3$$

$$V_{H_2O} = V_{tot} - V_{dioxane} - V_{NaClO_4}$$
$$= 5.00\ cm^3 - 3.00\ cm^3 - 0.25\ cm^3$$
$$= 1.75\ cm^3.$$

The densities of each of the mixtures and those of the pure components were determined using the sonic density meter set at 25.0 ± 0.1°C. In order to determine the calibration constant (A) of the instrument, the number of oscillations (T) in a set time was determined for both air and water. These were used to calculate A from the following equation:

$$^*\rho_1 - \rho_{H_2O} = A(T_1^2 - T_{H_2O}^2), \qquad 3.1$$

where $^*\rho_1$ represents the density of air when determining A, and the mixture in question otherwise.

The following values for the densities of air and water were used [74]:

$$\rho_{H_2O}^{25} = 0.99710\ g\ cm^{-3}$$

$$\rho_{AIR}^{25} = 0.001103\ g\ cm^{-3}$$

Once A, and T for the pure components and each of the mixtures, had been determined, the densities for each of the samples were calculated using the above equation. The number of oscillations (T) were recorded for three different sets of solutions. Representative density measurement data, including the contraction factor calculated for each mixture, are given in Table 3.2.

An example of the calculation of the contraction factor from the density measurements is given for a mixture containing 60% dioxane:

mass of dioxane $= {}^{*}\rho_{dioxane} \times V_{dioxane}$

$= 1.0276 \text{ g cm}^{-3} \times 3.00 \text{ cm}^{3}$

$= 3.0828 \text{ g}$

mass of $NaClO_4$ $= {}^{*} \rho_{NaClO_4} \times V_{NaClO_4}$

$= 1.0166 \text{ g cm}^{-3} \times 2.00 \text{ cm}^{3}$

$= 2.0332 \text{ g}$

true volume = total mass / density of mixture

$= 5.1160 \text{ g} / 1.0438 \text{ g cm}^{-3}$

$= 4.9013 \text{ cm}^{3}$

contraction factor = true volume / measured volume

$= 4.9013 \text{ cm}^{3} / 5.0000 \text{ cm}^{3}$

$= 0.9803$

where * represents the densities calculated using equation (3.1).

TABLE 3.2

Density measurement data for various dioxane-$NaClO_4$ mixtures and their pure components.

EXPERIMENT 1 : A = 2.22125 x 10^{-9} g cm^{-3}

PURE COMPONENTS	T	ρ/g cm^{-3}	V_{true}/cm^3	CONTRACTION FACTOR
air	32168	0.001103	-	-
H_2O	38512	0.99710	-	-
dioxane	38690	1.0276	-	-
*(0.25 M) $NaClO_4$	38626	1.0166	-	-
% (v/v) DIOXANE	T	ρ/g cm^{-3}	V_{true}/cm^3	CONTRACTION FACTOR
40	38737	1.0357	4.9290	0.9858
45	38757	1.0392	4.9151	0.9830
50	38767	1.0409	4.9097	0.9819
55	38779	1.0429	4.9030	0.9806
60	38784	1.0438	4.9013	0.9803
65	38785	1.0440	4.9031	0.9806
70	38789	1.0447	4.9024	0.9805
75	38788	1.0445	4.9060	0.9812
80	38781	1.0433	4.9142	0.9828

* M represents mol dm^{-3}

EXPERIMENT 2: $A = 2.22164 \times 10^{-9}$ g cm^{-3}

PURE COMPONENTS	T	ρ/g cm^{-3}	V_{true}/cm^3	CONTRACTION FACTOR
air	32168	0.001103	-	-
H_2O	38511	0.99710	-	-
dioxane	38689	1.0276	-	-
*(0.25 M) $NaClO_4$	38626	1.0166	-	-
% (v/v) DIOXANE	T	ρ/g cm^{-3}	V_{true}/cm^3	CONTRACTION FACTOR
40	38741	1.0366	4.9248	0.9850
45	38754	1.0388	4.9170	0.9834
50	38768	1.0412	4.9083	0.9817
55	38778	1.0429	4.9029	0.9806
60	38783	1.0438	4.9013	0.9803
65	38786	1.0443	4.9016	0.9803
70	38786	1.0443	4.9042	0.9808
75	38783	1.0438	4.9092	0.9818
80	38777	1.0428	4.9166	0.9833

EXPERIMENT 3 : A = 2.22094 x 10^{-9} g cm^{-3}

PURE COMPONENTS	T	ρ/g cm^{-3}	V_{true}/cm^3	CONTRACTION FACTOR
air	32167	0.001103	-	-
H_2O	38512	0.99710	-	-
dioxane	38688	1.0273	-	-
*(0.25 M) $NaClO_4$	38627	1.0168	-	-
% (v/v) DIOXANE	T	ρ/g cm^{-3}	V_{true}/cm^3	CONTRACTION FACTOR
40	38743	1.0367	4.9243	0.9849
45	38757	1.0391	4.9154	0.9831
50	38769	1.0412	4.9080	0.9816
55	38779	1.0429	4.9026	0.9805
60	38784	1.0438	4.9008	0.9802
65	38787	1.0443	4.9010	0.9802
70	38789	1.0447	4.9016	0.9803
75	38788	1.0445	4.9051	0.9810
80	38780	1.0431	4.9142	0.9828

The plot of density against % dioxane (v/v) for the three sets of solutions is shown in Figure 3.1. These curves are reproducible and parabolic in shape, with a maximum density at 70% (v/v) dioxane.

The density of pure dioxane obtained from the measurements in this study, viz. 1.0276 g cm^{-3}, compares well with that of 1.02797 g cm^{-3} reported in the literature [75]. This suggests that reliable results were obtained, hence the value of 0.9803 was confidently used as the contraction factor for the medium in this study, viz. 0.1 mol dm^{-3} $NaClO_4$ in 60% (v/v) dioxane.

Attempts were also made to measure density using pyknometry but this was abandoned due to the difficulty in removing air bubbles from the pyknometer, which led to results which were not reproducible.

3.2 CALIBRATION OF THE POTENTIOMETRIC CELL

Calibration of the potentiometric cell was a prerequisite for all complexometric titrations performed in this study. To ensure successful calibrations, the glass electrodes were conditioned and the regions of linear electrode response were determined.

The electrochemical cell used in these titrations to determine the equilibrium hydrogen ion concentration can be represented as follows:

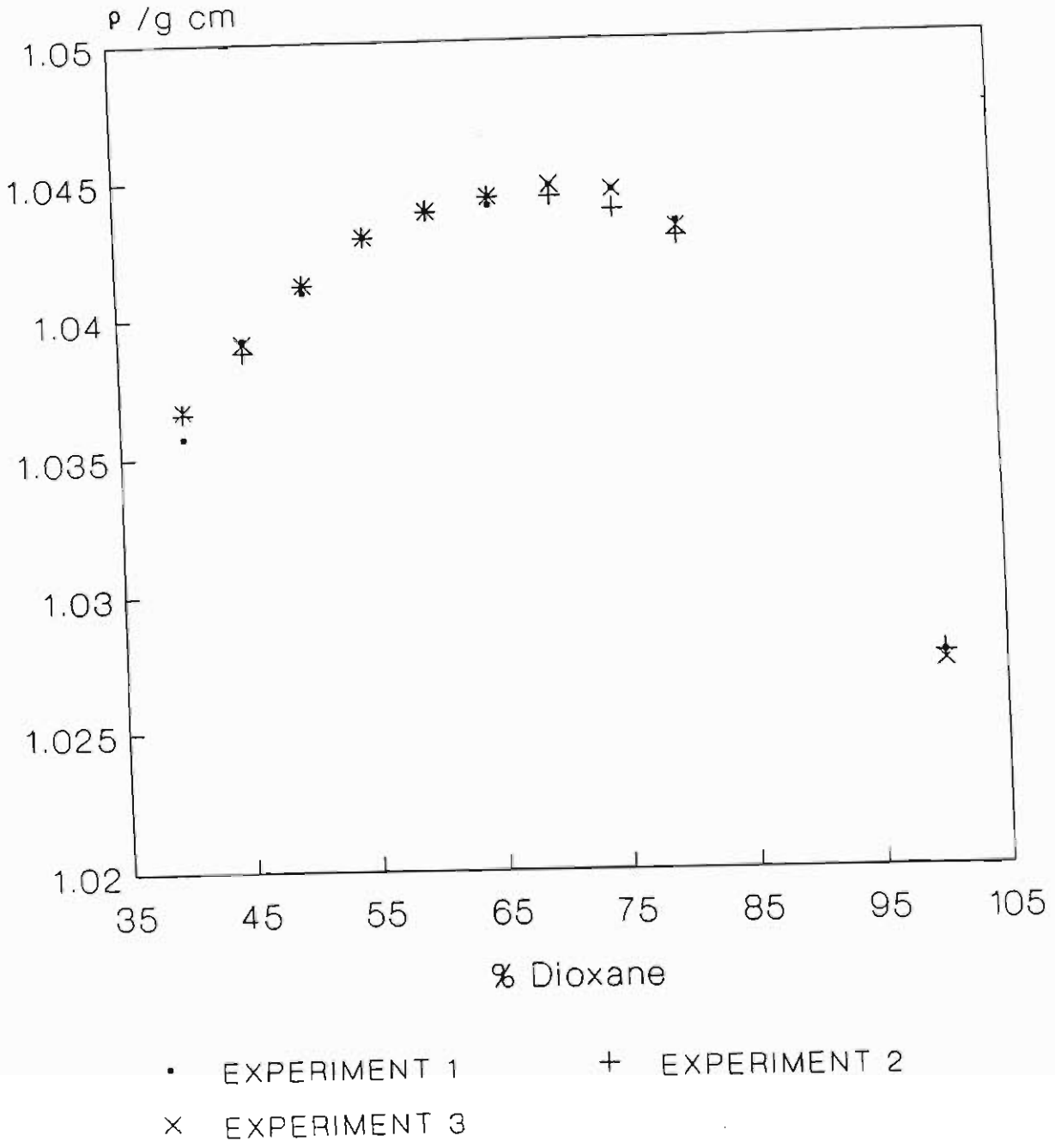

Figure 3.1 Variations in the densities of dioxane-$NaClO_4$ mixtures on changing the volume percentage of dioxane.

(-) RE | SB | test solution | glass electrode (+)
l L

where RE (reference electrode) = Ag/AgCl/0.01 mol dm^{-3} Cl^-, 0.09 mol dm^{-3} ClO_4^-, 0.1 mol dm^{-3} Na^+ in 60% (v/v) dioxane; and SB (salt bridge) = 0.1 mol dm^{-3} $NaClO_4$ in 60% (v/v) dioxane. This electrochemical cell has two liquid junctions, viz. one between the reference electrode and the salt bridge (l), and one between the salt bridge and the test solution (L).

There are four contributions to the potential difference measured between the glass electrode and the reference electrode, hence the measured EMF of the cell is given by the equation [31]:

$$E_{cell} = E_{ref} + E_L + E_l + E_g, \qquad 3.2$$

where E_{ref}, E_g, E_l and E_L represent the potentials of the reference electrode, the glass electrode and the liquid junction potentials respectively.

Equation (3.2) can be simplified to give [76];

$$E_{cell} = E_{ref} + E_j + E_g, \qquad 3.3$$

where E_j is the sum of the junction potentials.

Glass electrodes exhibit a Nernstian response provided that the solutions are buffered with respect to the activity of the hydrogen ions. If in addition, the ionic strength of the test solution is kept constant,

the activity of the free hydrogen ions can be expressed in terms of concentration [31]. Thus equation (3.3) may be written as:

$$E_{cell} = E_o + s \log[H^+] + E_j, \qquad 3.4$$

where E_{cell} is the measured EMF of the cell, s is the slope which exhibits a value close to the Nernstian slope (viz. 59.2 mV at 25°C), E_o is a cell constant including all constant potentials and the hydrogen-ion activity coefficient, and E_j is the sum of the liquid junction potentials.

The potential difference across a junction, J, is given by [77]:

$$E_J = \frac{-RT}{F} \int_1^2 \sum_i \frac{T_i}{z_i} \, d \ln c_i \gamma_i, \qquad 3.5$$

where R represents the gas constant, T represents the absolute temperature, F represents the Faraday constant, z_i represents the charge number of the i^{th} ionic species, T_i represents the transport number of the ion i, c_i represents the concentration of ions i in mol dm^{-3}, γ_i represents the concentration scale activity coefficient of ion i, and 1 and 2 represent the bulk solutions between which the boundary is formed.

It is best to determine the liquid junction potential (E_j) experimentally when it becomes large, i.e. when the two adjoining solutions differ greatly in the

concentration, mobility or charge of the ions. However, E_j can be maintained small and constant by keeping the concentration of the inert background electrolyte constant and much higher than the concentration of the high mobility reagent H^+ and OH^- ions. Under these conditions E_j can be incorporated into E_o, so that equation (3.4) can be rewritten as:

$$E_{cell} = E^{o}_{cell} + s \log[H^+] . \qquad 3.6$$

In this study the potentiometric cell was calibrated by a strong acid - strong base titration. The calibration is required to ascertain the values of the constants E^o_{cell} and s. Equation (3.6) is linear with respect to $[H^+]$, therefore the cell can be used to measure the hydrogen ion concentration, once it has been calibrated.

The glass indicating electrode requires specific conditioning and maintenance procedures to ensure reliable and reproducible performance. The procedures followed are discussed in the following section.

3.2.1 CONDITIONING AND MAINTENANCE OF THE GLASS ELECTRODE

Surface hygroscopicity is important for the electrode to produce a p[H] response. (p[H] is a measure of acidity or basicity, and is equivalent to the negative logarithm of the hydrogen ion concentration.) Lithium containing glasses are more useful in partially aqueous media since they require less hydration [78].

Glass electrodes of the low sodium error type were used in this study, since sodium ions constituted a major part of the cations present in the solutions.

An extensive literature search to identify the appropriate conditioning procedure for glass electrodes in partially aqueous media revealed interesting contradictions.

According to the manufacturers of one brand of glass electrodes (METROHM) [79], p[H] glass electrodes used in non-aqueous media should be soaked in water between measurements as often as possible. R.G. Bates [80] reported that the performance of the glass electrode usually became less satisfactory as the membrane became partially dehydrated. He also mentioned that the usefulness of the glass electrode in non-aqueous solutions could be impaired by a defective response due to the dehydration and sometimes by the high resistance of the medium. However, he confirmed the restoration of the p[H] response by soaking the electrode in water after being immersed in non-aqueous media.

When conditioning the glass electrode for an acetonitrile medium, I.M. Kolthoff [81] reported that the electrode was stored in water. Just prior to use the glass bulb was thoroughly rinsed with absolute ethanol and dried in a current of dry nitrogen. The electrode was then soaked in purified acetonitrile for 20 min. and then inserted into the buffer solution in the glass electrode compartments. After completion of

a series of measurements, the electrode was rinsed with ethanol and dried as above. Kolhoff stated that in general, a stable potential (±2 mV/30 min.) was obtained in 5-10 min. This conditioning procedure appears drastic and contradicts the importance of surface hygroscopicity.

G. Mattock [82] has employed pH-sensitive glass electrodes in dioxane-water mixtures after conditioning them for 24 hours in the appropriate solvent. Similarly, A.G. Mitshell and W.F.K. Wynne-Jones [83] have suggested that glass electrodes be conditioned for 24 hours in the appropriate solvent before using them in peroxide-water mixtures. These findings are in keeping with the theoretical considerations described by J.J. Lagowski [84], and Boksay and Csákváry [85].

The phase-boundary potential of ion-selective membranes is given by the following equation [86]:

$$E_{B_{1(1)}} = E_o + \frac{RT}{z_i F} \ln \frac{(a_i)_1}{(a_i)_{(1)}}, \qquad 3.7$$

where $E_{1(1)}$ is the phase boundary potential, E_o is a constant and independent of activities, z_i is the valency of the i^{th} ion, F is the Faraday constant, a_i is the activity of the i^{th} ion, and 1 and (1) represent the solution and the membrane respectively.

Boksay and Csákváry [85] have found some contradictions when employing equation (3.7) to

describe the potential of an interphase between the glass electrode and the aqueous solution - the electrode process was found to be different from that described by the equation. In fact, the real electrode process should be described by taking into account that when an ion leaving the glass enters the solution a vacancy is produced in the glass. In the reverse process, the ion entering the glass from the solution can occupy a vacancy only. Accordingly, if this real electrode process is considered

$$Vacancy + H_1^+ \rightleftarrows H_{(1)}^+, \qquad 3.8$$

then the phase-boundary potential can be described by the following equation [84]:

$$E_{1_{(1)}} = E_o + \frac{RT}{F} \ln \left[C_v \frac{a_{H,1}}{a_{H,(1)}}\right]. \qquad 3.9$$

Thus, the potential of the glass electrode depends, in addition to the activity of the hydrogen ion, on the concentration of the vacancies (C_v). The concentration of the vacancies may change if the ion-exchange reaction is related to volume changes in the glass or if the vacancies in the glass phase are occupied by the neutral molecules in the solution. These possibilities must be taken into account, for example, when the solvent containing the ion tested is replaced by another one.

It has been found experimentally [84] that when a glass electrode is transferred from an aqueous

solution to a non-aqueous one, the potential of the glass electrode changes significantly (20-100 mV) as a function of time, and the final potential value is reached within 30-120 min., even when the oxonium ion activity is almost equal in the two appropriate solutions. This can be attributed either to a change in concentration of the vacancies, or to a variation in proton activity at the surface of the glass. (The change in proton activity does not necessarily involve a change in proton concentration, since the proton is bonded in the surface layer to different proton acceptors such as solvent molecules or certain groups in the silicate lattice.) Consequently if the glass electrode is intended to be used in non-aqueous media, then the electrode must be soaked for a few hours in the appropriate solvent in order to obtain an electrode surface layer having a constant proton activity as well as a constant vacancy concentration characteristic of the non-aqueous solvent. In this case the phase-boundary potential can be described as follows [84]:

$$E_{1_{(1)}} = E_o' + \frac{RT}{F} \frac{\ln a_{H1}}{a_{H(1)}}, \qquad 3.10$$

where E'_0 is a constant also involving the concentration of vacancies.

Conditioning in the appropriate solvent medium for 24 hours was also recommended by E.L. Purlee and E. Grunwald [87]. They cautioned against the practice of standardising the glass electrode in water when

subsequent measurements were to be made in another solvent, and also called attention to the slow equilibration of the glass electrode with the solvent medium. They reported that equilibrium EMFs, i.e. thermodynamically reversible values, could be obtained only after equilibrium between the glass membrane and solvent medium had been attained. They therefore recommended the storage of routinely used glass electrodes in the appropriate solvent medium.

In this study the glass electrodes were conditioned as follows:

a) The electrodes were soaked in 0.1 mol dm^{-3} aqueous HCl for at least 24 hours [88], then
b) rinsed with water, and finally
c) soaked in the partially aqueous medium used in this study, viz. 0.1 mol dm^3 $NaClO_4$ in 60% (v/v) dioxane taking into account the contraction factor of 0.9803.

After completion of each titration the electrode was rinsed thoroughly with water and reactivated as mentioned above. When the electrode was not in use for long periods of time it was stored in a pH 4 buffer solution.

The sensitivities of the glass electrodes, i.e. the Nernstian slopes, were checked as described in the RADIOMETER manual [89]. The sensitivity check was designed for aqueous media, however, it was especially useful in obtaining information regarding the performance of newly bought electrodes.

The RADIOMETER PHM 84 Research pH Meter was set as follows:

Electrical zero	→	Iso pH
Iso pH	→	pH 7.00
Sensitivity	→	100%
Temperature	→	25°C
Range	→	pH
Hold	→	off

The glass electrodes and the Ag/AgCl reference electrode (METROHM 6.0726.100) containing a 3.0 mol dm^{-3} KCl filling solution, were connected to the PHM 84 Research pH Meter. They were immersed in pH 7.00 buffer for 2 min. The "BUFFER" button was rotated until the display read 7.000 at 25°C. The electrodes were then rinsed with water, and immersed in pH 4.01 buffer for 2 min. The "SENS" button was adjusted until the display read 4.008 at 25°C. The adjustment value of the "SENS" button was then recorded and a value in the range of 97-102% indicated a sensitive glass electrode. Only glass electrodes which satisfied the sensitivity check were used in this study. The buffers were prepared as described in 'The Handbook of Chemistry and Physics' [90].

3.2.2 DETERMINATION OF THE REGIONS OF LINEAR ELECTRODE RESPONSE

The regions of linear electrode response refer to the specific p[H] ranges where E_{cell} varies linearly with p[H] according to equation (5.5). At these p[H] ranges the junction potential (E_j) is small and/or constant;

and the solutions are sufficiently buffered to give reliable cell EMF readings.

The experiments in this section were designed to investigate the solvent effects, i.e. to compare the regions of linear electrode response in an aqueous medium with the partially aqueous medium used in this work, and to determine the acid and base regions of linear electrode response. The latter was necessary in order to establish the acid and base solution concentrations required for the calibration of the potentiometric cell.

The experiments were conducted at 25°C in the following manner:

a) The linearity of the electrode response in acidic solution in an aqueous medium, viz. 0.1 mol dm^{-3} $NaClO_4$, was monitored with RADIOMETER G202B (low sodium ion error) glass electrodes and Ag/AgCl reference electrodes. A known volume of 0.10 mol dm^{-3} $NaClO_4$, was titrated with standard $HClO_4$ solutions. A sequence of $HClO_4$ titrant solutions of increasing $HClO_4$ concentration was used. The concentration of the titrant ranged from approximately 3.2×10^{-4} mol dm^{-3} to 0.10 mol dm^{-3}.

   A plot of E_{cell} against p[H] for the titration described is shown in Figure 3.2. Of the three titrations performed only one set of data is plotted for the sake of clarity. Representative

data for these titrations are given in Table 3.3. Table 3.3 and the following tables in this section start with a description of the concentrations of the components in the titrate solution (denoted $[\ ]_o$) and titrant solution (denoted $[\ ]_T$), and the initial volume (V_o) of the titrate solution. These concentrations and volumes include the dioxane added and the contraction factor when results from the partially aqueous medium are considered. All concentrations are reported in mol dm^{-3}. The description of the solutions are followed by a listing of volume of titrant added excluding dioxane (V_T), p[H] and cell EMF reported in mV.

For the totally aqueous medium a linear E_{cell} against p[H] response is obtained in the region: $2.23 \leq p[H] \leq 4.17$ (see Figure 3.2).

b) The linearity of the electrode response in acidic solutions in the partially aqueous medium, viz. 0.1 mol dm^{-3} $NaClO_4$ in 60% (v/v) dioxane, was also monitored using RADIOMETER G202B (low sodium ion error) glass electrodes and Ag/AgCl reference electrodes. A solution containing a 20.00 cm^3 aliquot of 0.245 mol dm^{-3} $NaClO_4$ and a 30.00 cm^3 aliquot of pure dioxane was titrated with standard $HClO_4$ solutions and appropriate amounts of dioxane in order to maintain a constant solvent composition. A sequence of $HClO_4$ titrant solutions of increasing $HClO_4$ concentration was used. The concentration of the titrant ranged from about

TABLE 3.3

Data from the titrations of the aqueous medium, i.e. 0.10 mol dm^{-3} $NaClO_4$, with acid solutions.

SOLUTION DESCRIPTION	V_T/cm^3	p[H]	EMF1/ mV	EMF2/ mV	EMF3/ mV
$[H^+]_o = 0.000$	1.00	5.203	-81.3	-50.9	-25.4
	2.00	4.910	-70.5	-32.3	-17.1
$[H^+]_T = 3.199 \times 10^{-4}$	3.00	4.742	-62.2	-21.7	-11.2
	4.00	4.625	-56.3	-14.3	-6.5
$V_o = 50.00\ cm^3$	5.00	4.536	-51.5	-8.8	-2.7
	6.00	4.465	-47.6	-4.9	0.7
	7.00	4.406	-44.5	-1.5	3.6
$[H^+]_o = 3.929 \times 10^{-5}$	1.00	4.175	-30.9	13.3	15.9
	2.00	4.029	-22.1	22.3	23.9
$[H^+]_T = 1.600 \times 10^{-3}$	3.00	3.924	-15.8	28.7	29.3
	4.00	3.841	-10.8	33.7	34.1
$V_o = 57.00\ cm^3$	5.00	3.774	-6.5	37.3	37.9
	6.00	3.718	-3.0	40.7	41.2
	7.00	3.669	0.2	43.4	43.9
$[H^+]_o = 2.100 \times 10^{-4}$	1.00	3.472	12.3	55.1	54.9
	2.00	3.340	20.5	62.9	62.8
$[H^+]_T = 7.998 \times 10^{-3}$	3.00	3.242	26.6	68.9	68.6
	4.00	3.165	31.5	73.4	73.1
$V_o = 64.00\ cm^3$	5.00	3.100	34.9	77.2	76.7
$[H^+]_o = 7.743 \times 10^{-4}$	1.00	2.865	49.8	90.5	89.7
	2.00	2.720	58.1	99.2	98.4
$[H^+]_T = 3.999 \times 10^{-2}$	3.00	2.609	64.2	105.4	104.6
	4.00	2.525	69.2	110.2	109.4
$V_o = 69.00\ cm^3$	5.00	2.456	73.1	113.9	113.2
	6.00	2.399	76.5	117.0	116.4
	7.00	2.349	79.0	119.6	119.3
$[H^+]_o = 4.386 \times 10^{-3}$	1.00	2.228	85.1	125.4	125.1
	2.00	2.152	89.5	129.7	129.6
$[H^+]_T = 9.998 \times 10^{-2}$	3.00	2.082	93.1	133.1	133.1
	5.00	1.973	98.4	138.4	138.5
$V_o = 76.00\ cm^3$	9.00	1.822	105.4	145.3	145.5
	14.00	1.698	110.5	150.7	150.8
	24.00	1.546	116.7	156.7	156.7
	34.00	1.451	120.4	160.3	160.1
	49.00	1.360	123.6	163.4	163.4
	74.00	1.269	126.4	165.9	165.9

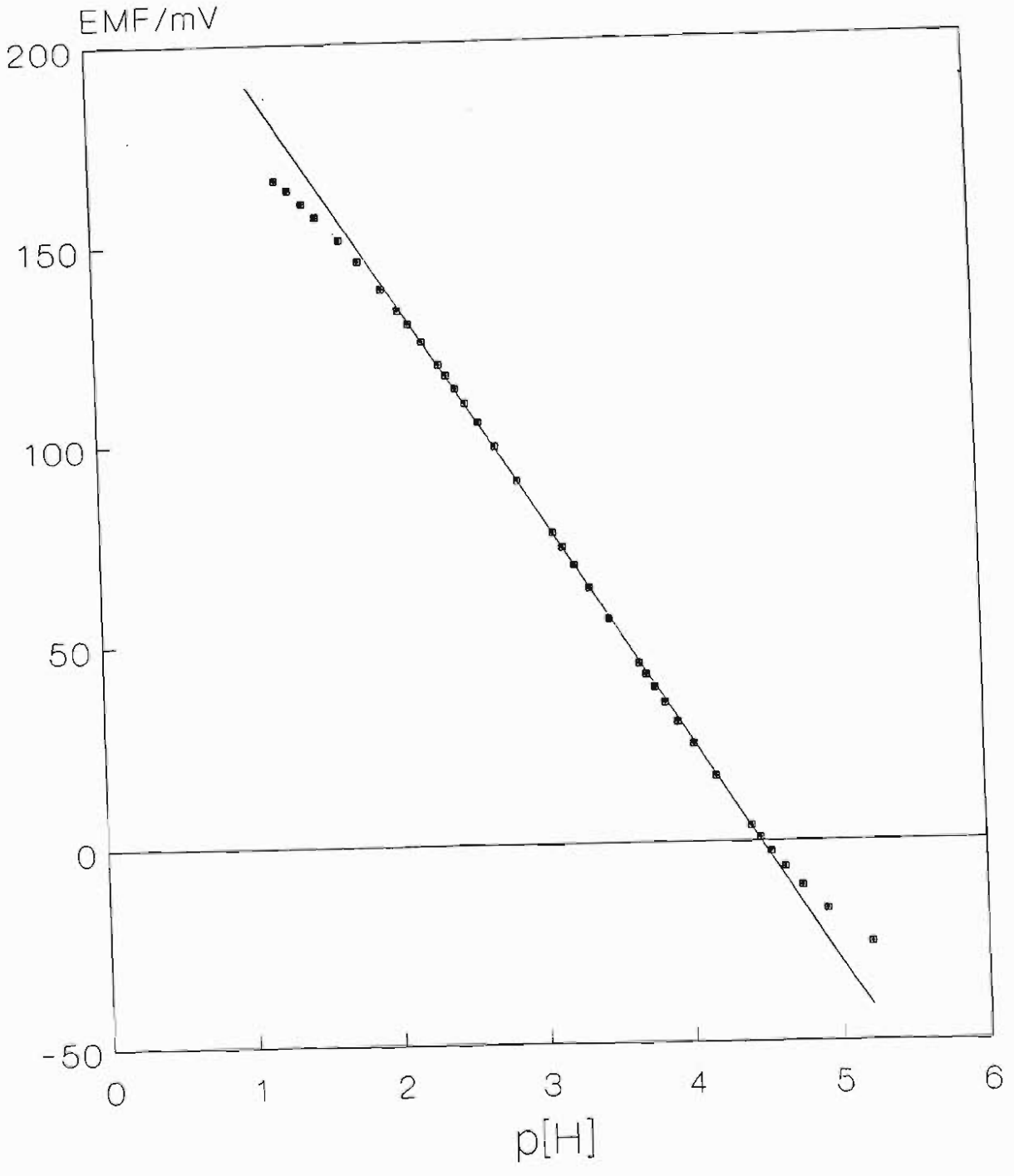

Figure 3.2 Determination of the acidic region of linear electrode response in the aqueous medium, by titrating a solution of the background electrolyte with a strong acid.

8×10^{-4} mol dm^{-3} to about 0.25 mol dm^{-3}.

A plot of E_{cell} versus p[H] for the titration described is shown in Figure 3.3. Representative data for the three titrations carried out is given in Table 3.4. A linear E_{cell} against p[H] response is obtained in the region: $2.22 \leq p[H] \leq 4.02$.

The solvent effect investigation revealed that the range of linear electrode response was reduced for the partially aqueous medium when compared to the totally aqueous medium. Figure 3.4. shows a plot of E_{cell} versus p[H] for the linear acid regions of electrode response in both the aqueous and partially aqueous media. The curve obtained from the data collected in the aqueous medium lies below the similar curve obtained in the partially aqueous medium. This observation is in keeping with the literature [91]. The E^{o}_{cell} and s are both higher in the partially aqueous medium, viz. 319.315 mV and 59.0462 mV, when compared to the totally aqueous medium, viz. 250.939 mV and 56.2544 mV.

c) The linearity of the electrode response in basic solutions in the partially aqueous medium, viz. 0.1 mol dm^{-3} $NaClO_4$ in 60% (v/v) dioxane, was monitored using RADIOMETER G202B (low sodium error) glass electrodes and Ag/AgCl reference electrodes. A solution containing a mixture of a 20.00 cm^3 aliquot of 0.245 mol dm^{-3} $NaClO_4$, a 0.80 cm^3 aliquot of a standard 0.25 mol dm^{-3} NaOH solution and a

TABLE 3.4

Data obtained for the titration of a solution containing a 20.00 cm^3 aliquot of 0.245 mol dm^{-3} $NaClO_4$ and a 30.00 cm^3 aliquot of pure dioxane with standard $HClO_4$ and appropriate volumes of dioxane so as to maintain a constant solvent composition.

SOLUTION DESCRIPTION	V_T/cm^3	p[H]	EMF1/ mV	EMF2/ mV	EMF3/ mV
$[H^+]_o = 0.000$	0.40	5.194	83.3	25.8	60.9
	0.80	4.901	84.5	36.8	64.5
$[H^+]_T = 8.002 \times 10^{-4}$	1.20	4.733	86.0	44.4	68.0
	1.60	4.617	87.5	50.3	72.6
$V_o = 49.02\ cm^3$	2.00	4.528	88.8	54.6	76.1
	2.40	4.456	89.9	58.3	79.2
	2.80	4.397	90.9	60.9	81.4
$[H^+]_o = 4.100 \times 10^{-5}$	0.40	4.166	96.5	72.8	90.1
	0.80	4.020	101.2	81.9	96.2
$[H^+]_T = 4.001 \times 10^{-3}$	1.20	3.915	105.0	88.2	102.0
	1.60	3.832	108.4	93.2	106.5
$V_o = 55.88\ cm^3$	2.00	3.765	111.0	97.2	110.0
	2.40	3.709	113.6	100.0	113.5
	2.80	3.660	115.5	102.8	116.0
$[H^+]_o = 2.143 \times 10^{-4}$	0.40	3.463	125.6	115.0	127.8
	0.80	3.332	131.6	123.2	136.0
$[H^+]_T = 2.000 \times 10^{-2}$	1.20	3.234	137.0	128.9	141.7
	1.60	3.156	141.0	133.5	146.4
$V_o = 62.74\ cm^3$	2.00	3.091	144.5	136.0	149.9
$[H^+]_o = 7.902 \times 10^{-4}$	0.40	2.856	158.6	150.6	164.5
	0.80	2.708	166.9	160.0	172.5
$[H^+]_T = 0.1000$	1.20	2.600	172.9	166.0	178.6
	1.60	2.516	177.4	170.9	183.5
$V_o = 67.64\ cm^3$	2.00	2.448	181.4	174.8	187.2
	2.40	2.390	184.5	178.2	190.6
	2.80	2.340	187.2	180.9	193.0
$[H^+]_o = 4.476 \times 10^{-3}$	0.40	2.230	193.0	186.9	197.8
	0.80	2.144	197.3	191.3	202.6
$[H^+]_T = 0.2500$	1.20	2.074	200.9	194.9	206.6
	2.00	1.964	206.4	200.1	212.6
$V_o = 74.50\ cm^3$	3.60	1.813	214.0	207.9	220.3
	5.60	1.690	220.4	214.0	226.6
	9.60	1.537	227.5	220.8	233.7
	13.60	1.442	231.5	224.9	237.6
	19.60	1.351	235.0	228.7	241.3
	29.60	1.260	238.2	231.9	244.5

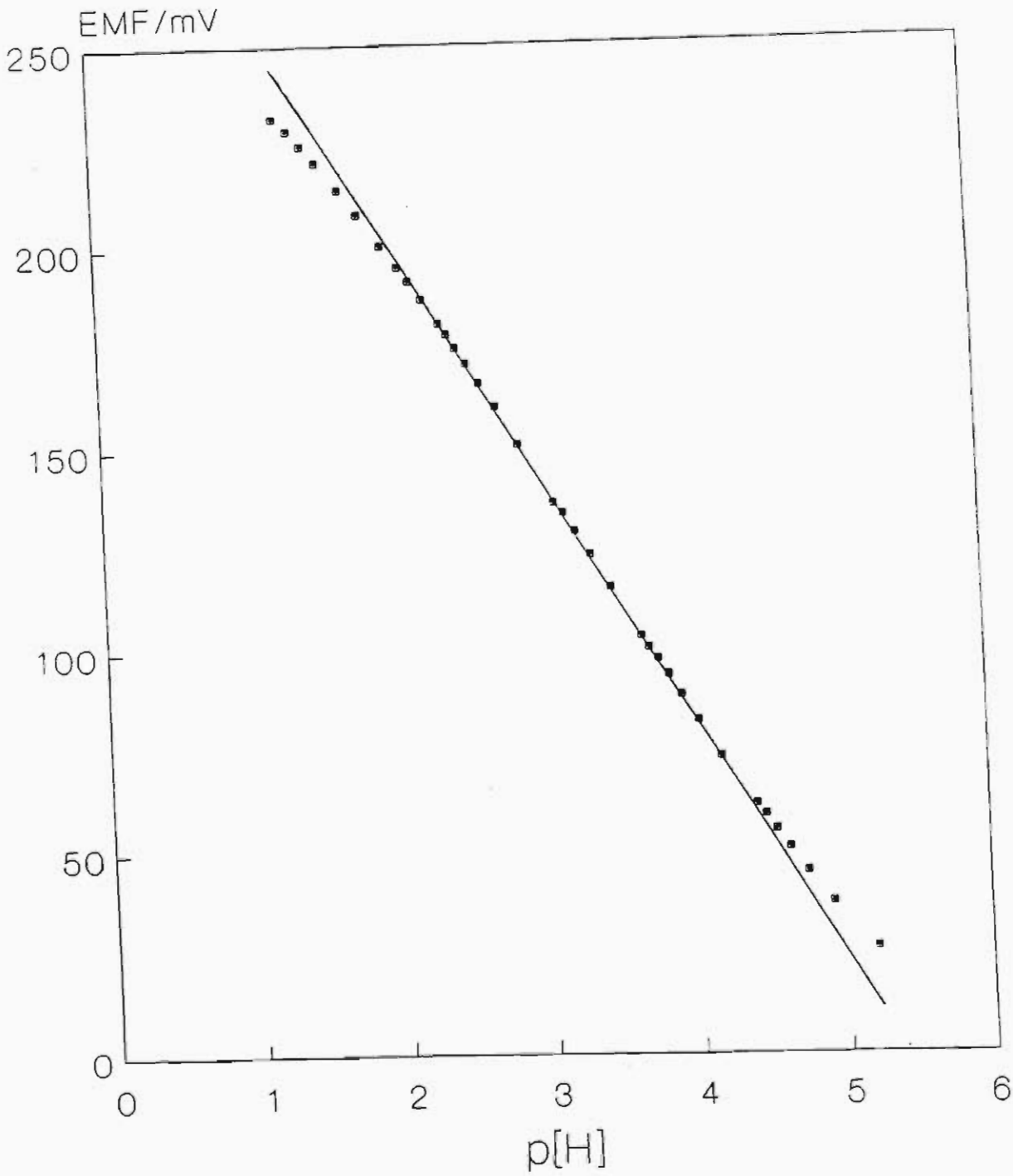

Figure 3.3 Plot used to ascertain the acidic region of linear electrode response in the partially aqueous medium used in this study, by titrating a solution of the background electrolyte in 60% (v/v) dioxane with a strong acid and appropriate volumes of dioxane in order to maintain a constant solvent composition.

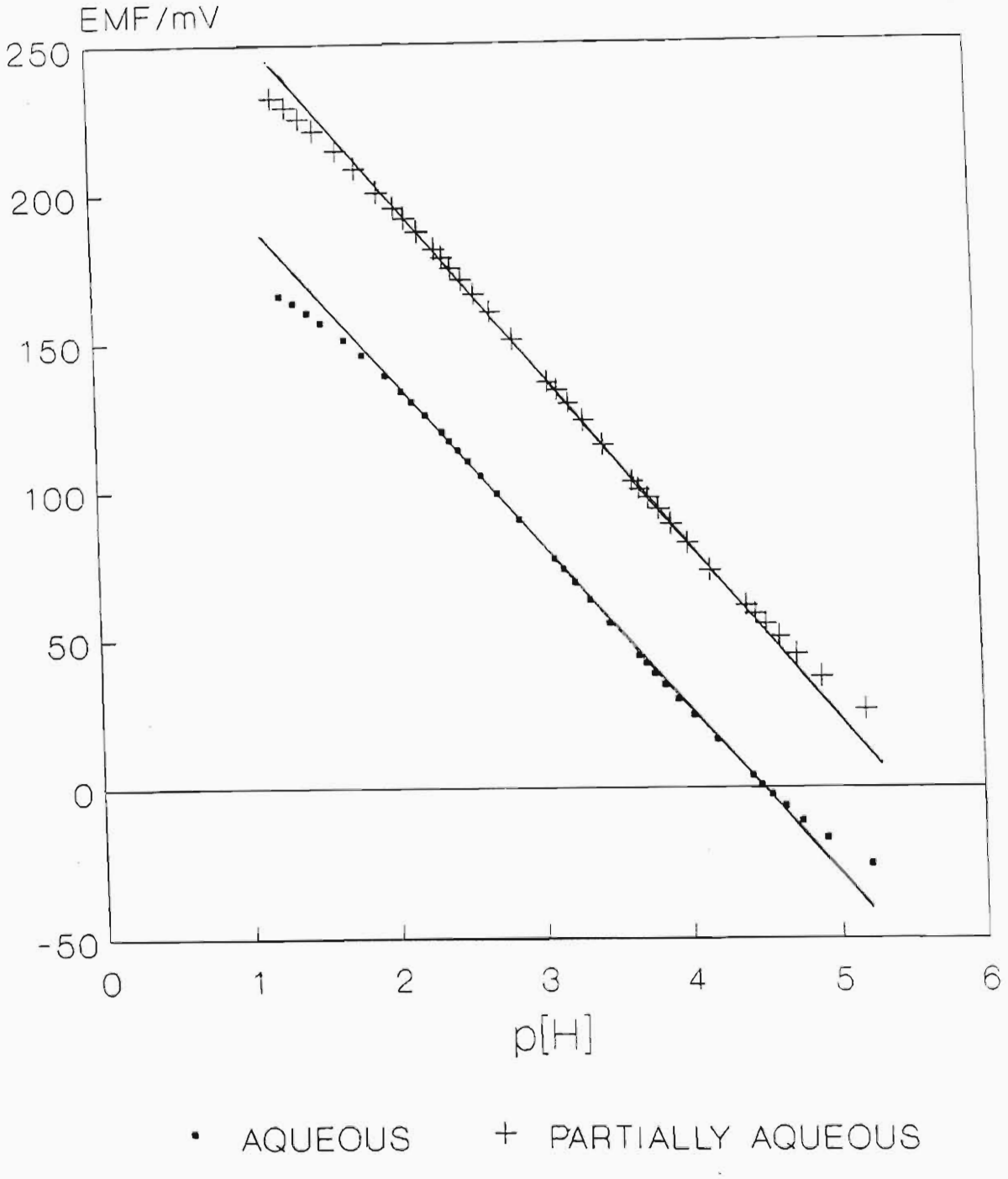

Figure 3.4 Plots demonstrating the difference in the regions of linear electrode response in acidic solutions for the aqueous and partially aqueous media.

31.20 cm^3 aliquot of pure dioxane, was titrated with standard $HClO_4$ solutions and appropriate volumes of dioxane, in order to maintain a constant solvent composition. A sequence of $HClO_4$ titrant solutions of decreasing $HClO_4$ concentration was used. The concentration of the titrant ranged from about 0.05 mol dm^{-3} to about 2 x 10^{-3} mol dm^{-3}. The titrant concentration was then increased to 0.025 mol dm^{-3} so that points in the acid region of linear electrode response, which had already been established, were collected. These points were used to extrapolate the linear response to the region of high p[H] in order to determine the corresponding base region of linear electrode response.

A plot of E_{cell} vs p[H] for this titration is shown in Figure 3.5. Representative data for Figure 3.5 is given in Table 3.5. The basic p[H] range covered included: $10.29 \leq p[H] \leq 13.48$, but did not produce a linear electrode response. However, this titration revealed that the linear electrode response of the basic solutions was at p[H] values greater than 13.48.

The experiments were then redesigned to cover the p[H] range $13.00 \leq p[H] \leq 14.80$. Here METROHM 6.0102.100 and RADIOMETER G202B (low sodium ion error) glass electrodes and a Ag/AgCl reference electrode were used to monitor the linear electrode response. A known volume of 0.245 mol dm^{-3} $NaClO_4$ was diluted to be 0.1 mol dm^{-3} in 60%(v/v) dioxane,

TABLE 3.5

Data obtained from the titration of a solution containing a mixture of a 20.00 cm^3 aliquot of 0.245 mol dm^{-3} $NaClO_4$, a 0.80 cm^3 aliquot of a standard 0.25 mol dm^{-3} NaOH solution and a 31.20 cm^3 aliquot of pure dioxane, with standard $HClO_4$ solutions and appropriate volumes of dioxane, in order to maintain a constant solvent composition.

SOLUTION DESCRIPTION	V_T/cm^3	p[H]	EMF/mV
$[OH^-]_o$ = 0.2016 mol dm^{-3}	0.00	13.54	-463.6
	0.40	13.48	-460.3
$[H^+]_T$ = 5.000 x 10^{-2} mol dm^{-3}	0.80	13.43	-456.6
	1.20	13.36	-452.2
V_o = 50.98 cm^3	1.60	13.29	-447.2
	2.00	13.21	-440.8
$[OH^-]_o$ = 1.818 x 10^{-3} mol dm^{-3}	0.40	13.16	-436.5
	0.80	13.10	-432.1
$[H^+]_T$ = 2.500 x 10^{-2} mol dm^{-3}	1.20	13.04	-426.8
	1.60	12.97	-421.0
V_o = 55.88 cm^3	2.00	12.89	-412.9
	2.40	12.80	-402.9
	2.80	12.68	-387.0
$[OH^-]_o$ = 5.037 x 10^{-4} mol dm^{-3}	0.40	12.62	-377.2
	0.80	12.56	-365.0
$[H^+]_T$ = 1.000 x 10^{-2} mol dm^{-3}	1.20	12.49	-347.2
	1.60	12.40	-319.7
V_o = 62.74 cm^3	2.00	12.29	-326.2
$[OH^-]_o$ = 1.715 x 10^{-4} mol dm^{-3}			
$[H^+]_T$ = 2.000 x 10^{-3} mol dm^{-3}	0.80	12.23	-221.3
V_o = 67.64 cm^3			
$[OH^-]_o$ = 1.437 x 10^{-4} mol dm^{-3}	1.20	3.662	110.3
	1.60	3.463	122.0
$[H^+]_T$ = 2.500 x 10^{-2} mol dm^{-3}	2.00	3.322	130.0
	2.40	2.231	135.8
V_o = 69.60 cm^3	2.80	3.143	140.7

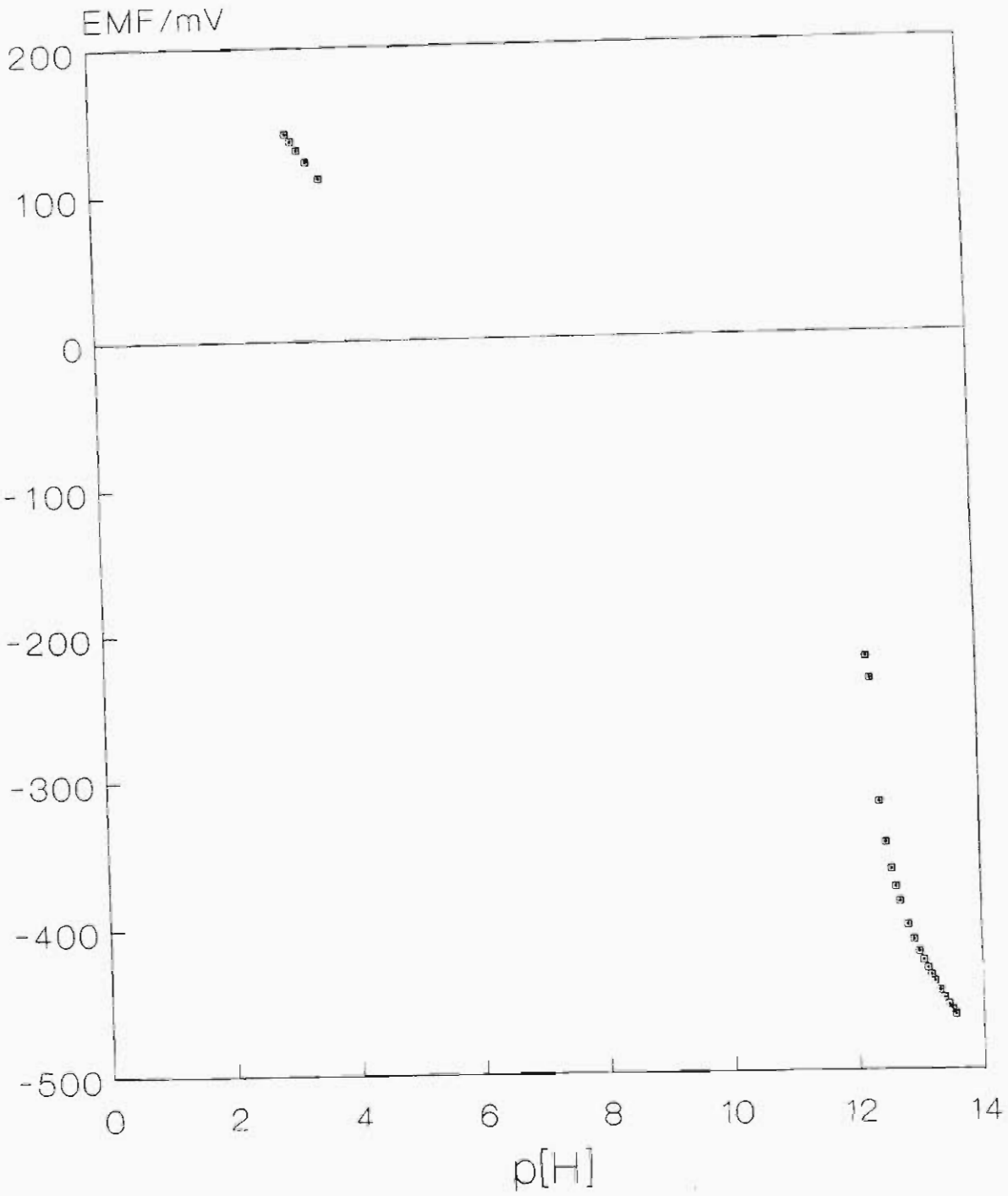

Figure 3.5 Plot used to ascertain the basic region of linear electrode response in the partially aqueous medium used in this study, by titrating a mixture of the background electrolyte and base solutions in 60% (v/v) dioxane with acid solutions and appropriate volumes of dioxane in order to maintain a constant solvent composition.

and the resulting solution was titrated with increments of standard NaOH solutions and appropriate volumes of dioxane so as to maintain a constant solvent composition. Two NaOH titrant solutions of differing hydroxide ion concentration were used. The concentrations of the titrant were ±0.045 mol dm^{-3} and ±0.245 mol dm^{-3} respectively. A plot of E_{cell} versus p[H] for the titration described is shown in Figure 3.6. Representative data for this titration, which was performed in duplicate, is given in Table 3.6.

The apparent linear region of electrode response for the basic solutions was verified by the titration of a 20.00 cm^3 aliquot of a 0.245 mol dm^{-3} $NaClO_4$ and a 30.00 cm^3 aliquot of pure dioxane with a standard 0.25 mol dm^{-3} NaOH solution and appropriate volumes of dioxane. This data is included in Table 3.6. A linear E_{cell} against p[H] response is obtained in the region:
$13.70 \leq p[H] \leq 14.70$.

Deviations from linearity below and above the linear p[H] ranges of the acid and the base regions respectively, can be attributed to values of E_j which are no longer negligible. Deviations from linearity above and below the linear p[H] ranges of the acid and the base regions respectively, can be attributed to insufficient concentration buffering in solutions that are very dilute in hydrogen ions [92,93].

TABLE 3.6

Data obtained from the titration of a known volume of 0.245 mol dm^{-3} $NaClO_4$ which was diluted to be 0.1 mol dm^{-3} in 60% (v/v) dioxane, with increments of standard NaOH solutions and appropriate volumes of dioxane so as to maintain a constant solvent composition.

SOLUTION DESCRIPTION	V_T/cm^3	p[H]	*EMF1/ mV	#EMF2/ mV	EMF3/ mV
$[OH^-]_o = 0.000$	0.80	12.79	-344.5	-419.9	-
	1.20	12.96	-359.0	-435.0	-
$[OH^-]_T = 4.500 \times 10^{-2}$	1.60	13.07	-368.8	-442.0	-
	2.00	13.16	-375.6	-448.0	-
$V_o = 50.98\ cm^3$	2.40	13.23	-381.0	-452.6	-
	0.40	13.51	-401.1	-470.6	-
	0.80	13.67	-412.3	-477.7	-
	1.20	13.79	-417.0	-484.7	-
	1.60	13.88	-422.9	-489.4	-
$[OH^-]_o = 2.119 \times 10^{-3}$	2.40	14.01	-431.6	-496.5	-
	3.60	14.14	-439.8	-503.5	-
$[OH^-]_T = 0.2500$	4.80	14.23	-444.6	-508.4	-
	6.80	14.34	-451.2	-514.0	-
$V_o = 54.90\ cm^3$	9.60	14.45	-457.1	-519.1	-
	13.60	14.54	-462.6	-523.8	-
	23.60	14.67	-469.9	-530.1	-
	33.60	14.73	-474.3	-533.3	-
	0.40	13.24	-	-	-446.5
	0.80	13.54	-	-	-467.3
	1.20	13.70	-	-	-477.5
	1.60	13.82	-	-	-484.0
$[OH^-]_o = 0.000$	2.00	13.91	-	-	-488.8
	2.40	13.98	-	-	-492.5
$[OH^-]_T = 0.2515$	3.60	14.13	-	-	-499.4
	5.20	14.27	-	-	-506.4
$V_o = 49.02\ cm^3$	7.60	14.39	-	-	-513.8
	11.20	14.51	-	-	-520.8
	16.80	14.61	-	-	-527.3
	28.00	14.72	-	-	-534.0
	40.00	14.78	-	-	-537.1

*$[OH]_T = 4.509 \times 10^{-2}$ and 0.2505 mol dm^{-3}

#$[OH]_T = 4.510 \times 10^{-2}$ and 0.2506 mol dm^{-3}

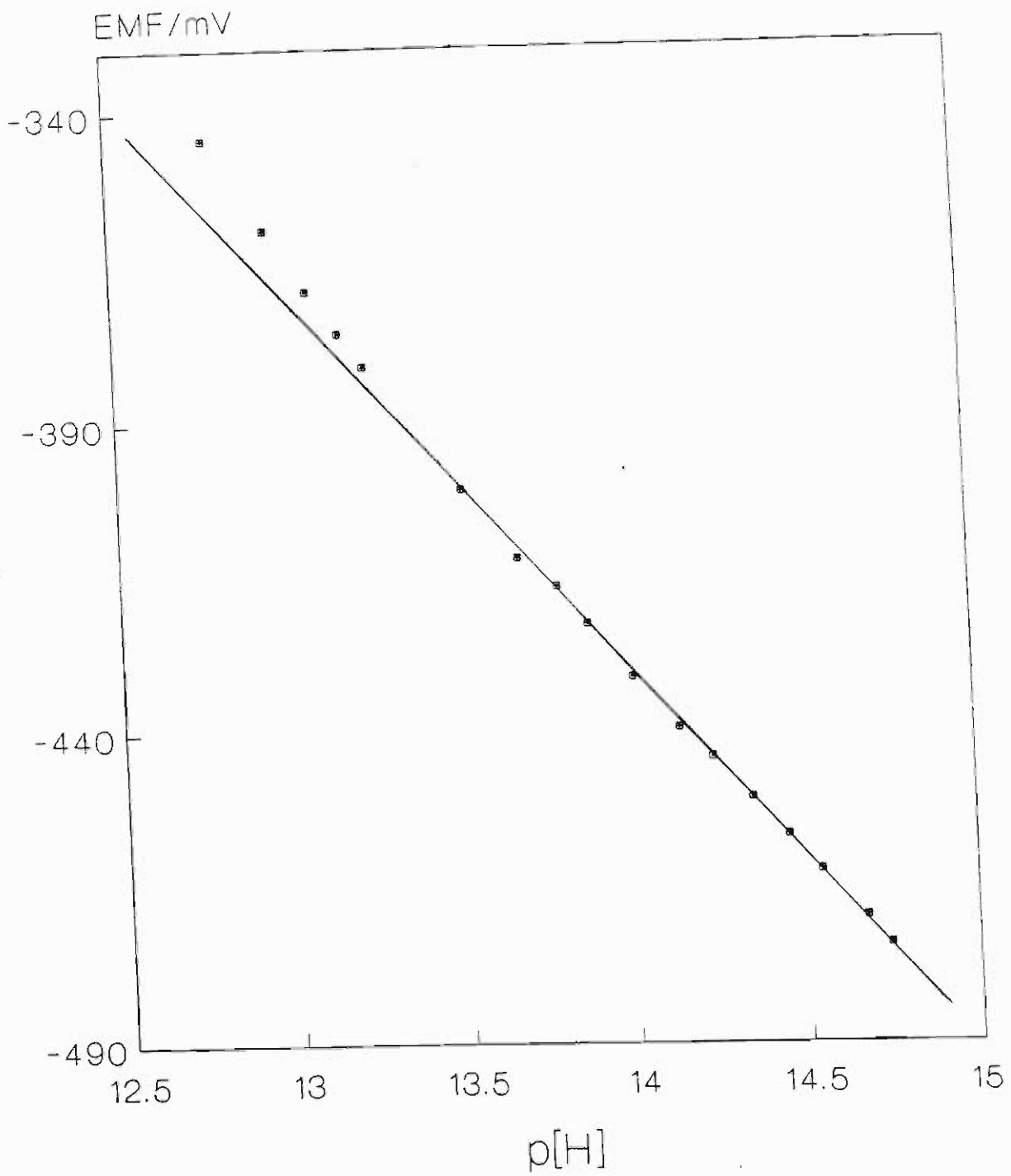

Figure 3.6 Determination of the basic region of linear electrode response in the partially aqueous medium used in this study, by titrating a solution of the background electrolyte in 60% (v/v) dioxane with a strong base and appropriate volumes of dioxane in order to maintain a constant solvent composition.

The results of these experiments indicate that in order to obtain linear E_{cell} against p[H] responses in the strong base-strong acid calibration procedure, the concentration of the titrant and titrate solutions should be in the order of 1×10^{-2} mol dm^{-3} and 1×10^{-1} mol dm^{-3} respectively, before introduction into the reaction vessel.

3.2.3 CELL CALIBRATION TECHNIQUE

The potentiometric cell used in this study was calibrated at the beginning of each titration, since the standard potential of the glass electrode membrane varies with time and it is difficult to reproduce liquid junction potentials with adequate precision [92].

A strong base-strong acid calibration technique was employed in this study. This entailed measuring equilibrium cell potentials before and after the equivalence point, and applying the Gran plot method (see Section 4.1) to determine the concentration of the NaOH solution and that of any inherent carbonate contamination.

All experiments were conducted at a temperature of 25.0 ± 0.1°C. The ionic strength of all solutions was made up to a final concentration of 0.10 mol dm^{-3} with $NaClO_4$ as inert background electrolyte in 60% (v/v) dioxane, taking into account the contraction factor of 0.9803.

The strong base-strong acid calibration was performed by titrating a solution containing background electrolyte, $NaClO_4$, and strong base, NaOH (approximately 0.1686 mol dm^{-3}), in 60% (v/v) dioxane, with a standard solution of a strong acid, $HClO_4$ (approximately 0.09803 mol dm^{-3}), and appropriate volumes of dioxane so as to maintain a constant solvent composition. After the addition of each increment of titrant the equilibrium cell potential was recorded. The Gran plot method was then used to determine the concentration of the NaOH solution.

The concentrations of the acid and base in the titrant and titrate, together with the value of K_w were supplied to the computer program CALIB (see Section 4.3.3) in order to calculate the p[H] at each point during the titration. The calculated p[H] values were plotted against the corresponding cell potential values. The points lying on the linear part of the curve were then used to obtain least-squares estimates of E^o_{cell} and s (using STATGRAPHICS - see Section 4.3.4), which are required for equation (3.6). Constant s was given by the gradient of the line and constant E^o_{cell} by the intercept of the line at p[H] = 0. Table 3.7 shows typical data for such a cell calibration. Figure 3.7 is a plot of E_{cell} against calculated p[H], from which E^o_{cell} and s were obtained by linear regression. For these data E^o_{cell} = 367.196 mV and s = 58.1539 mV with a correlation coefficient of 1.000.

TABLE 3.7

Data obtained for the calibration of a cell containing a glass electrode, with strong acid and strong base as calibrants, maintaining a constant solvent composition of 0.1 mol dm^{-3} $NaClO_4$ in 60% (v/v) dioxane.

SOLUTION CONCENTRATIONS	V_T/cm^3	p[H]	EMF/mV
	0.00	14.08	-451.3
	0.80	14.01	-447.7
	1.60	13.94	-443.4
$[OH^-]_o = 3.483 \times 10^{-3}$ mol dm^{-3}	2.40	13.85	-438.5
$[H^+]_T = 9.799 \times 10^{-2}$ mol dm^{-3}	3.20	13.75	-432.9
$V_o = 49.015$ cm^3	3.60	13.70	-429.3
	7.60	3.039	189.9
	8.00	2.832	202.5
	8.40	2.696	210.7
	8.80	2.595	216.5
	9.20	2.515	221.1

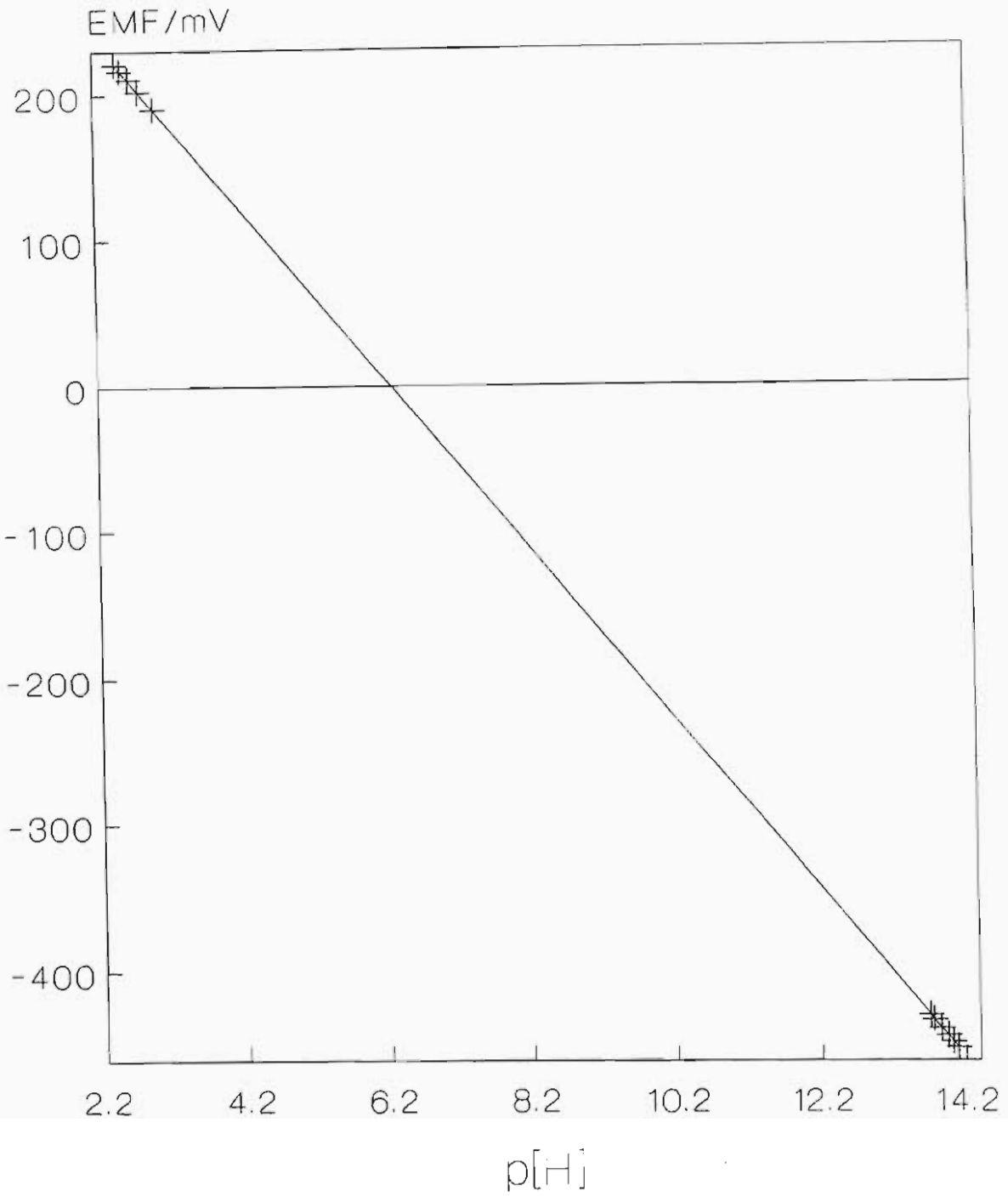

Figure 3.7 Calibration curve for a cell containing a glass electrode, obtained by using strong acid and strong base as calibrants.

Various authors [94] assume that the glass electrode has a perfectly Nernstian calibration slope and then determine, from their observations in the alkaline region of the calibration, that value of K_w which is most consistent with this assumption. In this study, however, a single value of 1.1482×10^{-16} [45] was used throughout for K_w, and the calibration slope determined as described above. Hence the assumption of a perfectly Nernstian slope was not made, in keeping with the ideas of workers in the field of ion-selective electrodes [95].

The strong base-strong acid calibration technique is advantageous since points in both the high and low p[H] regions are included, therefore E^o_{cell} and s can be determined with greater accuracy.

3.3 METHOD OF INVESTIGATION

This section describes the selection of experimental conditions for potentiometric measurements and the actual complexometric titrations carried out in order to obtain the stability constants of the complexes formed for each system studied. Numerical data obtained from these potentiometric titrations are included. Also outlined here, is the synthesis and analysis of the zinc 8-hydroxyquinolate precipitate.

3.3.1 SELECTION OF EXPERIMENTAL PROCEDURE

The conditions chosen in this study ensured that the measured quantity, viz. the hydrogen ion

concentration, was a sensitive function of the stability constant being determined.

The experiments were designed so that the concentration of each reactant was varied over as wide a range as was practically possible. This facilitated the measurement of reliable stability constants, and allowed the choice of extracting the stability constant for a particular species from a selected region where no other interfering species appeared to be present.

Four methods were available for the determination of the protonation constants of 8-hydroxyquinoline:

a) titration of acid into a solution containing deprotonated ligand,
b) titration of a solution of deprotonated ligand into an acid solution,
c) titration of hydroxide into a solution containing protonated ligand, and
d) titration of protonated ligand into a solution containing hydroxide.

It is imperative that only those p[H] readings which are sensitive to the values of the protonation constants be taken, i.e. in the range $pK_a \pm 1$, since readings outside this range are not useful. Method (c) was used for the determination of the protonation constants of 8-hydroxyquinoline due to the volatility of dioxane, which was used to make up the ligand solution, and to maintain consistency with the metal-8-hydroxyquinoline complexation procedure.

Three methods were available for the determination of the stability constants of the metal-ligand complexes:

a) addition of acid to a solution containing the metal-ligand complexes, i.e. decomposing the metal-ligand complexes with acid,
b) addition of a hydroxide solution to a solution containing the metal ion plus protonated ligand, i.e. deprotonating the ligand so that it can then complex with the metal ion, and
c) addition of deprotonated ligand to a solution containing metal ion and protonated ligand.

Method (b) was used for the complexes of 8-hydroxyquinoline due to the hydrolysis of metal ions, the precipitation of the resulting metal-ligand complex at moderate to high p[H] values and the volatility of the ligand solution.

To ensure the reproducibility of results, repeat potentiometric titrations were carried out with fresh stock solutions. Reverse potentiometric titrations were necessary to ascertain that equilibrium had been attained during the titration, since this study entails the investigation of equilibrium systems. The potentiometric titrations were conducted at several metal ion concentrations so that the presence of polynuclear species could be detected.

For the metal-ligand systems the working p[H] was kept fairly low in order to suppress hydrolysis and/or precipitation of the metal-ligand complexes. This was achieved largely by introducing some protonated ligand as part of the background electrolyte. However, this

method of lowering the working p[H] can cause loss of sensitivity if $[M]_t$ is much lower than $[L]_t$. On the other hand, reagent concentrations must not be too high in comparison with the concentration of background electrolyte, as this would cause fluctuations in the ionic strength and resultant changes in activity coefficients. The program HALTA1 (see Section 4.3.1) was therefore used to calculate the ionic strength at each point of the titrations to ensure, if possible, that an approximately constant ionic strength would be maintained.

The concentration levels of all reagents used in this study were at least millimolar, since sub-millimolar concentration levels are prone to experimental error.

Throughout this work the measurements were undertaken in a partially aqueous medium, viz. 0.1 mol dm^{-3} $NaClO_4$ in 60% (v/v) dioxane, and at a temperature of 25°C. This medium was chosen to ensure the solubility of the metal oxinates; and for comparison purposes since similar work is reported in the literature [23]. The background electrolyte was chosen to be $NaClO_4$ because the ClO_4^- anion has no affinity in aqueous solution for Zn^{2+} or Ge^{4+} [42]. Finally, the cation Na^+ has a very low tendency to form complexes. It was therefore hoped that this background electrolyte would have no unwanted effect on the equilibria being studied. The working temperature was chosen to be 25°C because this is the temperature most often used for thermodynamic measurements.

In the potentiometric measurements, the whole assembly was allowed to come to equilibrium over a period of at least 2½ hours after the first addition of calibrating titrant solution. After each subsequent addition of titrant solution, sufficient time was allowed to ensure that the system had come to equilibrium. An equilibration period of 10 to 15 min. was allowed for points in the low p[H] region, whereas for points in the high p[H] region 25 or more minutes were allowed. When successive cell EMF readings differed by less than 3 mV the volume of titrant solution added was doubled.

The actual details of the experiments are given in the following sections. The data collected from the potentiometric experiments are listed in full in Tables 3.8 to 3.10, together with the solution concentrations used. These tables begin with a listing of the concentrations of the components in the titrate solution (denoted $[\ ]_o$) and titrant solution (denoted $[\ ]_T$), and the initial volume (V_o) of the titrate solution. These concentrations and volumes include the dioxane added and the contraction factor. All concentrations are reported in mol dm^{-3}. The cell calibration constants (E^o_{cell} and s) together with the correlation coefficients (denoted r) have also been included, while the concentration of the background electrolyte has been omitted for simplicity. The description of the solutions are followed by a listing of volume of titrant added (V_T), total volume added at that point (V_{TOT}), i.e. ($V_T + V_{dioxane}$) x 0.9803, cell EMF in mV and several derived quantities. These

results will be discussed in Chapter 5.

In this study the data from approximately half the total number of titrations carried out for the protonation of oxine and the complexation of zinc with oxine were rejected, because the early phase of the study involved inappropriately conditioned glass electrodes (see Section 3.2.1) and the cell calibration method entailed the use of dilute solutions of strong base which produced data in the non-linear response region of the glass electrode (see Section 3.2.2), and therefore in retrospect was considered to be inadequate.

3.3.2 PROTONATION OF 8-HYDROXYQUINOLINE

The protonation constants for 8-hydroxyquinoline were determined potentiometrically by the addition of a titrant solution containing hydroxide plus an appropriate volume of dioxane in order to maintain a constant solvent composition of 0.1 mol dm^{-3} $NaClO_4$ in 60% (v/v) dioxane, into a titrate solution containing totally protonated 8-hydroxyquinoline. In these titrations the cell was calibrated by using strong acid and strong base. A mixture of 30.00 cm^3 dioxane, 16.00 cm^3 of a 0.245 mol dm^{-3} $NaClO_4$ solution and 4.00 cm^3 of the 0.1686 mol dm^{-3} NaOH solution was titrated with a solution of 0.09819 mol dm^{-3} $HClO_4$ plus an appropriate volume of dioxane, in order to maintain a constant solvent composition. This NaOH solution was subsequently diluted and used as the titrant in the same titration.

The concentrations of hydroxide and the constants E^{o}_{cell} and s were calculated from the cell potential readings as described in Section 3.2.3. Once the cell had been calibrated, a 6.00 cm^3 aliquot of a standard 0.06537 mol dm^{-3} 8-hydroxyquinoline solution in dioxane and a 4.00 cm^3 aliquot of a 0.245 mol dm^{-3} $NaClO_4$ solution were pipetted into the reaction mixture. The $NaClO_4$ solution was added in order to maintain a constant solvent composition. This was preceded by addition of an aliquot of a 0.09819 mol dm^{-3} $HClO_4$ solution (plus an appropriate volume of dioxane) to ensure the total protonation of oxine. This mixture was then titrated with a 0.045 mol dm^{-3} NaOH solution, i.e. a dilution of the solution whose concentration had been determined in the calibration stage of the experiment. The protonation of oxine was carried out in triplicate. The potentiometric titration data collected are presented in Table 3.8.

3.3.3 COMPLEXATION OF ZINC WITH 8-HYDROXYQUINOLINE

The potentiometric titrations for this system were carried out by adding a titrant solution containing hydroxide plus an appropriate volume of dioxane in order to maintain a constant solvent composition, to a titrate solution containing Zn^{2+} and totally protonated 8-hydroxyquinoline. For these titrations the potentiometric cell was calibrated with strong acid and strong base, as described in Sections 3.2.3 and 3.3.2. The choice of titration method for the complexation of zinc with 8-hydroxyquinoline was determined by the precipitation of zinc 8-

TABLE 3.8

Data obtained for the protonation of oxine.

TITRATION 1

E^{o}_{cell} = 329.2 mV s = 58.18 mV r = 0.9999

$[H^{+}]_{o} = 6.063 \times 10^{-3}$ $[oxine]_{o} = 4.421 \times 10^{-3}$

$[OH^{-}]_{T} = 1.796 \times 10^{-2}$ $[oxine]_{T} = 0$

V_{o} = 88.72 cm^{3}

V_T/cm^3	V_{TOT}/cm^3	EMF/mV	p[H]	$\bar{j}$
0.00	0.00	169.1	2.752	1.97
0.40	0.98	166.3	2.800	1.96
0.80	1.96	163.2	2.853	1.96
1.20	2.94	160.0	2.908	1.95
1.60	3.92	156.6	2.967	1.94
2.00	4.90	153.0	3.029	1.92
2.40	5.88	149.1	3.096	1.91
2.80	6.86	145.0	3.166	1.89
3.20	7.84	140.9	3.237	1.87
3.60	8.82	136.2	3.317	1.85
4.00	9.80	131.9	3.391	1.82
4.40	10.78	127.2	3.472	1.79
4.80	11.76	122.9	3.546	1.76
5.20	12.74	116.1	3.663	1.73
5.60	13.72	111.6	3.740	1.70
6.00	14.70	106.6	3.826	1.66
6.40	15.68	102.7	3.893	1.62
6.80	16.67	98.9	3.959	1.58
7.20	17.65	94.5	4.034	1.54
7.60	18.63	90.2	4.108	1.50
8.00	19.61	85.5	4.189	1.46
8.40	20.59	80.6	4.273	1.41
8.80	21.57	75.8	4.356	1.37
9.20	22.55	70.5	4.447	1.33
9.60	23.53	64.7	4.546	1.29
10.00	24.51	58.3	4.656	1.24
10.40	25.49	50.7	4.787	1.20
10.80	26.47	40.6	4.961	1.16
11.20	27.45	26.4	5.205	1.11
11.60	28.43	2.00	5.624	1.07
12.00	29.41	-233.3	9.668	1.02
12.40	30.39	-274.4	10.38	0.98
12.80	31.37	-290.0	10.64	0.94
13.20	32.35	-300.1	10.82	0.89
13.60	33.33	-308.4	10.96	0.85
14.00	34.31	-315.0	11.07	0.80
14.40	35.29	-321.3	11.18	0.76
14.80	36.27	-326.6	11.27	0.72
15.20	37.25	-331.4	11.36	0.67
15.60	38.23	-336.2	11.44	0.63
16.00	39.21	-340.5	11.51	0.59
16.40	40.19	-344.8	11.59	0.55
16.80	41.17	-348.9	11.66	0.50
17.20	42.15	-352.8	11.72	0.46
17.60	43.13	-356.9	11.79	0.42
18.00	44.11	-360.9	11.86	0.38
18.40	45.09	-365.2	11.94	0.34
18.80	46.07	-369.6	12.01	0.30
19.20	47.05	-374.2	12.09	0.27
19.60	48.03	-378.9	12.17	0.23
20.00	49.02	-383.8	12.26	0.20

TITRATION 2

E^{o}_{cell} = 372.4 mV s = 58.19 mV r = 1.000

$[H^{+}]_{o}$ = 6.813 x 10^{-3} $[oxine]_{o}$ = 4.302 x 10^{-3}

$[OH^{-}]_{T}$ = 1.837 x 10^{-2} $[oxine]_{T}$ = 0

V_{o} = 91.17 cm^{3}

V_T/cm^3	V_{TOT}/cm^3	EMF/mV	p[H]	$\bar{j}$
0.00	0.00	222.8	2.572	1.96
0.80	1.96	218.5	2.645	1.95
2.00	4.90	211.6	2.764	1.93
2.80	6.86	205.7	2.865	1.92
3.60	8.82	199.5	2.972	1.90
4.00	9.80	195.9	3.034	1.89
4.40	10.78	192.4	3.094	1.87
4.80	11.76	188.6	3.159	1.85
5.20	12.74	184.9	3.223	1.83
5.60	13.72	180.7	3.295	1.81
6.00	14.70	176.0	3.376	1.78
6.40	15.68	168.7	3.501	1.76
6.80	16.67	164.4	3.575	1.73
7.20	17.65	160.2	3.647	1.69
7.60	18.63	156.0	3.719	1.66
8.00	19.61	152.2	3.785	1.62
8.40	20.59	148.2	3.853	1.58
8.80	21.57	144.3	3.921	1.54
9.20	22.55	139.5	4.003	1.50
9.60	23.53	135.3	4.075	1.46
10.00	24.51	131.1	4.147	1.41
10.40	25.49	126.6	4.225	1.37
10.80	26.47	121.9	4.305	1.33
11.20	27.45	116.9	4.391	1.29
11.60	28.43	111.0	4.493	1.24
12.00	29.41	104.8	4.599	1.20
12.40	30.39	97.6	4.723	1.15
12.80	31.37	88.8	4.874	1.11
13.20	32.35	76.8	5.080	1.07
13.60	33.33	57.8	5.407	1.02
14.00	34.31	-11.8	6.603	0.98
14.40	35.29	-212.9	10.06	0.93
14.80	36.27	-237.0	10.47	0.89
15.20	37.25	-250.7	10.71	0.84
15.60	38.23	-260.3	10.87	0.80
16.00	39.21	-268.1	11.01	0.75
16.40	40.19	-274.5	11.12	0.71
16.80	41.17	-280.2	11.22	0.66
17.20	42.15	-285.2	11.30	0.62
17.60	43.13	-289.8	11.38	0.57
18.00	44.11	-294.4	11.46	0.53
18.40	45.09	-298.6	11.53	0.49
18.80	46.07	-302.7	11.60	0.44
19.20	47.05	-307.0	11.68	0.40
19.60	48.03	-311.2	11.75	0.36
20.00	49.02	-315.4	11.82	0.32
20.40	50.00	-319.6	11.89	0.27
20.80	50.98	-323.8	11.96	0.23
21.20	51.96	-328.2	12.04	0.20
21.60	52.94	-332.7	12.12	0.16
22.00	53.92	-337.1	12.19	0.12
22.40	54.90	-341.8	12.27	0.09
22.80	55.88	-346.8	12.36	0.07

TITRATION 3

E^{o}_{cell} = 372.4 mV s = 58.19 mV r = 1.000

$[H^{+}]_{o}$ = 6.726 x 10^{-3} $[oxine]_{o}$ = 4.302 x 10^{-3}

$[OH^{-}]_{T}$ = 1.858 x 10^{-2} $[oxine]_{T}$ = 0

V_{o} = 91.17 cm^{3}

V_T/cm^3	V_{TOT}/cm^3	EMF/mV	p[H]	$\bar{j}$
0.00	0.00	172.7	2.620	2.00
0.80	1.96	168.1	2.700	2.00
1.60	3.92	162.1	2.793	1.99
2.00	4.90	159.8	2.843	1.98
2.40	5.88	156.7	2.897	1.97
2.80	6.86	153.8	2.947	1.96
3.20	7.84	150.3	3.007	1.94
3.60	8.82	146.7	3.069	1.93
4.00	9.80	143.1	3.131	1.91
4.40	10.78	139.6	3.192	1.89
4.80	11.76	135.9	3.256	1.86
5.20	12.74	132.0	3.323	1.83
5.60	13.72	128.0	3.392	1.80
6.00	14.70	124.0	3.461	1.77
6.40	15.68	119.8	3.534	1.74
6.80	16.67	115.6	3.606	1.71
7.20	17.65	111.2	3.682	1.67
7.60	18.63	107.0	3.755	1.63
8.00	19.61	103.2	3.820	1.59
8.40	20.59	99.1	3.891	1.55
8.80	21.57	95.2	3.959	1.51
9.20	22.55	90.7	4.036	1.47
9.60	23.53	86.3	4.112	1.43
10.00	24.51	82.0	4.187	1.38
10.40	25.49	77.4	4.266	1.34
10.80	26.47	72.6	4.349	1.30
11.20	27.45	67.2	4.442	1.25
11.60	28.43	61.1	4.548	1.21
12.00	29.41	54.4	4.663	1.16
12.40	30.39	46.6	4.798	1.12
12.80	31.37	36.7	4.696	1.07
13.20	32.35	22.8	5.209	1.03
13.60	33.33	-5.1	5.691	0.98
14.00	34.31	-221.8	9.433	0.94
14.40	35.29	-269.6	10.26	0.89
14.80	36.27	-289.4	10.60	0.85
15.20	37.25	-300.8	10.80	0.80
15.60	38.23	-309.5	10.95	0.76
16.00	39.21	-316.2	11.06	0.71
16.40	40.19	-322.2	11.17	0.66
16.80	41.17	-327.7	11.26	0.62
17.20	42.15	-332.8	11.35	0.57
17.60	43.13	-337.2	11.43	0.53
18.00	44.11	-341.3	11.50	0.49
18.40	45.09	-345.4	11.57	0.44
18.80	46.07	-349.4	11.64	0.35
19.20	47.05	-353.2	11.70	0.31
19.60	48.03	-357.0	11.77	0.27
20.00	49.02	-360.8	11.83	0.23
20.40	50.00	-364.8	11.90	0.19
20.80	50.98	-368.6	11.97	0.15
21.20	51.96	-372.5	12.04	0.11
21.60	52.94	-376.4	12.10	0.07
22.00	53.92	-380.6	12.18	0.04

hydroxyquinolate dihydrate at p[H] ≈ 3.6.

In all the titrations neither the metal ion concentration nor that of the ligand was kept constant. Two titrations (nos 1 and 3) were carried out in duplicate in order to check the reproducibility of the results obtained. The repeat titrations were 5 and 7. A limited number of points were collected during a titration due to precipitation at p[H] ≈ 3.6, and this influenced the decision of not conducting a reverse titration. The initial concentrations of Zn^{2+} and oxine were varied within the limits $2.1x10^{-3} \leq [Zn^{2+}]_o \leq 6.0x10^{-3}$ mol dm^{-3} and $1.8x10^{-2} \leq [oxine]_o \leq 2.1x10^{-2}$ mol dm^{-3}. The following initial metal to ligand ratios were studied: 1:3, 1:5, 1:6, 1:7.5 and 1:10. The potentiometric titration data collected in this work are presented in Table 3.9.

3.3.4 ANALYSIS OF THE ZINC 8-HYDROXYQUINOLATE PRECIPITATE

8-Hydroxyquinoline is known to precipitate zinc quantitatively as a greenish-yellow, crystalline precipitate [96] in the p[H] range 3.3 to 4.4 [11]. This precipitate has the formula $Zn(C_9H_6ON)_2$, viz. zinc 8-hydroxyquinolate, and is used for the gravimetric determination of zinc [4].

The precipitate obtained from the potentiometric titrations, referred to as the experimental precipitate in this work, was analysed by comparison with the zinc 8-hydroxyquinolate synthesized

TABLE 3.9

Data obtained for the complexation of zinc with 8-hydroxyquinoline.

TITRATION 1

E^{o}_{cell} = 371.5 mV s = 58.35 mV r = 0.9999

$[H^{+}]_{o}$ = 2.205 x 10^{-2}, $[Zn^{2+}]_{o}$ = 2.139 x 10^{-3},

$[oxine]_{o}$ = 2.087 x 10^{-2},

$[OH^{-}]_{T}$ = 6.955 x 10^{-2}, $[Zn^{2+}]_{T}$ = 0, $[oxine]_{T}$ = 0,

V_{o} = 107.83 cm^{3}

V_T/cm^3	V_{TOT}/cm^3	EMF/mV	p[H]	-log[L]	$\bar{Z}$
0.00	0.00	217.2	2.645	11.96	0.06
0.40	0.98	212.4	2.728	11.80	0.09
0.80	1.96	207.5	2.812	11.65	0.12
1.20	2.94	202.7	2.894	11.49	0.15
1.60	3.92	197.8	2.978	11.34	0.19
2.00	4.90	193.2	3.057	11.19	0.23
2.40	5.88	189.0	3.129	11.06	0.27
2.80	6.86	185.1	3.195	10.94	0.33
3.20	7.84	181.5	3.257	10.83	0.38
3.60	8.82	178.2	3.314	10.73	0.44
4.00	9.80	174.9	3.370	10.64	0.49
4.40	10.78	171.9	3.422	10.55	0.55
5.00	12.25	167.8	3.492	10.43	0.65
5.60	13.72	163.9	3.559	10.32	0.75

TITRATION 2

E^{o}_{cell} = 330.0 mV s = 58.11 mV r = 0.9999

$[H^+]_o = 2.155 \times 10^{-2}$, $[Zn^{2+}]_o = 2.789 \times 10^{-3}$,

$[oxine]_o = 2.040 \times 10^{-2}$,

$[OH^-]_T = 6.966 \times 10^{-2}$, $[Zn^{2+}]_T = 0$, $[oxine]_T = 0$,

V_o = 110.28 cm^3

V_T/cm^3	V_{TOT}/cm^3	EMF/mV	p[H]	-log[L]	$\bar{Z}$
0.00	0.00	174.9	2.668	11.92	0.03
0.40	0.98	170.3	2.747	11.77	0.05
0.80	1.96	165.7	2.827	11.63	0.08
1.20	2.94	161.0	2.907	11.47	0.11
1.60	3.92	156.6	2.983	11.33	0.14
2.00	4.90	152.2	3.059	11.20	0.17
2.40	5.88	148.1	3.129	11.07	0.21
2.80	6.86	144.4	3.193	10.95	0.25
3.20	7.84	141.0	3.252	10.85	0.30
3.60	8.82	137.8	3.307	10.76	0.34
4.00	9.80	134.7	3.360	10.66	0.39
4.60	11.27	130.5	3.432	10.54	0.47
5.20	12.74	126.5	3.501	10.43	0.54
6.20	15.19	120.3	3.608	10.26	0.67

TITRATION 3

E^{o}_{cell} = 369.4 mV s = 58.10 mV r = 1.000

$[H^+]_o = 2.105 \times 10^{-2}$, $[Zn^{2+}]_o = 3.410 \times 10^{-3}$,

$[oxine]_o = 1.996 \times 10^{-2}$,

$[OH^-]_T = 7.009 \times 10^{-2}$, $[Zn^{2+}]_T = 0$, $[oxine]_T = 0$,

V_o = 112.73 cm^3

V_T/cm^3	V_{TOT}/cm^3	EMF/mV	p[H]	-log[L]	$\bar{Z}$
0.00	0.00	215.6	2.648	11.98	0.06
0.40	0.98	211.3	2.722	11.84	0.08
0.80	1.96	206.8	2.800	11.69	0.10
1.20	2.94	202.2	2.879	11.54	0.12
1.60	3.92	197.9	2.953	11.41	0.15
2.00	4.90	194.0	3.020	11.28	0.19
2.40	5.88	190.2	3.085	11.16	0.22
2.80	6.86	186.7	3.146	11.06	0.26
3.20	7.84	183.3	3.204	10.95	0.30
3.60	8.82	180.3	3.256	10.86	0.34
4.20	10.29	176.0	3.330	10.74	0.41
4.80	11.76	172.1	3.397	10.63	0.48
5.40	13.23	168.4	3.460	10.52	0.55
6.00	14.70	165.2	3.516	10.44	0.63

TITRATION 4

E^{o}_{cell} = 329.5 mV s = 58.05 mV r = 0.9999

$[H^+]_o = 1.905 \times 10^{-2}$, $[Zn^{2+}]_o = 6.151 \times 10^{-3}$,

$[oxine]_o = 1.800 \times 10^{-2}$,

$[OH^-]_T = 6.931 \times 10^{-2}$, $[Zn^{2+}]_T = 0$, $[oxine]_T = 0$,

V_o = 124.99 cm^3

V_T/cm^3	V_{TOT}/cm^3	EMF/mV	p[H]	-log[L]	$\bar{Z}$
0.40	0.98	173.7	2.684	11.96	0.07
0.80	1.96	169.7	2.753	11.83	0.08
1.20	2.94	165.8	2.820	11.71	0.09
1.60	3.92	162.1	2.884	11.59	0.11
2.00	4.90	158.5	2.946	11.47	0.13
2.40	5.88	155.0	3.006	11.36	0.15
2.80	6.86	151.8	3.061	11.27	0.17
3.20	7.84	148.8	3.113	11.17	0.19
3.80	9.31	144.7	3.183	11.05	0.23
4.40	10.78	140.9	3.249	10.94	0.27
5.00	12.25	137.4	3.309	10.84	0.31
5.60	13.72	134.1	3.366	10.75	0.35
6.20	15.19	131.1	3.418	10.67	0.39
7.00	17.16	127.0	3.488	10.55	0.45

TITRATION 5

E^{o}_{cell} = 328.9 mV s = 57.98 mV r = 0.9999

$[H^+]_o = 2.221 \times 10^{-2}$, $[Zn^{2+}]_o = 2.139 \times 10^{-3}$,

$[oxine]_o = 2.087 \times 10^{-2}$,

$[OH^-]_T = 6.782 \times 10^{-2}$, $[Zn^{2+}]_T = 0$, $[oxine]_T = 0$,

V_o = 107.83 cm^3

V_T/cm^3	V_{TOT}/cm^3	EMF/mV	p[H]	-log[L]	$\bar{Z}$
0.00	0.00	176.5	2.628	11.99	0.05
0.40	0.98	171.8	2.709	11.84	0.07
0.80	1.96	167.0	2.792	11.68	0.10
1.20	2.94	162.1	2.876	11.52	0.13
1.60	3.92	157.5	2.956	11.38	0.17
2.00	4.90	153.1	3.032	11.24	0.21
2.40	5.88	148.9	3.104	11.10	0.25
2.80	6.86	145.0	3.171	10.98	0.30
3.20	7.84	141.4	3.233	10.87	0.35
3.60	8.82	137.9	3.294	10.77	0.40
4.00	9.80	134.8	3.347	10.68	0.46
4.60	11.27	130.4	3.423	10.55	0.54
5.20	12.74	126.4	3.492	10.43	0.64
5.80	14.21	122.4	3.561	10.32	0.72
6.40	15.68	118.6	3.627	10.22	0.81

TITRATION 6

E^{o}_{cell} = 328.8 mV s = 58.10 mV r = 0.9999

$[H^+]_o = 2.068 \times 10^{-2}$, $[Zn^{2+}]_o = 4.005 \times 10^{-3}$,

$[oxine]_o = 1.953 \times 10^{-2}$,

$[OH^-]_T = 6.918 \times 10^{-2}$, $[Zn^{2+}]_T = 0$, $[oxine]_T = 0$,

V_o = 115.19 cm^3

V_T/cm^3	V_{TOT}/cm^3	EMF/mV	p[H]	-log[L]	$\bar{Z}$
0.00	0.00	175.8	2.633	12.02	0.06
0.40	0.98	171.3	2.710	11.87	0.07
0.80	1.96	166.9	2.786	11.73	0.09
1.20	2.94	162.2	2.867	11.57	0.10
1.60	3.92	158.0	2.939	11.44	0.13
2.00	4.90	154.0	3.008	11.31	0.15
2.40	5.88	150.2	3.074	11.20	0.18
2.80	6.86	146.6	3.136	11.08	0.21
3.20	7.84	143.3	3.192	10.98	0.24
3.60	8.82	140.1	3.247	10.89	0.28
4.20	10.29	135.9	3.320	10.76	0.33
4.80	11.76	131.9	3.389	10.65	0.39
5.40	13.23	128.3	3.450	10.55	0.45
6.00	14.70	124.8	3.511	10.45	0.50
6.60	16.18	121.8	3.562	10.37	0.57

TITRATION 7

E^{o}_{cell} = 327.5 mV s = 57.90 mV r = 1.000

$[H^+]_o = 2.102 \times 10^{-2}$, $[Zn^{2+}]_o = 3.410 \times 10^{-3}$,

$[oxine]_o = 2.000 \times 10^{-2}$,

$[OH^-]_T = 7.044 \times 10^{-2}$, $[Zn^{2+}]_T = 0$, $[oxine]_T = 0$,

V_o = 112.73 cm^3

V_T/cm^3	V_{TOT}/cm^3	EMF/mV	p[H]	-log[L]	$\bar{Z}$
0.00	0.00	172.7	2.673	11.92	0.04
0.40	0.98	168.2	2.751	11.78	0.06
0.80	1.96	163.8	2.827	11.64	0.08
1.20	2.94	159.4	2.903	11.49	0.11
1.60	3.92	155.1	2.977	11.36	0.14
2.00	4.90	151.0	3.048	11.23	0.17
2.40	5.88	147.2	3.114	11.11	0.20
2.80	6.86	143.8	3.172	11.00	0.24
3.20	7.84	140.3	3.233	10.90	0.28
3.60	8.82	137.2	3.286	10.81	0.32
4.20	10.29	132.9	3.361	10.68	0.38
4.80	11.76	128.9	3.430	10.56	0.45
5.40	13.23	125.0	3.497	10.45	0.52
6.00	14.70	121.5	3.557	10.36	0.59
6.60	16.18	118.3	3.613	10.27	0.66

according to Vogel [97], and referred to as the synthetic precipitate in this work. The method of preparation of the synthetic precipitate is briefly described below. A solution containing 5.0 g of sodium acetate and 3.81 cm^3 of glacial acetic acid was made up to 100 cm^3 with water. A mass of 0.18 g of ZnO, i.e. 0.15 g of zinc, was added to this solution and heated to 60°C. The solution was then treated with a slight excess of a 2% solution of oxine in 95% ethanol, boiled for a few minutes, filtered and washed with hot water.

A comparison of the composition of the precipitates obtained from the potentiometric titrations and that from the synthesis described above was carried out by subjecting each precipitate to elemental analysis (recorded on a PERKIN ELMER CHN ANALYSER), uv (recorded on a VARIAN DMS 300 UV VISIBLE SPECTROPHOTOMETER), ir (recorded on a PYE UNICAM SP3-300 INFRARED SPECTROPHOTOMETER), em (recorded on a JEOL JSM 35 Scanning Electron Microscope fitted with a KEVEX 7000/77 energy dispersive x-ray analysis system), proton and ^{13}C nmr (recorded on a VARIAN GEMINI 200 mHz SPECTROMETER) and mass (recorded on a FINNIGAN-1020 GCMS) spectroscopy.

The precipitates were also titrated by a method described by Vogel [98] that reveals the number of oxine molecules attached to the metal ion. This titration entailed dissolving an accurate amount of the precipitate in warm concentrated hydrochloric acid (HCl) followed by the addition of a few drops of

indicator (0.1% solution of the sodium salt of methyl red) and 0.75 g of pure potassium bromide (KBr). The solution was then titrated slowly with standard 0.05 mol dm^{-3} potassium bromate solution ($KBrO_3$) until a pure yellow colour was observed. A slight excess of the standard $KBrO_3$ solution was added to ensure that free bromine was present, and this was tested for by removing a drop of the liquid on to potassium iodide starch paper, which turned black thus indicating a positive result. The solution was diluted with about 7.0 cm^3 of a 2 mol dm^{-3} HCl solution (to prevent the precipitation of 5,7-dibromo-8-hydroxyquinoline during the titration). After 5 min. 10 cm^3 of a 10% potassium iodide solution (KI) was added and the liberated iodine was titrated with a standard 0.02 mol dm^{-3} sodium thiosulphate ($Na_2S_2O_3$) solution, using starch as the indicator.

The analysis of the results obtained will be discussed in Section 5.3.

3.3.5 COMPLEXATION OF GERMANIUM WITH 8-HYDROXYQUINOLINE

The potentiometric titrations for this system were carried out by adding a titrant solution containing hydroxide plus an appropriate volume of dioxane (in order to maintain a constant solvent composition) to a titrate solution containing Ge^{4+} and totally protonated oxine. For these titrations the potentiometric cell was calibrated with strong acid

and strong base, as described in Sections 3.2.3 and 3.3.2.

In all the titrations neither the metal ion concentration nor that of the ligand was kept constant. Two titrations (nos 1 and 2) were carried out in duplicate in order to check the reproducibility of the results obtained. The repeat titrations were nos 4 and 5. The initial concentrations of Ge^{4+} and oxine were varied within the limits $1.9 \times 10^{-3} \leq [Ge^{4+}]_o \leq 2.1 \times 10^{-3}$ mol dm^{-3} and $4.3 \times 10^{-3} \leq [oxine]_o \leq 1.2 \times 10^{-2}$ mol dm^{-3}. The following initial metal to ligand ratios were studied: 1:2, 1:4 and 1:6. The potentiometric titration data collected in this work are presented in Table 3.10.

TABLE 3.10

Data obtained for the complexation of germanium with 8-hydroxyquinoline.

TITRATION 1

E^{o}_{cell} = 330.4 mV s = 57.98 mV r = 0.9999

$[H^{+}]_{o} = 5.379 \times 10^{-3}$, $[Ge^{4+}]_{o} = 2.027 \times 10^{-3}$,

$[oxine]_{o} = 4.107 \times 10^{-3}$,

$[OH^{-}]_{T} = 2.075 \times 10^{-2}$, $[Ge^{4+}]_{T} = 0$, $[oxine]_{T} = 0$,

V_{o} = 116.53 cm^3

V_T/cm^3	V_{TOT}/cm^3	EMF/mV	p[H]	-log[L]	$\bar{Z}$
2.00	4.90	150.3	3.105	11.79	0.00
2.40	5.88	147.0	3.162	11.69	0.00
2.80	6.86	143.7	3.219	11.59	0.01
3.20	7.84	140.2	3.280	11.48	0.02
3.60	8.82	136.6	3.342	11.37	0.03
4.00	9.80	133.1	3.402	11.27	0.04
4.40	10.78	129.4	3.466	11.16	0.04
4.80	11.76	125.7	3.530	11.05	0.05
5.20	12.74	122.0	3.594	10.94	0.06
5.60	13.72	118.6	3.652	10.84	0.07
6.00	14.70	115.0	3.714	10.74	0.07
6.40	15.68	111.3	3.778	10.64	0.08
6.80	16.67	107.6	3.842	10.54	0.08
7.20	17.65	104.0	3.904	10.45	0.09
7.60	18.63	100.1	3.971	10.35	0.09
8.00	19.61	96.4	4.035	10.25	0.09
8.40	20.59	92.3	4.106	10.15	0.09
8.80	21.57	88.0	4.180	10.05	0.09
9.20	22.55	83.5	4.257	9.941	0.09
9.60	23.53	78.6	4.342	9.829	0.09
10.00	24.51	73.5	4.430	9.716	0.08
10.40	25.49	67.5	4.533	9.587	0.08
10.80	26.47	60.2	4.659	9.434	0.06
11.20	27.45	51.9	4.802	9.268	0.06
11.60	28.43	40.2	5.004	9.041	0.04
12.00	29.41	22.1	5.316	8.707	0.03
12.40	30.39	-43.1	6.441	7.563	0.02
12.80	31.37	-231.5	9.690	4.332	0.07
13.20	32.35	-253.0	10.06	3.984	0.12
13.60	33.33	-260.3	10.19	3.882	0.19
14.00	34.31	-268.6	10.33	3.763	0.25
14.40	35.29	-275.8	10.45	3.665	0.31

TITRATION 2

E^{o}_{cell} = 367.3 mV s = 58.26 mV r = 1.000

$[H^{+}]_{o}$ = 1.355 x 10^{-2}, $[Ge^{4+}]_{o}$ = 1.908 x 10^{-3},

$[oxine]_{o}$ = 1.192 x 10^{-2},

$[OH^{-}]_{T}$ = 3.724 x 10^{-2}, $[Ge^{4+}]_{T}$ = 0, $[oxine]_{T}$ = 0,

V_{o} = 118.96 cm^{3}

V_T/cm^3	V_{TOT}/cm^3	EMF/mV	p[H]	-log[L]	$\bar{Z}$
0.00	0.00	213.0	2.647	12.20	0.04
0.40	0.98	209.9	2.700	12.10	0.04
0.80	1.96	206.9	2.752	12.00	0.05
1.20	2.94	203.9	2.803	11.91	0.07
1.60	3.92	200.9	2.855	11.81	0.08
2.00	4.90	197.7	2.910	11.71	0.10
2.40	5.88	194.6	2.963	11.61	0.12
2.80	6.86	191.4	3.018	11.51	0.14
3.20	7.84	188.2	3.073	11.41	0.16
3.60	8.82	185.2	3.124	11.32	0.18
4.00	9.80	182.2	3.176	11.23	0.20
4.40	10.78	179.2	3.227	11.14	0.22
4.80	11.76	176.0	3.282	11.04	0.24
5.60	13.72	170.7	3.373	10.88	0.29
6.00	14.70	167.9	3.421	10.80	0.32
6.80	16.67	162.6	3.512	10.65	0.36
7.40	18.14	158.8	3.577	10.54	0.39
8.00	19.61	154.9	3.644	10.43	0.41
8.60	21.08	151.1	3.710	10.32	0.44
9.20	22.55	147.2	3.776	10.22	0.45
9.80	24.02	143.3	3.843	10.11	0.46
10.40	25.49	139.5	3.909	10.02	0.48
11.00	26.96	135.6	3.976	9.916	0.48
11.60	28.43	131.4	4.048	9.811	0.48
12.20	29.90	127.3	4.118	9.712	0.48
12.80	31.37	122.8	4.195	9.604	0.47
13.20	32.35	119.8	4.247	9.535	0.46
13.60	33.33	116.4	4.305	9.456	0.44
14.00	34.31	113.2	4.360	9.385	0.44
14.40	35.29	109.4	4.425	9.301	0.42
14.80	36.27	105.5	4.492	9.217	0.40
15.20	37.25	101.2	4.566	9.126	0.38
15.60	38.23	96.4	4.648	9.027	0.35
16.00	39.21	90.9	4.743	8.916	0.32
16.40	40.19	84.3	4.856	8.787	0.29
16.80	41.17	76.0	4.999	8.628	0.25
17.20	42.15	65.7	5.175	8.437	0.23
17.60	43.13	47.8	5.483	8.114	0.19
18.00	44.11	-12.6	6.519	7.064	0.16
18.40	45.09	-200.6	9.746	3.848	0.19
18.80	46.07	-223.1	10.13	3.477	0.21
19.20	47.05	-234.7	10.33	3.292	0.24
19.60	48.03	-242.9	10.47	3.167	0.28
20.00	49.02	-249.7	10.59	3.065	0.30
20.40	50.00	-255.4	10.69	2.983	0.32
20.80	50.98	-260.1	10.77	2.919	0.35
21.20	51.96	-264.2	10.84	2.865	0.39
21.60	52.94	-267.8	10.90	2.821	0.43
22.00	53.92	-271.0	10.95	2.783	0.48
22.40	54.90	-274.2	11.01	2.746	0.52
23.00	56.37	-278.0	11.08	2.709	0.63
23.60	57.84	-282.2	11.15	2.667	0.70
24.20	59.31	-285.8	11.21	2.637	0.80
25.00	61.27	-290.4	11.29	2.602	0.95

TITRATION 3

E^{o}_{cell} = 324.006 mV s = 57.9169 mV r = 1.000

$[H^{+}]_{o}$ = 9.775 x 10^{-3}, $[Ge^{4+}]_{o}$ = 1.990 x 10^{-3},

$[oxine]_{o}$ = 8.299 x 10^{-3},

$[OH^{-}]_{T}$ = 2.925 x 10^{-2}, $[Ge^{4+}]_{T}$ = 0, $[oxine]_{T}$ = 0,

V_{o} = 114.06 cm^{3}

V_T/cm^3	V_{TOT}/cm^3	EMF/mV	p[H]	-log[L]	$\bar{Z}$
0.00	0.00	166.6	2.718	12.22	0.02
0.40	0.98	163.5	2.771	12.12	0.02
1.00	2.45	159.2	2.846	11.98	0.03
1.60	3.92	154.4	2.928	11.83	0.04
2.20	5.39	149.6	3.011	11.67	0.06
2.80	6.86	144.8	3.094	11.52	0.08
3.40	8.33	139.8	3.181	11.37	0.10
4.00	9.80	135.2	3.260	11.23	0.12
4.60	11.27	130.2	3.346	11.07	0.14
5.20	12.74	125.7	3.424	10.94	0.17
5.80	14.21	121.3	3.500	10.81	0.19
6.40	15.68	117.0	3.574	10.69	0.21
7.00	17.16	112.8	3.647	10.57	0.23
7.60	18.63	108.5	3.721	10.45	0.25
8.20	20.10	104.1	3.797	10.33	0.26
8.80	21.57	99.8	3.871	10.22	0.27
9.40	23.04	95.5	3.945	10.11	0.28
10.00	24.51	91.2	4.020	9.998	0.29
10.60	25.98	86.7	4.097	9.888	0.30
11.20	27.45	81.8	4.182	9.770	0.29
11.80	28.92	76.6	4.272	9.649	0.28
12.40	30.39	71.1	4.367	9.525	0.28
12.80	31.37	67.0	4.437	9.434	0.27
13.20	32.35	62.5	4.515	9.337	0.26
13.60	33.33	57.5	4.602	9.232	0.25
14.00	34.31	52.1	4.695	9.123	0.24
14.40	35.29	45.4	4.810	8.989	0.22
14.80	36.27	37.6	4.945	8.839	0.21
15.20	37.25	27.2	5.125	8.644	0.20
15.60	38.23	8.9	5.441	8.311	0.17
16.00	39.21	-43.3	6.342	7.397	0.16
16.40	40.19	-242.2	9.776	3.975	0.20
16.80	41.17	-265.3	10.18	3.593	0.22
17.20	42.15	-277.5	10.39	3.400	0.24
17.60	43.13	-286.1	10.53	3.269	0.27
18.00	44.11	-292.2	10.64	3.182	0.31
18.40	45.09	-297.6	10.73	3.108	0.35
18.80	46.07	-302.1	10.81	3.050	0.39
19.20	47.05	-306.2	10.88	2.999	0.43
19.60	48.03	-309.9	10.95	2.956	0.48
20.00	49.02	-313.5	11.01	2.916	0.52

TITRATION 4

E^{o}_{cell} = 330.5 mV s = 58.07 mV r = 0.9999

$[H^{+}]_{o}$ = 5.852 x 10^{-3}, $[Ge^{4+}]_{o}$ = 2.079 x 10^{-3},

$[oxine]_{o}$ = 4.316 x 10^{-3},

$[OH^{-}]_{T}$ = 2.047 x 10^{-2}, $[Ge^{4+}]_{T}$ = 0, $[oxine]_{T}$ = 0,

V_{o} = 109.16 cm^{3}

V_T/cm^3	V_{TOT}/cm^3	EMF/mV	p[H]	-log[L]	$\bar{Z}$
0.60	1.47	166.6	2.822	12.30	0.00
1.20	2.94	162.5	2.893	12.17	0.01
1.80	4.41	157.7	2.976	12.02	0.01
2.40	5.88	152.8	3.060	11.87	0.02
3.00	7.35	147.6	3.150	11.70	0.03
3.40	8.33	143.8	3.215	11.58	0.03
3.80	9.31	140.2	3.277	11.47	0.04
4.20	10.29	136.3	3.344	11.36	0.04
4.60	11.27	132.5	3.410	11.24	0.05
5.00	12.25	128.9	3.472	11.13	0.06
5.40	13.23	125.1	3.537	11.02	0.07
5.80	14.21	121.3	3.602	10.91	0.07
6.20	15.19	117.7	3.664	10.81	0.08
6.60	16.18	114.0	3.728	10.71	0.09
7.00	17.16	110.3	3.792	10.61	0.09
7.40	18.14	106.6	3.856	10.51	0.10
7.80	19.12	103.1	3.916	10.42	0.10
8.20	20.10	99.1	3.985	10.32	0.11
8.60	21.08	95.2	4.052	10.22	0.11
9.00	22.06	91.2	4.121	10.12	0.11
9.40	23.04	86.8	4.196	10.02	0.11
9.80	24.02	82.2	4.276	9.908	0.11
10.20	25.00	77.5	4.357	9.802	0.11
10.60	25.98	71.7	4.456	9.673	0.10
11.00	26.96	65.5	4.563	9.541	0.09
11.40	27.94	57.7	4.698	9.379	0.08
11.80	28.92	48.1	4.863	9.189	0.07
12.20	29.90	34.9	5.090	8.938	0.05
12.60	30.88	9.80	5.522	8.483	0.04
13.00	31.86	-208.7	9.285	4.714	0.05
13.40	32.84	-246.9	9.943	4.079	0.09
13.80	33.82	-261.1	10.19	3.857	0.15
14.20	34.80	-269.2	10.33	3.742	0.21
14.60	35.78	-277.1	10.46	3.631	0.26
15.00	36.76	-283.6	10.58	3.546	0.32

TITRATION 5

E^{o}_{cell} = 367.2 mV s = 58.15 mV r = 1

$[H^{+}]_{o}$ = 1.356 x 10^{-2}, $[Ge^{4+}]_{o}$ = 1.908 x 10^{-3},

$[oxine]_{o}$ = 1.192 x 10^{-2},

$[OH^{-}]_{T}$ = 3.724 x 10^{-2}, $[Ge^{4+}]_{T}$ = 0, $[oxine]_{T}$ = 0,

V_{o} = 118.96 cm^{3}

V_T/cm^3	V_{TOT}/cm^3	EMF/mV	p[H]	-log[L]	$\bar{Z}$
0.00	0.00	212.9	2.653	12.19	0.03
0.60	1.47	208.6	2.727	12.05	0.04
1.20	2.94	204.1	2.805	11.90	0.06
1.80	4.41	199.6	2.882	11.76	0.09
2.40	5.88	195.0	2.961	11.62	0.12
3.00	7.35	190.3	3.042	11.47	0.15
3.60	8.82	185.5	3.124	11.32	0.18
4.20	10.29	181.2	3.198	11.19	0.22
4.80	11.76	176.9	3.272	11.06	0.25
5.40	13.23	172.8	3.343	10.94	0.29
6.00	14.70	168.9	3.410	10.82	0.33
6.60	16.18	164.8	3.480	10.70	0.36
7.20	17.65	161.1	3.544	10.60	0.39
7.80	19.12	157.4	3.608	10.49	0.43
8.40	20.59	153.6	3.673	10.39	0.45
9.00	22.06	149.9	3.737	10.28	0.48
9.60	23.53	146.0	3.804	10.18	0.49
10.20	25.00	142.3	3.867	10.08	0.51
10.80	26.47	138.5	3.933	9.984	0.52
11.40	27.94	134.6	4.000	9.886	0.53
12.00	29.41	130.8	4.065	9.793	0.54
12.60	30.88	126.6	4.137	9.691	0.54
13.20	32.35	122.3	4.211	9.590	0.54
13.80	33.82	117.5	4.294	9.479	0.52
14.40	35.29	112.5	4.380	9.367	0.51
14.80	36.27	108.7	4.445	9.284	0.49
15.20	37.25	104.7	4.514	9.198	0.47
15.60	38.23	100.5	4.586	9.111	0.46
16.00	39.21	96.0	4.663	9.019	0.45
16.40	40.19	90.0	4.767	8.898	0.42
16.80	41.17	83.6	4.877	8.774	0.40
17.20	42.15	75.8	5.011	8.626	0.38
17.60	43.13	64.8	5.200	8.422	0.35
18.00	44.11	48.2	5.485	8.124	0.33
18.40	45.09	-2.5	6.357	7.241	0.31
18.80	46.07	-198.4	9.726	3.882	0.35
19.20	47.05	-221.2	10.12	3.505	0.38
19.60	48.03	-233.4	10.33	3.310	0.41
20.00	49.02	-242.0	10.48	3.178	0.43
20.40	50.00	-249.1	10.60	3.071	0.45
20.80	50.98	-255.3	10.70	2.981	0.46
21.20	51.96	-259.8	10.78	2.920	0.50
21.60	52.94	-264.0	10.85	2.865	0.53
22.00	53.92	-267.5	10.91	2.822	0.58
22.60	55.39	-272.7	11.00	2.760	0.63
23.20	56.86	-277.0	11.08	2.715	0.71
23.80	58.33	-281.0	11.15	2.676	0.80
24.40	59.80	-284.7	11.21	2.644	0.89
25.00	61.27	-288.2	11.27	2.618	1.00

CHAPTER 4

CALCULATION TECHNIQUES

This chapter outlines the Gran plot method for equivalence point determination in potentiometric titrations; the derivation of formation curves from potentiometric data and the various computer programs employed to analyse these data.

4.1. GRAN PLOTS

Gran plots provide an accurate determination of the equivalence point of a potentiometric titration. This equivalence point can be determined from the point of inflection of the titration curve (a plot of the cell EMF (E) as a function of the volume (V) of titrant added). When there is only a small potential change at the end-point, e.g. in the titration of weak acids by strong bases, the equivalence point is usually determined from the peak of the 'differential curve' ($\Delta E/\Delta V$ as a function of the volume of titrant added) or the zero value point of the 'second derivative curve' ($\Delta^2 E/\Delta V^2$ plotted as a function of the volume of titrant). These methods do not use the data points which are far from the equivalence point and the results obtained may be erroneous if the titration curve is not symmetrical about the equivalence point.

Gran [99,100] devised a method of linearising the titration curve such that all the points in the titration are used, rather than just those in the

region of the equivalence point. The Gran [99-102] method entails linearising the titration curve by calculating functions ϕ and ϕ' (derived below) from the titration data which give straight lines that can be extrapolated to the equivalence point when plotted against the volume of titrant. The Gran plot method can be applied to potentiometric titrations involving acids, bases, ionic precipitates, complex formation and oxidation-reduction reactions.

In this study the Gran plot method was used for the standardisation of the strong base solutions and the quantitation of any carbonate contamination. The method of titrating a strong base with a strong acid was used and is described below. All titrations were carried out in a partially aqueous medium, viz. 0.1 mol dm^{-3} $NaClO_4$ in 60% (v/v) dioxane, at a temperature of 25°C.

4.1.1 TITRATION OF A STRONG BASE WITH A STRONG ACID

When V_o cm^3 of a strong base, with an initial concentration of C_B, is titrated with a strong acid of concentration C_A, the concentration of hydroxide ions, C_{OH}, after the addition of V cm^3 of acid will be:

$$C_{OH} = C_B \frac{V_o}{V_o + V} - C_A \frac{V}{V_o + V}. \qquad 4.1$$

At the equivalence point

$$C_B V_o = C_A V_e \ , \qquad 4.2$$

where V_e is the volume of acid added when the equivalence point is reached.

Substitution of equation (4.2) into equation (4.1) leads to

$$C_{OH} = C_A \frac{V_e - V}{V_o + V} \qquad 4.3$$

Now,

$$antilog(-pOH) = 10^{-pOH} = a_{OH} = \gamma_{OH} \times C_{OH}, \qquad 4.4$$

where a_{OH} and γ_{OH} represent the activity and activity coefficient of the hydroxide ion, respectively.

Equation (4.3) and (4.4) together give:

$$10^{-pOH} = \gamma_{OH} \frac{C_A}{V_o + V} (V_e - V), \qquad 4.5$$

which can be transformed to

$$(V_o + V)\ 10^{-pOH} = \gamma_{OH} C_A (V_e - V), \qquad 4.6$$

Substituting $pOH = pK_w - pH$ in equation (4.6) leads to

$$(V_o + V)\ 10^{pH - pK_w} = \gamma_{OH} C_A (V_e - V) \qquad 4.7$$

Rearranging equation (4.7), results in

$$(V_o + V)\ 10^{pH} = \frac{\gamma_{OH}\ C_A}{10^{-pK_w}} (V_e - V), \qquad 4.8$$

therefore

$$(V_o + V)\ 10^{pH} = K_1\ (V_e - V), \qquad 4.9$$

where K_1 is a constant, including the activity coefficient which can be considered constant by holding the ionic strength constant during a titration.

Similarly it can be shown that when the equivalence point has been passed, the concentration of hydrogen ions, C_H, is given by

$$C_H = C_A \frac{V}{V_o + V} - C_B \frac{V_o}{V_o + V} \qquad 4.10$$

$$= \frac{C_A}{V_o + V} (V - V_e) \qquad 4.11$$

Now,

$$antilog(-pH) = 10^{-pH} = a_H = \gamma_H \times C_H \qquad 4.12$$

$$= \frac{\gamma_H C_A}{(V_o + V)} (V - V_e). \qquad 4.13$$

Thus

$$(V_o + V)\ 10^{-pH} = K_2\ (V - V_e), \qquad 4.14$$

where K_2 is a constant, including the activity coefficient, which can be considered constant when the ionic strength is held constant during a titration.

If the cell potential, E, of the galvanic cell

(+) electrode reversible to hydrogen ions	titration solution	reference (-) half cell

is measured, then, assuming ideal electrode behaviour, E is related to the hydrogen ion activity, a_H, by the Nernst equation:

$$E = E^o + \frac{2.303RT}{nF} \log a_H. \qquad 4.15$$

Since it is assumed that the cell behaves reversibly and that the junction potentials are constant, the value of E^o is constant. Rearranging equation (4.15) leads to

$$\frac{nEF}{2.303RT} = \frac{nE^oF}{2.303RT} + \log a_H. \qquad 4.16$$

The first term on the right hand side of equation (4.16) is a constant so that

$$pH = \frac{nE^{\circ}F}{2.303RT} - \frac{nEF}{2.303RT}. \qquad 4.17$$

Equations (4.9) and (4.14) may therefore be written as

$$(V_o + V)\ 10^{\frac{-EF}{2.303RT}} = K_1^*\ (V_e - V) \qquad 4.18$$

and

$$(V_o + V)\ 10^{\frac{EF}{2.303RT}} = K_2^*\ (V - V_e) \qquad 4.19$$

Two quantities ϕ and ϕ' can now be defined as

$$\phi = (V_o + V)\ 10^{\frac{EF}{2.303RT}} \qquad 4.20$$

and

$$\phi' = (V_o + V)\ 10^{\frac{-EF}{2.303RT}} \qquad 4.21$$

From equations (4.18) and (4.19) it is clear that the quantities ϕ and ϕ' are linear functions of V, such that $\phi(V)$ and $\phi'(V)$ both intersect on the abscissa at the point $(V_e, 0)$.

The contraction factor, the total volume at each point and the corresponding equilibrium cell potential were supplied to the computer program GRAN (see Section 4.3.3) in order to calculate ϕ or ϕ' at each point in the titration. The ϕ and ϕ' values thus calculated were then plotted against the corresponding total volume.

An example of a Gran plot for the titration of a strong base with a strong acid is shown in Figure 4.1.

The ionic strength of all the solutions were made up to a final concentration of 0.10 mol dm^{-3} with $NaClO_4$ in 60% (v/v) dioxane, taking into account the contraction factor of 0.9803. This procedure entailed titrating a mixture of 4.00 cm^3 of approximately 0.17 mol dm^{-3} NaOH and 16.00 cm^3 of 0.10 mol dm^{-3} $NaClO_4$ plus 30.00 cm^3 of dioxane with small aliquots of 0.0980 mol dm^{-3} $HClO_4$ and appropriate volumes of dioxane in order to maintain a constant solvent composition. The data collected and the results of the calculations performed to obtain the Gran plot are shown in Table 4.1.

From Figure 4.1 one obtains V_e = 66.20 cm^3, from whence the concentration of the sodium hydroxide solution can be calculated to be 0.1718 mol dm^{-3}.

The functions ϕ and ϕ' sometimes deviate from linearity because of one or more of the following factors.

a) The activity coefficients and junction potentials are not constant at extreme values of hydrogen and hydroxide ion concentrations. This is indicated by the curvature of the Gran plots at values of V remote from V_e . If such plots are linear near the equivalence point the value of V_e must be obtained from this region alone [102]. An example of this is shown in Figure 4.2 and representative data is given in Table 4.2.

TABLE 4.1

Titration of a mixture of 4.00 cm^3 of approximately 0.17 mol dm^{-3} NaOH + 16.00 cm^3 0.10 mol dm^{-3} $NaClO_4$ + 30.00 cm^3 dioxane, with 0.0980 mol dm^{-3} $HClO_4$. (V_o = 49.02 cm^3.)

V/cm^3	$(V_o + V)/cm^3$	EMF/mV	$\phi(V) \times 10^9/cm^3$
0.80	50.98	-445.0	1.693
1.60	52.94	-440.6	1.482
2.40	54.90	-435.8	1.275
3.20	56.86	-429.8	1.045
3.60	57.84	-426.4	0.9316
			$\phi'(V) \times 10^5/cm^3$
7.60	67.64	190.7	1.131
8.00	68.62	203.7	1.903
8.40	69.60	212.1	2.676
8.80	70.58	218.4	3.468
9.20	71.56	223.0	4.206

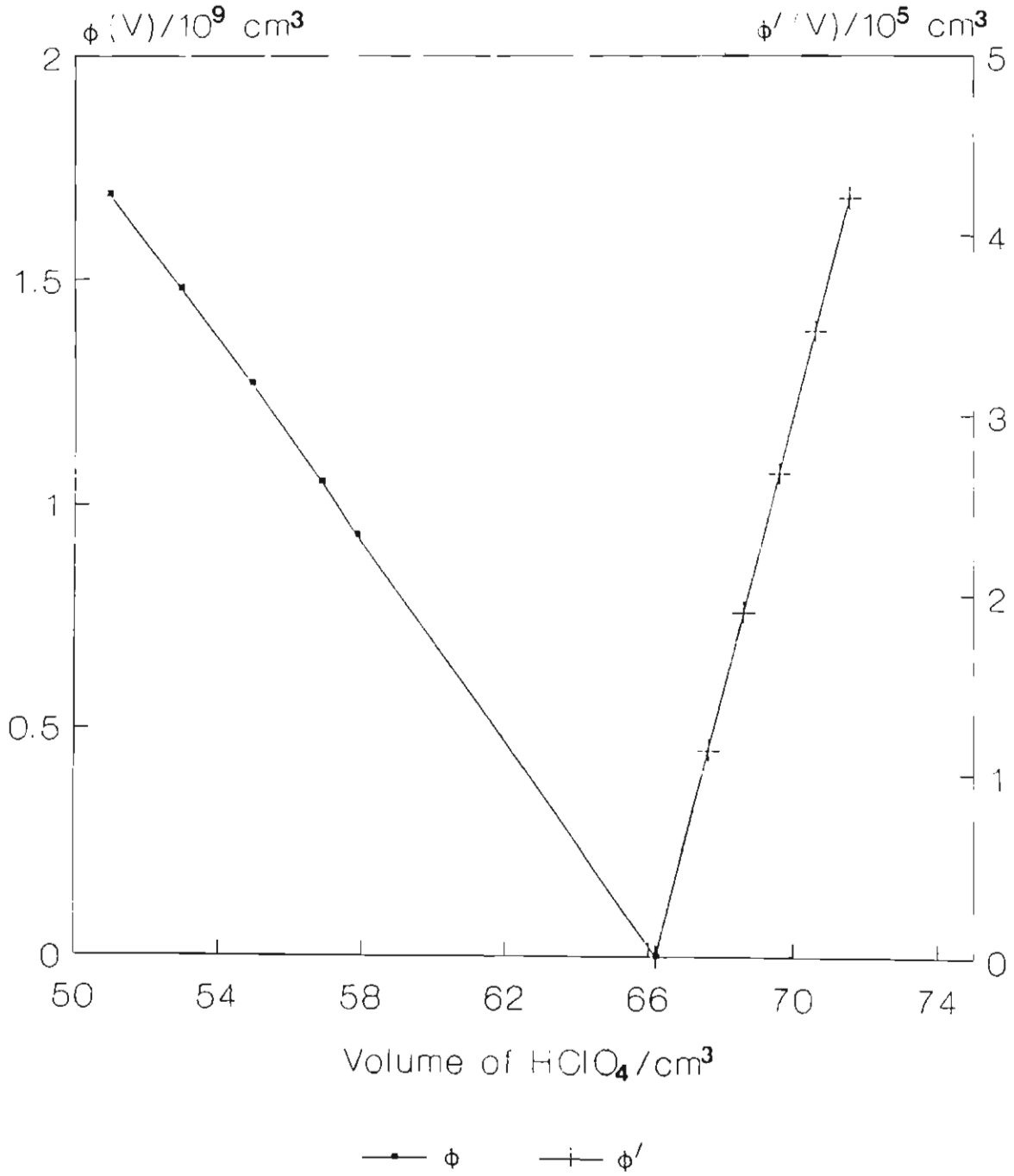

Figure 4.1 Gran plots ϕ and ϕ′ for the titration of a strong base with a strong acid.

TABLE 4.2

Titration of a mixture of 4.00 cm^3 of approximately 0.17 mol dm^{-3} NaOH + 16.00 cm^3 0.10 mol dm^{-3} $NaClO_4$ + 30.00 cm^3 dioxane, with 0.0980 mol dm^{-3} $HClO_4$. (V_o = 49.02 cm^3.)

V/cm^3	$(V_o + V)/cm^3$	EMF/mV	$\phi(V) \times 10^9/cm^3$
0.00	49.02	-487.9	8.646
0.80	50.98	-484.0	7.726
1.60	52.94	-480.2	6.920
2.40	54.90	-475.3	5.930
3.20	56.86	-469.5	4.901
3.60	57.84	-466.0	4.351
			$\phi'(V) \times 10^4/cm^3$
7.60	67.64	152.4	2.547
8.00	68.62	165.7	4.336
8.40	69.60	173.6	5.982
8.80	70.58	179.3	7.572
9.20	71.56	184.0	9.218

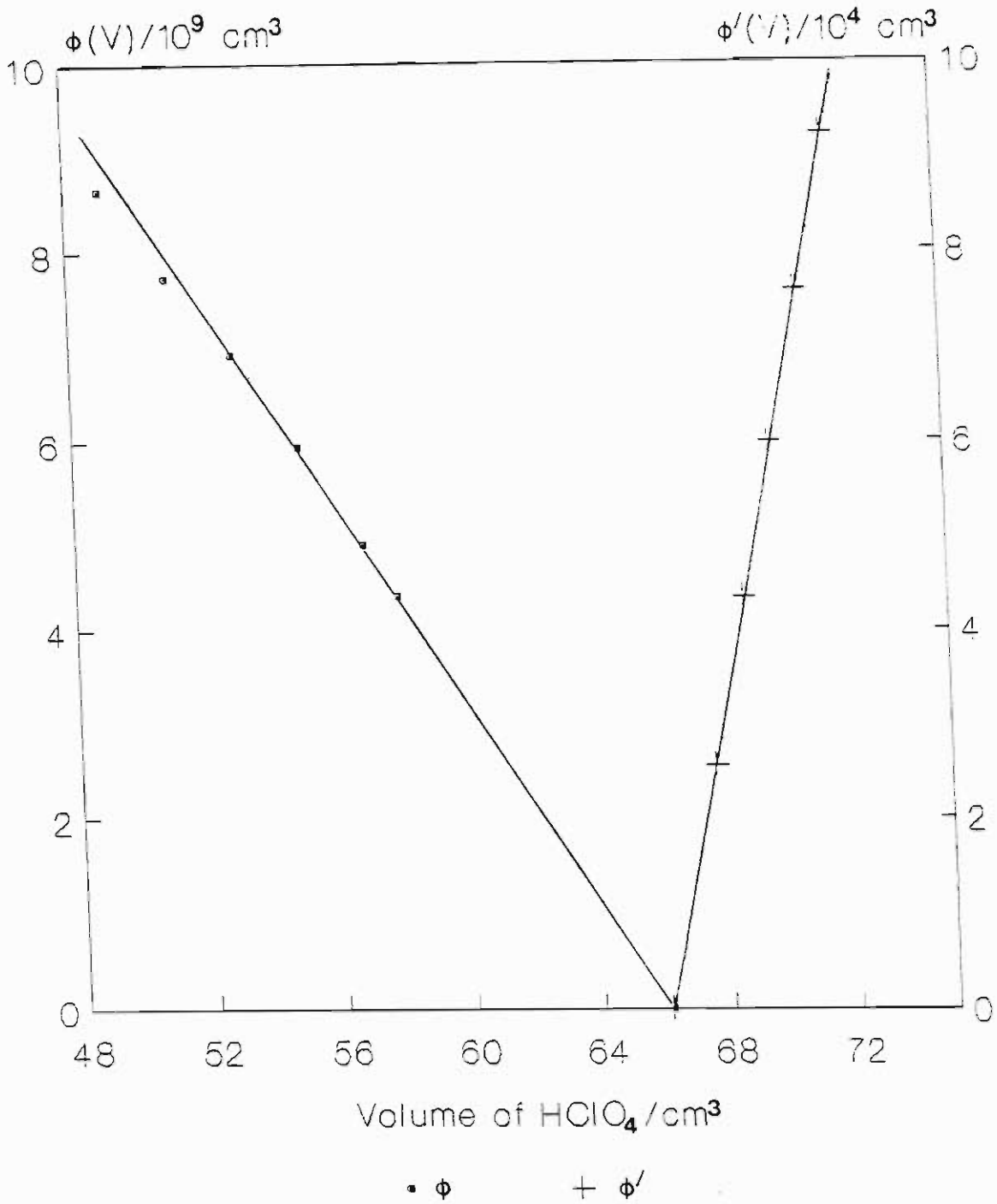

Figure 4.2 Gran plots ϕ and ϕ′ for the titration of a strong base with a strong acid, demonstrating the deviation of ϕ from linearity at high $[OH^-]$.

b) The carbonate contamination of the strong base. This is indicated by the curvature of ϕ, the function on the alkaline side of the equivalence point V_e, in the vicinity of that point, and ϕ', the function on the acidic side, now cuts the horizontal axis at some point $V'_e > V_e$. In this case

$$V'_e = \frac{V_o C_B}{C_A}, \qquad 4.22$$

where $C_B = [OH^-] + 2[CO_3^{2-}]$, the total concentration of base. If the function ϕ is linear over an appreciable range of V it may be extrapolated to cut the horizontal axis [102] at the point

$$V_e = \frac{V_o\ [OH]}{C_A}\ , \qquad 4.23$$

i.e. from this point the concentration of hydroxide ions in the strong base can be obtained. Thus the concentration of carbonate in the base can be estimated from the difference between V_e' and V_e, which can be written as:

$$[CO_3^{2-}] = \frac{(V'_e - V_e)\ C_A}{2V_o}. \qquad 4.24$$

Dissolved carbonate in the hydroxide solution is an example of an impurity which will affect the value of $[H^+]$, owing to the following protonation equilibria:

$$H^+ + CO_3^{2-} \rightleftharpoons HCO_3^- \qquad 4.25$$

$$H^+ + HCO_3^- \rightleftharpoons H_2CO_3 \rightleftharpoons H_2O + CO_2 \qquad 4.26$$

Gran plots can estimate the total carbonate concentration, and the computer program HALTAFALL (see Section 4.3.1) can be used to calculate the value of $[H^+]$, so that the effect of the presence of dissolved carbonate can be accounted for. In this work the carbonate content was negligible and hence not taken into account.

4.2 FORMATION CURVES

It is advisable to plot formation curves before calculating stability constants by computerised methods, since these formation curves give a general idea of the behaviour of the system and the presence of errors. The construction and interpretation of formation curves will now be discussed. The ligand used in this study is a weak diprotic acid. Hence the theory outlined in Sections 4.2.1 and 4.2.2 is applicable to such a ligand only.

4.2.1 $\bar{n}$(log[H]) plots

The stability constants of the complexes studied in this work were determined by a method involving competition between metal ions and hydrogen ions for the ligand L. It was therefore necessary to determine

the protonation constants of the ligand first.

For a diprotic acid there are two deprotonation reactions:

$$HL_2 \rightleftharpoons 2H + L \qquad 4.27$$

and

$$HL \rightleftharpoons H + L \qquad 4.28$$

for which we can write the following stability constants respectively:

$$\beta_{201} = \frac{[H_2L]}{[H]^2\ [L]} \qquad 4.29$$

and

$$\beta_{101} = \frac{[HL]}{[H]\ [L]} \qquad 4.30$$

(charges have been omitted for clarity.)

The total concentrations of the ligand and hydrogen ion may be expressed as

$$[L]_t = [L] + [HL] + [H_2L] \qquad 4.31$$

and

$$[H]_t = [H] + [HL] + 2[H_2L] - [OH]. \qquad 4.32$$

Since the equilibrium concentrations of HL, H_2L and OH

can be given in terms of the equilibrium concentrations of H and L and the appropriate stability constants, we get:

$$[L]_t = [L] + \beta_{101}[H][L] + \beta_{201}[H]^2[L] \qquad 4.33$$

and

$$[H]_t = [H] + \beta_{101}[H][L] + 2\beta_{201}[H]^2[L] - K_w[H]^{-1}. \qquad 4.34$$

The extent of protonation is expressed by the quantity $\bar{j}$, defined as the average number of hydrogen ions bound to each ligand. Thus

$$\bar{j} = \frac{bound\ H}{total\ L}$$

$$= \frac{[H]_t - [H] + [OH]}{[L]_t}$$

$$= \frac{[H]_t - [H] + K_w[H]^{-1}}{[L]_t}, \qquad 4.35$$

and therefore by using equations (4.34) and (4.33), we arrive at

$$\bar{j} = \frac{\beta_{101}[H] + 2\beta_{201}[H]^2}{1 + \beta_{101}[H] + \beta_{201}[H]^2}. \qquad 4.36$$

Using equation (4.35), values of $\bar{j}$ can be calculated from the experimental values of $[H]_t$, $[L]_t$ and $[H]$. From equation (4.36) we see that $\bar{j}$ is a function only of $[H]$ and is independent of $[H]_t$ and $[L]_t$. The way in

which $\bar{j}$ varies with [H] depends on the values of β_{101} and β_{201}.

Plots of $\bar{j}$ against log[H] can therefore be drawn to show this variation with [H]. Such plots are called "formation curves". The formation curve of a diprotic ligand has the following characteristics:

a) The points plotted form a single curve for all values of $[H]_t$ and $[L]_t$.
b) The curve is horizontal near $\bar{j} = 0$ and $\bar{j} = 2$.
c) The only other plateau is at $\bar{j} = 1$.
d) The formation curve is symmetrical under rotation through 180°C about its midpoint.

Deviations from the above characteristics, imply an error either in the measurements or in the species assumed to be present. An error in the measurements can arise through use of an incorrect value for $[L]_t$ or $[H]_t$ due to incorrect standardisation of a stock solution.

The formation curves are calculated using the computer program ESTA (see Section 4.3.2). A description of how one can deduce the types of species present in solution from formation curves will be given in the following section.

4.2.2 $\bar{Z}$ (log[L]) plots

For equilibrium systems involving a metal ion the formation curves of interest are plots of $\bar{Z}$ against

log (concentration of free ligand, L) also termed log A, where $\bar{Z}$ is the average number of ligands bound to each metal ion and is given by

$$\bar{Z} = \frac{\textit{conc. of ligand bound to metal}}{\textit{total metal ion concentration}} \qquad 4.37$$

In this study metal complex formation was monitored by measuring the hydrogen ion concentration with a glass electrode. The ligand used can complex with both metal ions and hydrogen ions. These considerations are important when deriving mass balance expressions for the total concentrations of metal ion, ligand and hydrogen ion. Thus, if we assume that only mononuclear species ML to ML_N are present, and that there is no hydrolysis of the metal aquo ion, we obtain equations (4.38)-(4.40) for the total concentrations.

$$M_t = \sum_{i=0}^{N} [ML_i]$$

$$= \sum_{i=0}^{N} \beta_{01i} [M] [L]^i, \qquad 4.38$$

where $\beta_{01i} = \dfrac{[ML_i]}{[M][L]^i}$ and $\beta_{010} = 1$.

$$[L]_t = \sum_{i=1}^{N} i\,[ML_i] + \sum_{j=0}^{2} [H_jL]$$

$$= \sum_{i=0}^{N} i\ \beta_{01i}[M]\,[L]^{i} + \sum_{j=0}^{2} \beta_{j01}[H]^{j}[L], \qquad 4.39$$

where $\beta_{001} = 1$.

$$[H]_t = [H] - [OH] + \sum_{j=1}^{2} j\ [H_jL]$$

$$= [H] - K_w[H]^{-1} + \sum_{j=1}^{2} j\ \beta_{j01}[H]^{j}[L]. \qquad 4.40$$

Equation (4.37) may be expressed as

$$\bar{Z} = \frac{\sum_{i=1}^{N} i\,[ML_i]}{\sum_{i=0}^{N} [ML_i]}$$

$$= \frac{\sum_{i=0}^{N} i\ \beta_{01i}[L]^{i}}{\sum_{i=0}^{N} \beta_{01i}[L]^{i}} \qquad 4.41$$

Using equations (4.38) and (4.39) we obtain the following expressions for $\bar{Z}$:

$$\bar{Z} = \frac{[L]_t - \sum_{j=0}^{2} [H_jL]}{[M]_t}$$

$$= \frac{[L]_t - [L] - \beta_{101}[H][L] - \beta_{201}[H]^2[L]}{[M]_t} . \qquad 4.42$$

From equation (4.40)

$$[L] = \frac{[H]_t - [H] + K_w[H]^{-1}}{\beta_{101}[H] + 2\beta_{201}[H]^2} . \qquad 4.43$$

Substituting equation (4.43) into equation (4.42) and using equation (4.36) we obtain

$$\bar{Z} = \frac{[L]_t - \bar{j}^{-1}([H]_t - [H] + K_w[H]^{-1})}{[M]_t} . \qquad 4.44$$

Thus $\bar{Z}$ can easily be calculated since $[M]_t$, $[L]_t$ and $[H]_t$ are usually known, [H] is measured experimentally, and β_{101} and β_{201} have usually been determined previously.

The derivation of the expressions (4.41), (4.42) and (4.44) for the quantity $\bar{Z}$ assumes that no polynuclear or ternary species are present. Under these assumptions $\bar{Z}$ is identical to the quantity $\bar{n}$ used by various other authors. If such species are present, calculation of $\bar{Z}$ would require knowledge of the stability constants for these species.

From equation (4.41) we see that $\bar{Z}$ is a function of the stability constants and the free ligand concentration if only mononuclear species ML_i are present. If polynuclear species are present $\bar{Z}$ (as

given by equation 4.42) will depend on [M] in addition to [L] and the stability constants. However, if the complexes are mononuclear but include hydrolysed or protonated complexes, $\overline{Z}$ will be independent of [M] but will vary according to $[H]_t$, $[L]_t$ and the stability constants.

Thus, if plots of $\overline{Z}$ against log[L] are superimposable for differing values $[M]_t$, polynuclear species are absent. If the formation curve plots are superimposable for widely differing values of $[H]_t$ and $[L]_t$, the possibility of protonated or hydroxo-complexes may be excluded [18, 19]. Formation curves thus give an indication of the types of complexes present in system being studied.

If the highest value of $\overline{Z}$ obtained (e.g. N) lies on a plateau and is an integer, then the highest mononuclear complex formed is ML_N. However it is not always possible to obtain a complete formation curve. Nevertheless some information can be obtained in that case. For instance, if the highest value of $\overline{Z}$ obtained is slightly greater than 1, the highest complex present is at least ML_2, whereas if a maximum value of $\overline{Z}$ just below 2 is obtained but there is no decrease in slope, then the presence of at least ML_3 can tentatively be assumed. Another feature exhibited by formation curves is a "curl-back" effect which seems to indicate the presence of ternary hydroxy metal complexes [93].

In practice formation curves obtained from experimental measurements are compared with theoretical formation curves obtained for the various models postulated. The model which best reproduces the experimental formation curve is then accepted as giving a satisfactory description of the system. (For the calculation of experimental and theoretical formation curves see Section 4.3.2)

Formation curves can reveal the presence of errors. This enables outlying points to be discarded, and some systematic errors, e.g. those due to incorrect solution concentrations, to be detected.

4.3 COMPUTER PROGRAMS USED

A description of the computer programs used to analyse potentiometric data obtained in this study follows.

4.3.1 HALTAFALL

The computer program HALTAFALL [103] is used for calculating the concentrations of species in an equilibrium mixture. A mixture of several components which can form a number of complexes and solid phases can be treated. One needs to specify the concentrations of the components, the relevant equilibrium constants expressed as stability constants and the composition of the mixture, before calculations can be carried out.

In this study the program was used to simulate

titrations in a single solution phase. The conditions of the experiments for optimum formation of the desired species without interference from side reactions was chosen on the basis of the species distribution tables obtained for various reagent concentrations. The program was also used to determine the experimental procedure with the greatest sensitivity of $[H^+]$ to the stability constant/s being determined. This was done by changing the estimate of the stability constant under consideration by one log unit at a time and noting the effect on the estimated p[H].

HALTA1 [104], a modified version of the HALTAFALL program, was used to calculate the ionic strength at each point of a titration. The only additional input information required here is the concentration of the inert electrolyte and the charges of all the components present. This version of the program is useful in verifying that an approximately constant ionic medium is present during a titration.

Once the stability constants for a particular system were known, species distribution curves were calculated using the HALTAFALL program.

4.3.2 ESTA

Equilibrium Simulation for Titration Data (ESTA) is a suite of five programs which perform calculations concerned with competitive solution equilibria [105].

This program is used for simulating equilibrium distributions of chemical species and for the analysis of potentiometric data. The calculations are performed by two main program modules :

a) THE SIMULATION MODULE (ESTA1), produces results on a point by point basis. It can determine a single value for almost any of the parameters which characterise a titration by setting up and solving the mass balance equations.

b) THE OPTIMIZATION MODULE (ESTA2), is used to determine the 'best' values of the stability constants of the proposed species and is based on a least squares procedure over a whole system of titrations.

One of the major problems in solution chemistry is still that of identifying the chemical model for a particular equilibrium mixture. The choice of a chemical model entails finding the set of pqr triples and corresponding stability constants β_{pqr} that best reproduce the experimental data. In this work ESTA was used to calculate the stability constants for the various complexes studied. The most likely models were submitted to ESTA and the adequacy of each model was evaluated by looking at the value of the objective function and the Hamilton R-factor. That model which yields the lowest value of the objective function and the Hamilton R-factor gives the best fit to the experimental data. The Gauss - Newton method is used to minimize the objective function which is based on weighted EMF residuals. To determine the weights, the program was supplied with the estimated random errors

in the titre volumes (0.01 cm^3) and observed EMF (0.10 mV).

This program was also used to calculate values of $\overline{Z}$(calc) for various postulated models of the species present in solution. These were then compared with $\overline{Z}$(obs) values which were also determined using the ESTA program. Species distribution plots for the systems studied were also obtained by means of the SPEC task in the program.

The BETA simulation task aided in identifying the minor species present in the systems studied. The program required estimates of the stability constants of the major species assumed present and a list of likely minor species to calculate the stability constant, at each point, for the minor species. Each minor species is regarded as the only remaining complex required to produce agreement between calculated and observed data at each titration point.

Further details of this program can be found in the ESTA Users Manual [106].

4.3.3 GRAN AND CALIB

GRAN and CALIB are programs written by my colleague, Mr. S.C. Edwards, in BASIC [107]. GRAN was used to calculate the functions ϕ and ϕ' for the Gran plot, whilst CALIB was used to calculate the p[H] values for the cell calibration.

4.3.4 STATGRAPHICS

The STATGRAPHICS Statistical Graphics System is a PC software package integrating a variety of statistical functions with high resolution colour graphics. In this study STATGRAPHICS was used for linear regression analyses and to plot formation curves.

Further details of this program can be found in the STATGRAPHICS User's Guide [108].

CHAPTER 5

RESULTS AND DISCUSSION

In this chapter the results derived from the potentiometric data are described and discussed in detail. The results of the spectroscopic and titrimetric studies of the zinc 8-hydroxyquinolate precipitate are also discussed.

The analysis of the potentiometric data listed in Section 3.3 was started by plotting the appropriate formation curve. Once the choice of model had been made the final stability constants were calculated by using the computer program ESTA. These stability constants were then used to arrive at 'calculated' formation curves. These are depicted as striped lines in the various figures.

For all the results obtained in this work the standard deviation calculated by ESTA is shown in parentheses after the appropriate result. In the calculation of stability constants fixed values of certain constants were used, most of which were taken from the literature. Table 5.1 lists those values.

5.1 PROTONATION OF 8-HYDROXYQUINOLINE

The formation curves for this system are shown in Figure 5.1 and can be seen to be superimposable. Hence the titrations were considered to be reproducible. The formation curves are also symmetrical under rotation

TABLE 5.1

Constants used in the calculation of stability constants. All data are for 25°C and μ = 0.1 mol dm^{-3}, except where indicated.

REACTIONS	log β	REF
$H_2O \rightleftharpoons H^+ + OH^-$	-15.94	45
$Zn^{2+} + H_2O \rightleftharpoons Zn(OH)^+ + H^+$	-11.37†	109
$Zn^{2+} + 2H_2O \rightleftharpoons Zn(OH)_2 + 2H^+$	-21.42†	109
$Zn^{2+} + 3H_2O \rightleftharpoons Zn(OH)_3^- + 3H^+$	-34.86†	109
$Zn^{2+} + 4H_2O \rightleftharpoons Zn(OH)_4^{2-} + 4H^+$	-49.39†	109
$2Zn^{2+} + OH^- \rightleftharpoons Zn_2(OH)^{3+}$	5.00†	109
$Ge^{4+} + H_2O \rightleftharpoons Ge(OH)^{3+} + H^+$	-15.76	28
$Ge^{4+} + 2H_2O \rightleftharpoons Ge(OH)_2^{2+} + 2H^+$	-31.9	28
$Ge^{4+} + 3H_2O \rightleftharpoons Ge(OH)_3^+ + 3H^+$	-48.3	28
$Ge^{4+} + 4H_2O \rightleftharpoons Ge(OH)_4 + 4H^+$	-64.95	28
$Ge(OH)_4 + OH^- \rightleftharpoons GeO(OH)_3^- + H_2O$	5.42*	27
$Ge(OH)_4 + 2OH^- \rightleftharpoons GeO_2(OH)_2^{2-} + 2H_2O$	8.83*	27

† corrected from μ = 0 to μ = 0.1 with the Davies equation [110].

* value for μ = 0.5 mol dm^{-3}.

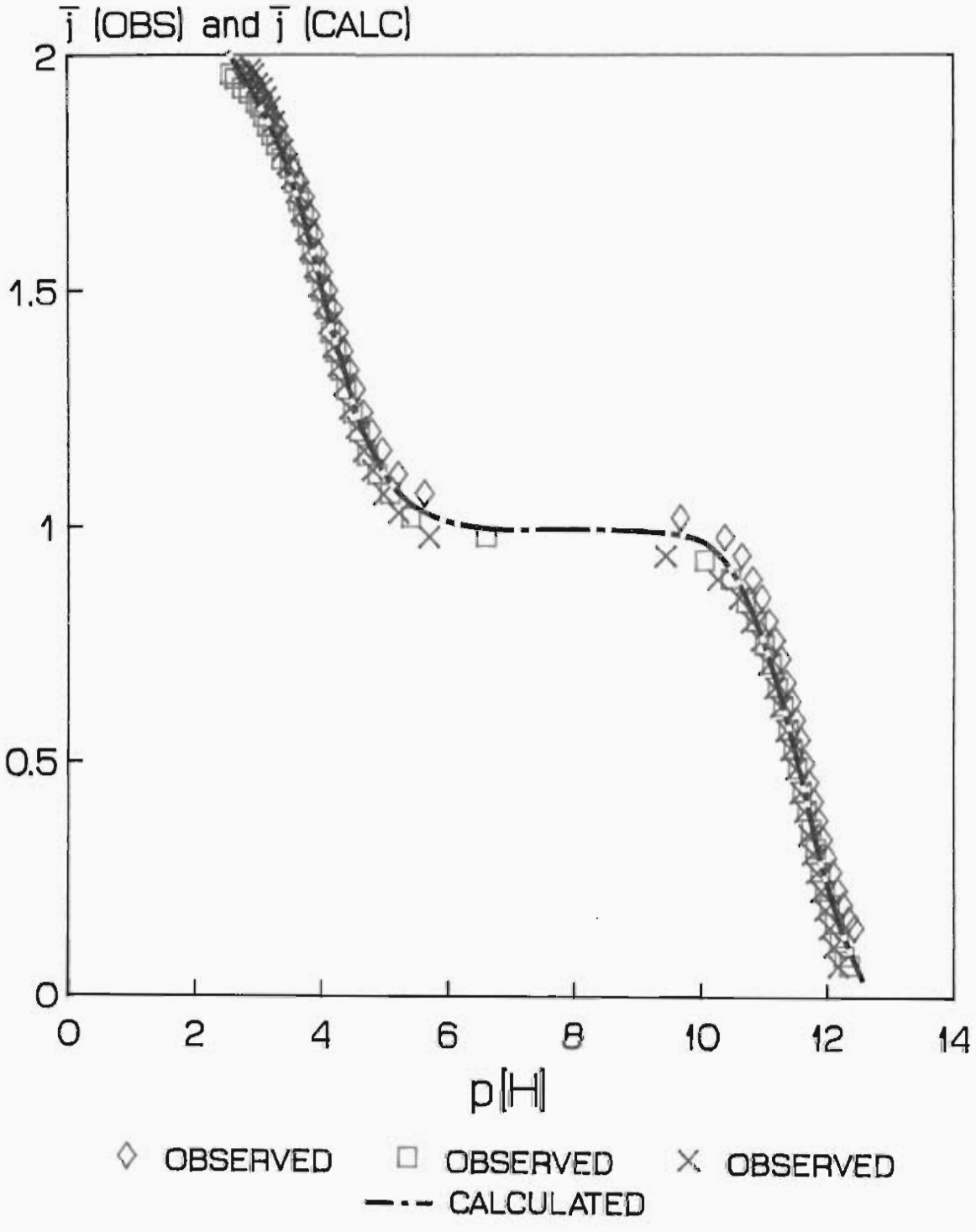

Figure 5.1 Formation curves for the protonation of 8-hydroxyquinoline.

about their midpoint – a property of formation curves for a diprotic ligand. The fact that $\bar{j}$(log[H]) curves level off at $\bar{j}$ = 1 and $\bar{j}$ = 2 is consistent with the diprotic nature of 8-hydroxyquinoline. The plateau at $\bar{j}$ = 1 is observed since the difference between the stepwise formation constants, viz. pK_{101} and pK_{102}, of 7.47 is sufficient to prevent overlap of the successive protonation steps.

A single value was used for the ionic product of water throughout the calculation of the protonation constants of 8-hydroxyquinoline. The values obtained for these constants, together with selected values available from the literature are shown in Table 5.2.

An increase in pK_{101} and concomitant decrease in pK_{102} with increasing organic content has previously been reported for oxine [10]. The results obtained in this work fall in line with the literature reported for other dioxane percentages.

The values of both the protonation constants of 8-hydroxyquinoline, viz. pK_{101} and pK_{102}, obtained in this work are higher than those reported for the same conditions [23]. This is probably a result of the higher value of K_w, viz. 16.34, used by Steger [23], since substitution of this higher K_w value in this work showed a decrease in the protonation constants of 8-hydroxyquinoline. Nevertheless, the protonation constants of 8-hydroxyquinoline obtained from this study agree reasonably well with those from literature.

TABLE 5.2

Protonation constants of 8-hydroxyquinoline, together with selected values reported in the literature. (All values are for 25°C unless otherwise stated.) Numbers in parenthesis refer to the standard deviation.

pK_{101}	pK_{102}	MEDIUM	REF
11.51 (0.01)	4.04 (0.02)	0.1 mol dm^{-3} $NaClO_4$ in 60% dioxane	This work
9.89 (0.03)	5.13 (0.02)	* μ = 0.01	3
10.80	4.48	* 0.3 mol dm^{-3} $NaClO_4$ in 50% dioxane	19
11.48 (0.01)	3.97 (0.01)	0.1 mol dm^{-3} $NaClO_4$ in 60% dioxane	23
12.33	3.18	70% dioxane	4

* Temperature = 20°C

The protonation constants obtained were then used to calculate a formation curve for the protonation of 8-hydroxyquinoline. This curve (see Figure 5.1) fits the experimental values fairly well thus indicating that the calculated protonation constants explain the experimental data adequately.

A species distribution diagram for 8-hydroxyquinoline is shown in Figure 5.2. From this distribution diagram it is evident that totally protonated ligand is present at the start of the titration and on addition of base, the increasing p[H] results in the following successive steps:

a) a decrease in the amount of totally protonated ligand (H_2L^+),
b) an increase in the amount of singly protonated ligand (HL),
c) a decrease in the amount of singly protonated ligand (HL), and
d) an increase in the amount of deprotonated ligand (L^-), until totally deprotonated ligand is present at the end of the titration.

The protonation constant with the smaller pK value indicates the first site of dissociation. In this work pK_{102} can be attributed to the -NH group which has a weaker dative bond in comparison to the covalent bond present in the -OH group whose dissociation as the second site is described by the larger pK_{101} value.

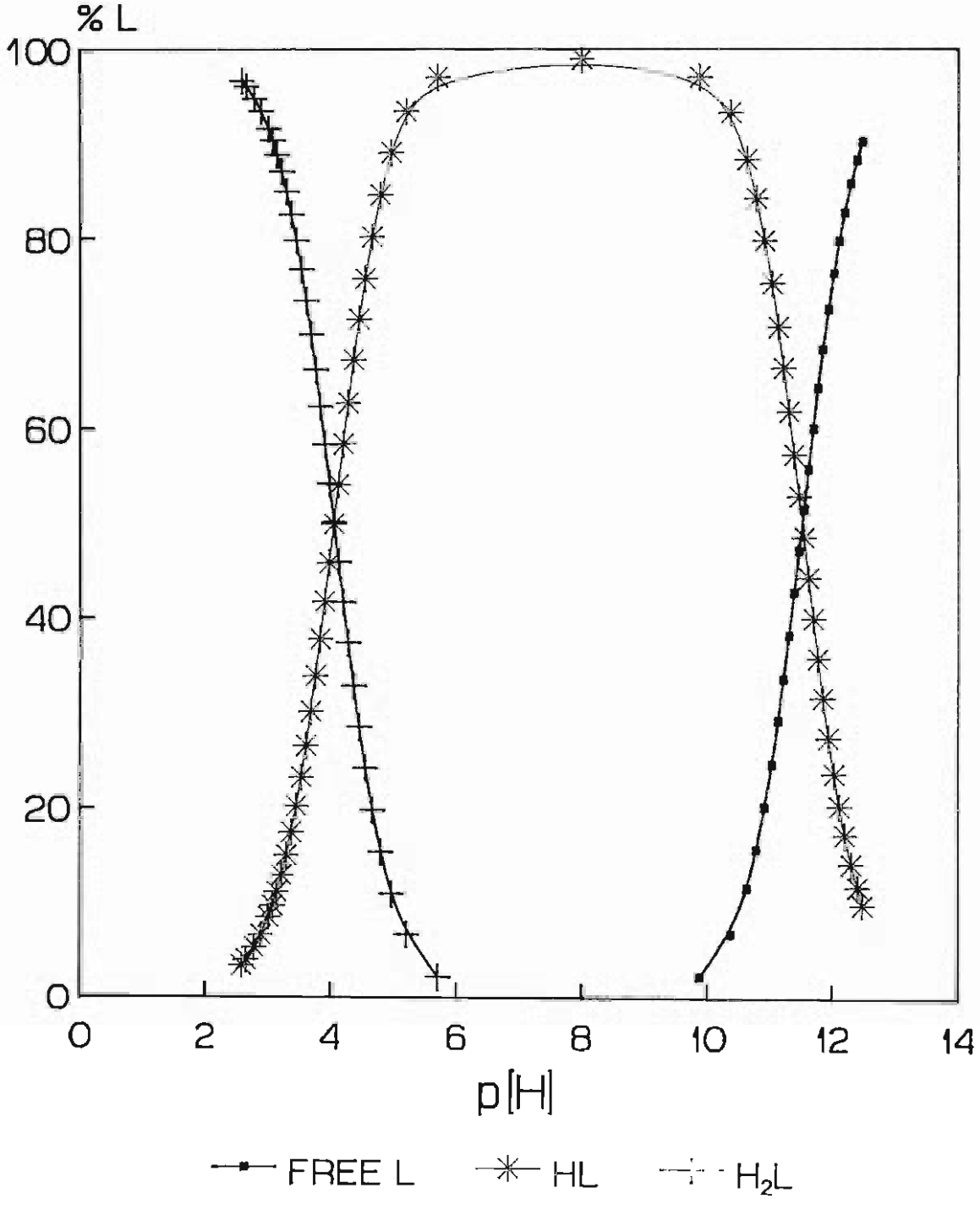

Figure 5.2 Species distribution diagram for the protonation of 8-hydroxyquinoline, for the case $[oxine]_o = 4.302 \times 10^{-3}$.

5.2 COMPLEXATION OF ZINC WITH 8-HYDROXYQUINOLINE

The formation curves for this system are shown in Figure 5.3. The various zinc:8-hydroxyquinoline ratios gave superimposable formation curves. This is typical of a binary system, and also suggests that the titrations are reproducible. The reproducibility of the titrations was verified by performing repeat titrations (nos 1 & 4) which yielded completely superimposable formation curves. The various metal concentrations also gave superimposable plots thus again confirming the absence of polynuclear species.

Complexation of zinc with 8-hydroxyquinoline resulted in precipitation at a p[H] ≈ 3.6. The precipitate was identified as zinc 8-hydroxyquinolate dihydrate (see Section 5.3). Due to the precipitation, the titrations were not carried out to p[H] values high enough to achieve complete complexation of zinc with 8-hydroxyquinoline, therefore the $\overline{Z}$(log[L]) curves revealed no other properties that could have aided in choosing possible models.

The fact that $\overline{Z}$(log[L]) curves show no sign of levelling as they approach $\overline{Z}$ = 1 suggests that the highest mononuclear complex formed is greater than ML. The highest value of $\overline{Z}$ reached is 0.81. This suggests that ML_2 is the highest mononuclear complex formed.

For species selection purposes, ML and ML_2 were treated as the major complexes present. Attempts were then made to introduce protonated and hydrolysed

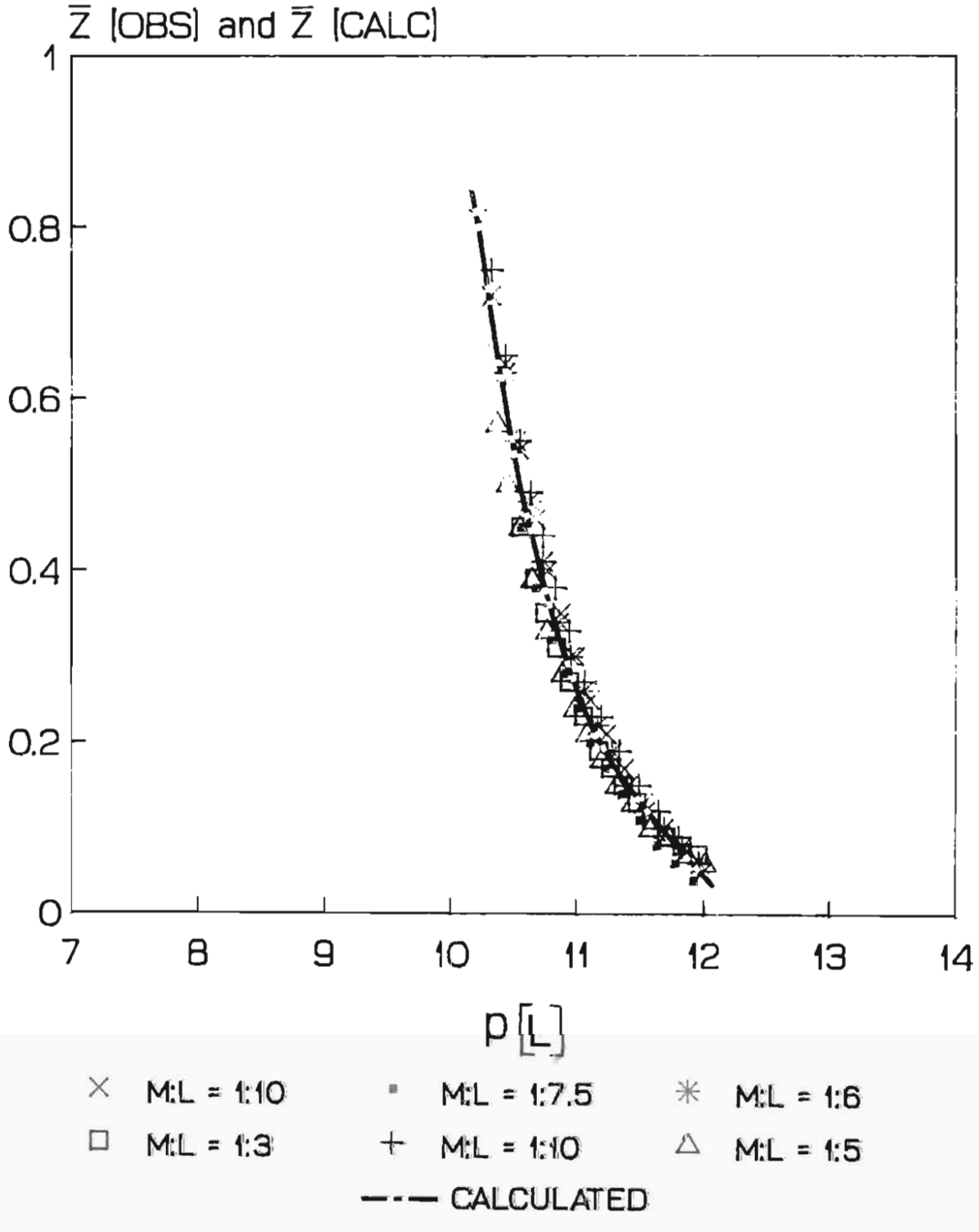

Figure 5.3 Formation curves for the zinc-8-hydroxyquinoline system.

species into the model [111]. Fixed values were used for the stability constants of the species H_2O, HL, H_2L^+, $Zn(OH)^+$, $Zn(OH)_2$, $Zn(OH)_3^-$, $Zn(OH)_4^{2-}$ and $Zn_2(OH)^{3+}$. Table 5.3 lists the results obtained for the 'successful' models tried, i.e. those models for which the program ESTA yielded successful refinements.

The p[H] range covered in these titrations, viz. $2.6 \leq p[H] \leq 3.6$, suggests the presence of protonated species rather than hydroxy species. On this basis, models 4 and 5 were discarded. Model 2 was also discarded since it was not representative of the experimental data when $\bar{Z}(\log[L])$ curves were plotted. Of all the proposed models, 1 and 3 averaged the experimental data most aptly when comparing the $\bar{Z}(\log[L])$ curves.

The values for the objective function, U, for models 1 and 3 were too close for a reliable comparison. Even though model 1 has the slightly lower U value, model 3 appears more favourable when structural stabilities of the complexes are considered.

Model 3 contains three complexes, two of which have 5-membered rings which are known to be remarkably stable. Model 1 on the other hand contains two complexes, both of which are protonated species. These major species from model 1 have less stable 5-membered ring structures since the negative charge density on the oxygen atom available for bonding to the metal is reduced by the dative bond formed with the proton. Model 3 was therefore chosen to be the best

TABLE 5.3

Stability constants for zinc-8-hydroxyquinoline complexes obtained from different models. (All titrations were used.)

MODEL	1	2	3	4	5
ML^+		10.53	10.39	10.31	10.43
ML_2			20.12		
MLH^{2+}	13.79	13.18	13.56	13.58	13.51
ML_2H^+	24.34				
$ML(OH)$				6.40	
$ML(OH)_2^-$					2.50
No. OF POINTS	101	101	101	101	101
U_{ESTA}	51	79	53	61	59
R_{ESTA}	0.005	0.006	0.005	0.005	0.005

description of the species present in solution. Zinc oxinate (ZnL_2) is reported [55] to have a tetrahedral configuration in solution. Isotopic exchange studies on zinc oxinate [112] gave evidence for the existence of labile bonding between zinc and oxine. This indicated that the chelate exchanged its metal content rapidly in the presence of excess zinc ion. Figure 5.4 depicts a space-filled diagram of the species ZnL_2 (zinc oxinate).

The results obtained for model 3 are compared with the literature values in Table 5.4. The formation curves calculated by using the stability constants from model 3 are shown in Figure 5.3. One can see that they reproduce the observed formation curves well.

Maley and Mellor [4] have reported that an increasing proportion of dioxane in the solvent diminishes its dielectric constant, hence increasing both $\log K_{011}$ and $\log K_{012}$. The results obtained from this study fall in line with the literature reported for other dioxane percentages.

Table 5.4 also shows that the results obtained for $\log K_{011}$ and $\log K_{012}$ in this work are higher than those reported for the same conditions [113]. It is possible that the values reported by Steger [23] are lower for the following reasons:

a) He did not consider the possibility of any species other than ML and ML_2 being present in solution.

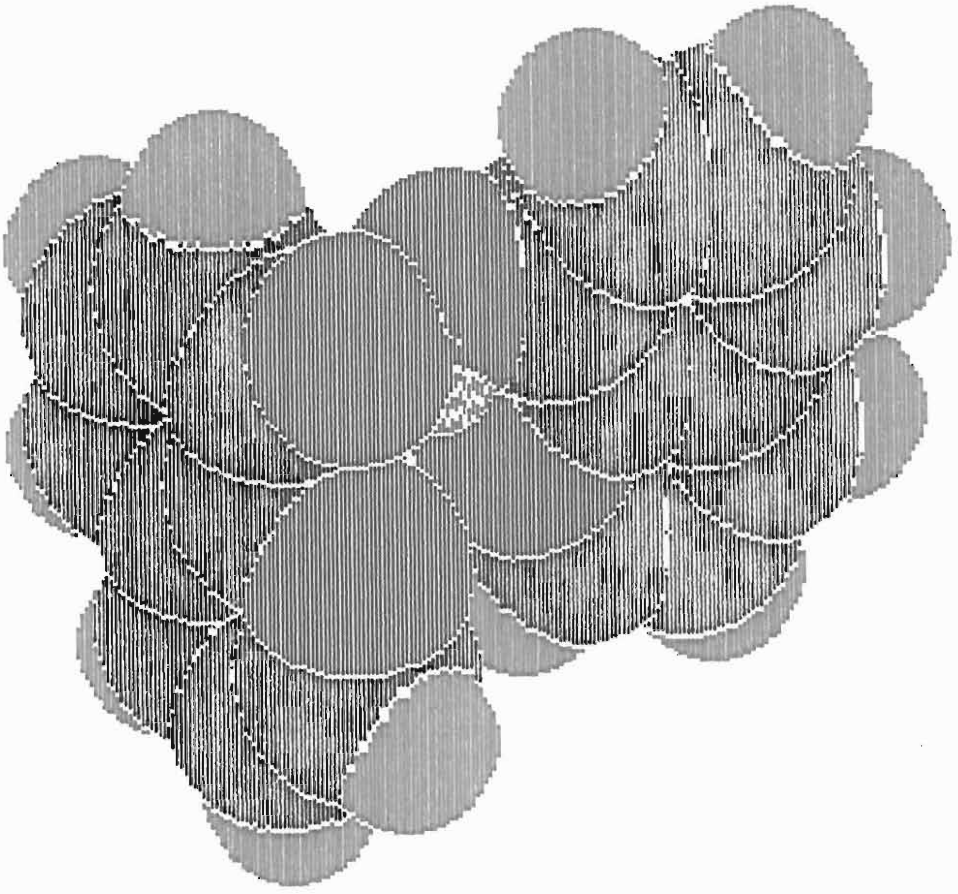

Figure 5.4 Space-filled diagram of the highest mononuclear complex formed in the zinc-8-hydroxyquinoline system, viz. zinc 8-hydroxyquinolate.

TABLE 5.4

Stability constants obtained for the zinc-8-hydroxyquinoline system together with values reported in the literature. (All values are for 25°C unless otherwise stated.) Numbers in parenthesis in the first three columns refer to the standard deviation.

$\log K_{011}$	$\log K_{012}$	$\log \beta_{111}$	MEDIUM	REF
10.39 (0.02)	9.73 (0.05)	13.56 (0.04)	0.1($NaClO_4$) 60% dioxane	This work
10.91	9.90	-	70% dioxane	4
9.96 (0.04)	9.02 (0.04)	-	0.1($NaClO_4$) 60% dioxane	23 & 113
9.96	8.90	-	50% dioxane	18
9.34	8.22	-	*0.3($NaClO_4$) 50% dioxane	19

* Temperature = 20°C

b) Steger [23] used a larger value of K_w compared to that used in this work. Substitution of this higher K_w value, viz. 16.34, in this work shows a decrease in the stability constants for the zinc-8-hydroxyquinoline system.

The $\overline{Z}(\log[L])$ curve shows no sign of levelling as it approaches $\overline{Z} = 1$. One would expect this when the literature values of the stepwise formation constants are considered, i.e. the difference between $\log K_{011}$ and $\log K_{012}$ of 0.94 is insufficient to prevent overlap of the successive formation steps.

Due to the precipitation of zinc 8-hydroxyquinolate no points were obtained for $\overline{Z} > 0.81$, therefore the value of $\log K_{012}$ would be expected to be less precise than that for $\log K_{011}$, where points for almost the entire range, viz. $0.01 < \overline{Z} < 0.81$, were obtained. This could explain the larger discrepency observed for $\log K_{012}$ (cf. $\log K_{011}$) when compared with the literature values [23].

There are no literature values available for comparison with the stability constant obtained for the protonated complex. If one considers the titration procedure, the p[H] range covered and the fact that totally protonated 8-hydroxyquinoline constitutes part of the background electrolyte (see Section 3.3.1), one would expect to find ZnLH, i.e. the protonated complex, as an intermediate species during the titration.

In order to visualize the amount of protonated complex present during the titration a species distribution diagram was constructed for an intermediate metal to ligand ratio of 1:5 with $[Zn^{2+}]_o$ = 4.005 x 10^{-3} mol dm^{-3} (see titration 6). This is represented in Figure 5.5 and shows that the protonated species constitutes 17% of the total zinc at a p[H] ≈ 3.6 under these conditions.

The following structures were hypothesized for the protonated complex (ZnLH):

a) The zinc ion attached to one 'arm' of oxine, i.e. only the nitrogen atom of oxine is bonded to the zinc ion, while the oxygen atom of oxine remains covalently bonded to the proton.

b) A 5-membered ring formed between the zinc ion and oxine, i.e. both the nitrogen and oxygen atoms of oxine are bonded to the zinc ion, whilst a dative bond is formed between the proton and the oxygen atom of oxine.

The latter hypothesis is preferred because it includes a stable 5-membered ring.

5.3 ANALYSIS OF THE ZINC 8-HYDROXYQUINOLATE PRECIPITATE

8-Hydroxyquinoline is known to precipitate zinc quantitatively in the p[H] range 3.3 to 4.4 as zinc 8-hydroxyquinolate [11]. The author therefore analysed the precipitate obtained from the potentiometric titrations, termed experimental precipitate in this

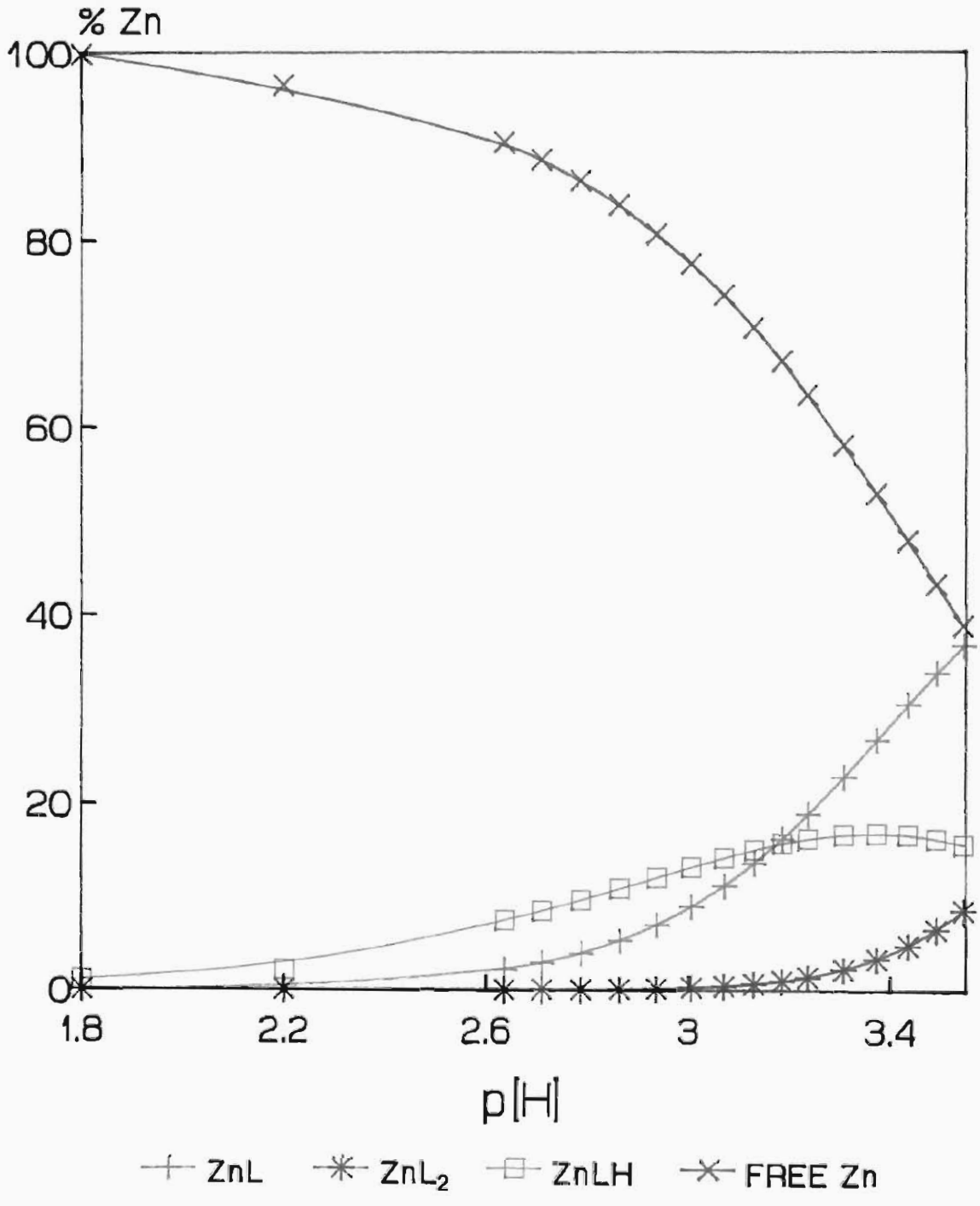

Figure 5.5 Species distribution diagram for the zinc-8-hydroxyquinoline system, for the case $[Zn^{2+}]_o/[oxine]_o \approx 5$ and $[Zn^{2+}]_o = 4.005 \times 10^{-3}$ mol dm^{-3}.

work, by comparison with the synthesized zinc 8-hydroxyquinolate (see Section 3.3.4), termed synthetic precipitate in this study.

Both precipitates were greenish-yellow, crystalline and soluble in chloroform. Photometric studies of the coloured chloroform solutions revealed absorption in the region of 400 nm. This behaviour is in keeping with the literature [96], and is attributable to conjugated systems.

The number of 8-hydroxyquinoline molecules attached to the zinc ion in each precipitate was determined by a titration (see Section 3.3.4). The major reactions that occur during this titration include the following:

$$BrO_3^- + 5Br^- + 6H^+ \rightleftharpoons 3Br_2 + 3H_2O \qquad 5.1$$

$$C_9H_7ON + 2Br_2 \rightleftharpoons C_9H_5ONBr_2 + 2H^+ + 2Br^- \qquad 5.2$$

$$2KI + Br_2 \rightleftharpoons 2KBr + I_2 \qquad 5.3$$

$$2Na_2S_2O_3 + I_2 \rightleftharpoons Na_2S_4O_6 + 2NaI \qquad 5.4$$

The total number of moles of free bromine was calculated using reaction (5.1), while reaction (5.2) gave an indication of the amount of bromine taken up by the 8-hydroxyquinoline. Reaction (5.3) then converts the excess free bromine to an equivalent

amount of free iodine, so that the number of moles of excess bromine could be calculated indirectly using reaction (5.4). The number of moles of bromine taken up by the oxine was then calculated as the difference between the amounts calculated from reactions (5.1) and (5.4). The number of moles of zinc present was calculated using the following equivalence [11]:

1 millimole BrO_3 ≡ 0.008175 g Zn

The ratio of zinc:8-hydroxyquinoline was calculated to be 1:1.997 for the experimental precipitate and 1:1.991 for the synthetic precipitate. The results of these titrations confirmed a formula of $Zn(C_9H_6ON)_2$ for both precipitates.

The elemental analysis of zinc 8-hydroxyquinolate dihydrate ($Zn(C_9H_6ON)_2.2H_2O$) calculated from this formula gave the following results: C: 55.48%, H: 4.15%, N: 7.19%, O: 16.41%, Zn: 16.77% and (Zn+O): 33.18%. Elemental analysis of the experimental precipitate gave the following results: C: 56.07%, H: 4.20%, N: 6.98%, (Zn+O): 32.75%, while the following results were obtained from the synthetic precipitate: C: 55.06%, H: 3.89%, N: 7.19%, (Zn+O): 33.86%. The acceptable limits of agreement between the observed and calculated values confirmed that the structure of the precipitate is zinc 8-hydroxyquinoline dihydrate.

The energy dispersive x-ray microanalysis spectra for both the experimental and synthetic precipitates are shown in Figures 5.6(a) and 5.6(b) respectively. Only elements with atomic masses above that of beryllium

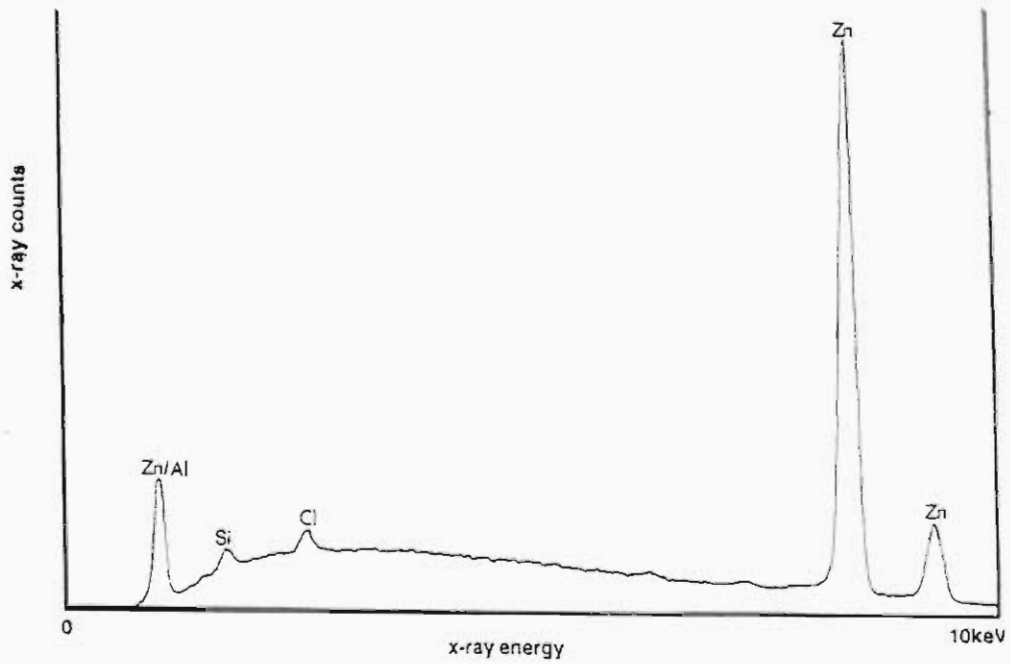

Figure 5.6(a) The energy dispersive spectrum of the experimental precipitate obtained from the zinc-8-hydroxyquinoline system.

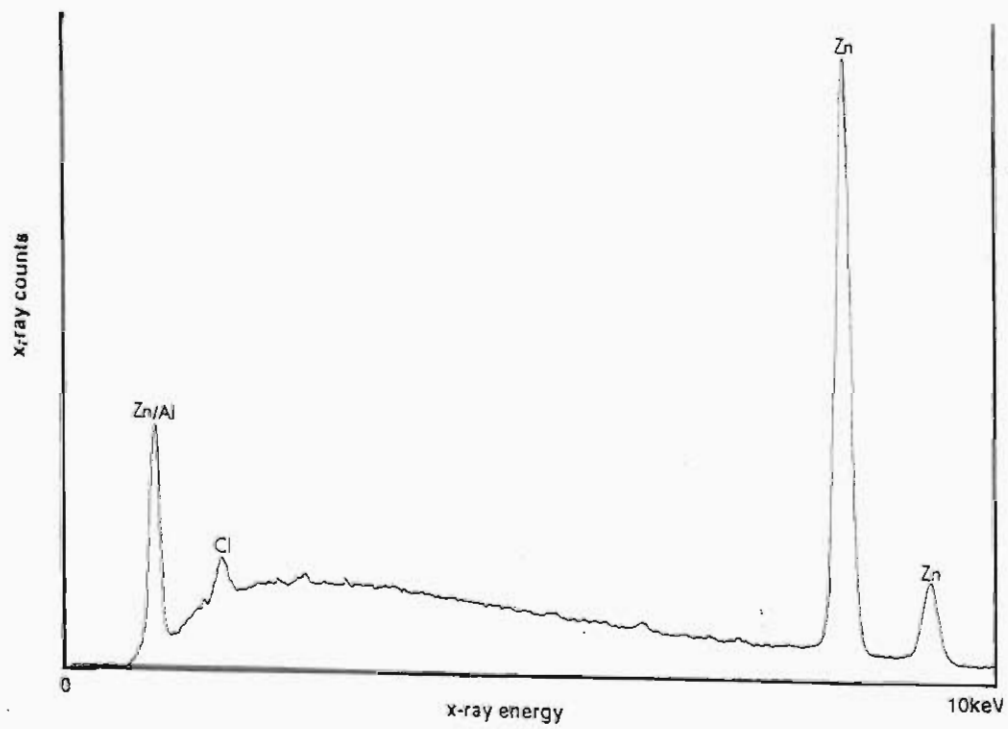

Figure 5.6(b) The energy dispersive spectrum of the synthetic zinc 8-hydroxyquinolate precipitate.

are detected from these spectra since the instrument has a beryllium window which absorbs x-rays of lighter elements. The spectra obtained were comparable and gave a 90.14% and 89.13% zinc by mass for the experimental and synthetic precipitates respectively. This indicates a comparable content of zinc in both precipitates.

Proton nmr spectra of the experimental and synthetic precipitates are similar and are shown in Figures 5.7(a) and 5.7(b) respectively. The $^{1}H_{nmr}$ spectra (200 mHz; C_5D_5N) showed the following δ/ppm: 8.92 (1H, dd, 2-H), 7.93 (1H, dd, 4-H), 7.58-7.54 (2H, m, 3-, 6-H), 6.98 (1H, dd, 5-H) and 6.87 (1H, dd, 7-H). These assignments correspond to those reported for zinc-oxinate in DMSO [55]. However, the reported δ values are further downfield - most probably an effect of the solvent. The magnetic equivalence of the two ligands about the central zinc atom in the nmr time scale is established by the presence of 6 proton resonances with well resolved splittings, corresponding to the six ring protons of the ligand.

^{13}C and adept nmr spectra of the experimental and synthetic precipitates are alike and shown in Figures 5.8(a) and 5.8(b) respectively. The $^{13}C_{nmr}$ (200 mHz) showed the following δ/ppm: 149.8-150.9, 135.5-136.5 and 123.3-124.4 (due to the solvent - C_5D_5N [114]; 165.5 (8-C), 141.7 (9-C) and 131.0 (4-C) (i.e. totally substituted carbons which are known to have a low intensity and are not observed in the adept spectra); 145.2, 138.9, 131.5, 121.8, 113.5 and 109.5 (doublets

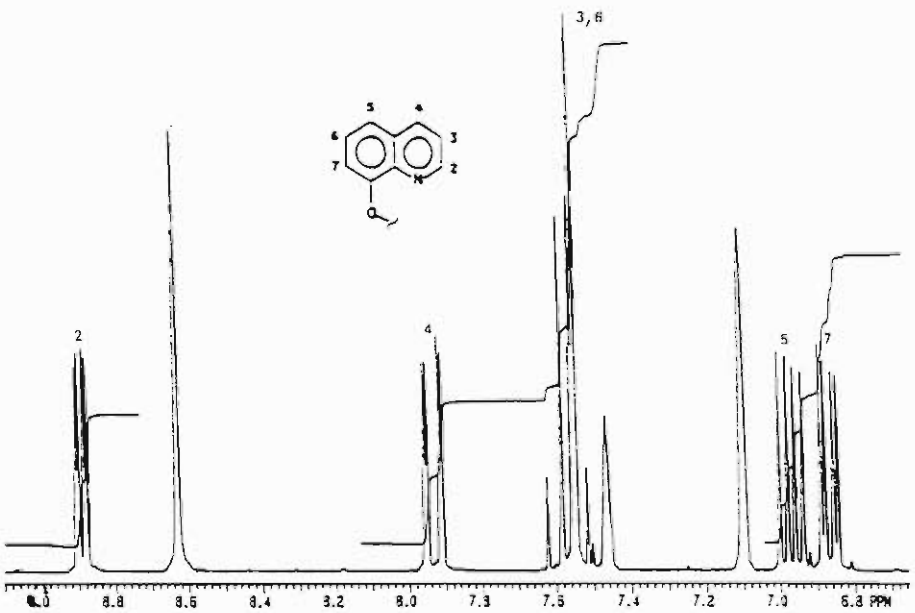

Figure 5.7(a) The proton nmr spectrum of the experimental precipitate obtained from the zinc-8-hydroxyquinoline system.

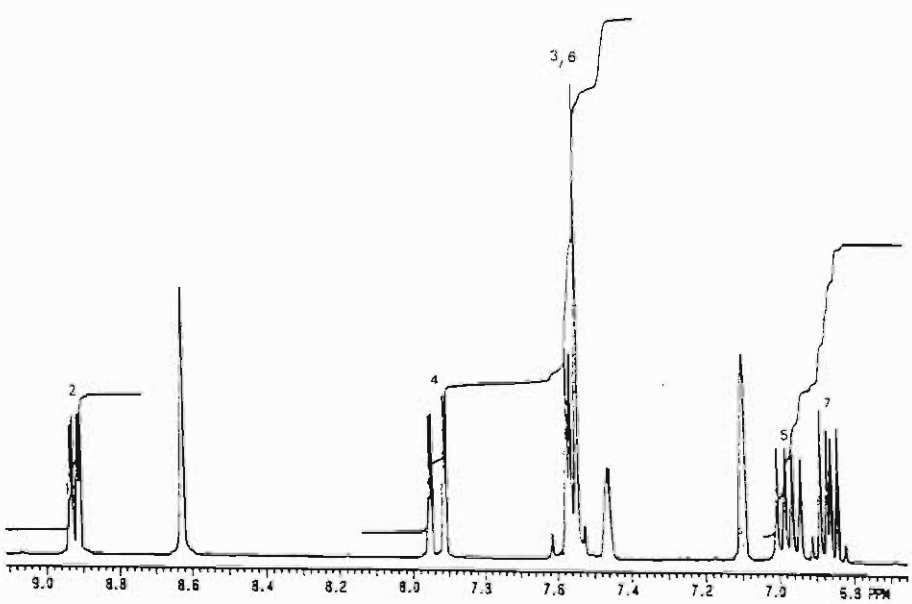

Figure 5.7(b) The proton nmr spectrum of the synthetic zinc 8-hydroxyquinolate precipitate.

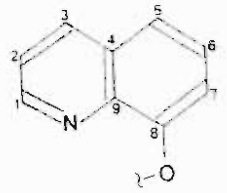

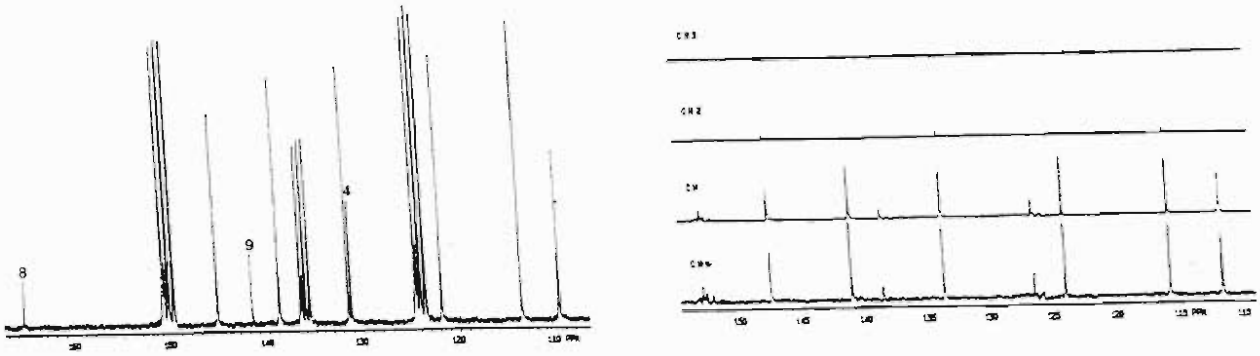

Figure 5.8(a) The carbon-13 nmr and adept spectra of the experimental precipitate obtained from the zinc-8-hydroxyquinoline system.

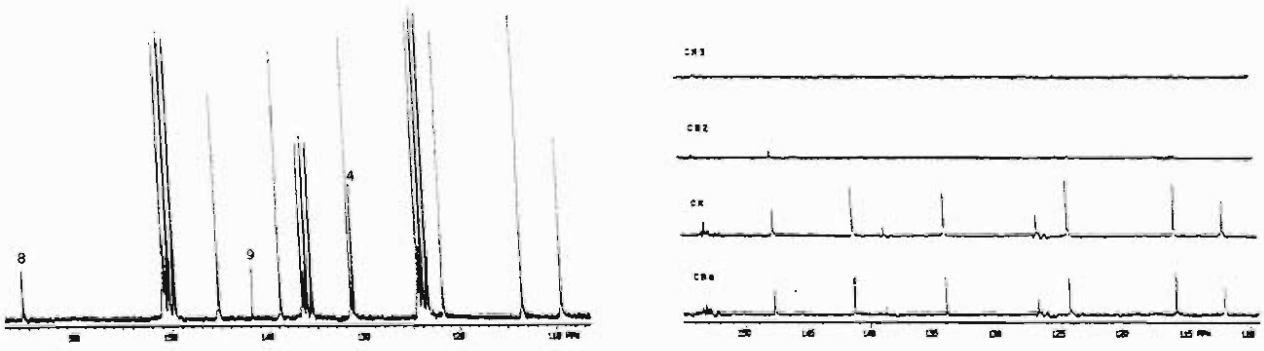

Figure 5.8(b) The carbon-13 nmr and adept spectra of the synthetic zinc 8-hydroxyquinolate precipitate.

which cannot be accurately assigned without an x-ray crystal structure of the molecule). However, the presence of 9 carbon resonances with well resolved splittings, corresponding to the nine ring carbons of the ligand establishes that the two ligands about the central zinc atom are magnetically equivalent in the nmr time scale.

Ir spectra of the experimental and synthetic precipitates are similar and are shown in Figures 5.9(a) and 5.9(b) respectively. These ir spectra showed the following ν/cm^{-1}: 1570 (s, C=C-CO vibrations); 1570, 1500, 1465 (s, Ar-vibrations), 1110 (s, C-O- vibrations), 820-745 (s, Ar-substitution).

The mass spectra of the experimental and synthetic precipitates are shown in Figures 5.10(a) and 5.10(b) respectively. These spectra show analogous fragmentation. The molar masses of zinc 8-hydroxyquinolate are 352.23 g mol^{-1}, 354.23 g mol^{-1} and 356.23 g mol^{-1} corresponding to the zinc isotopes ^{64}Zn, ^{66}Zn and ^{68}Zn in the order of decreasing natural abundance percentage [114]. Hence the triplet fragmentation at 352, 354 and 356 is attributable to zinc 8-hydroxyquinoline. Oxine complexed with the zinc isotope of highest occurrence (^{64}Zn with a natural abundance of 48.89%), explains the major fragment at 352. Other major fragments at 208, 145 and 116 can be attributed to the zinc complexed with one oxine (i.e. loss of an oxine; oxine (i.e. loss of ^{64}Zn); and oxine minus an aldehyde group (CH=O) respectively.

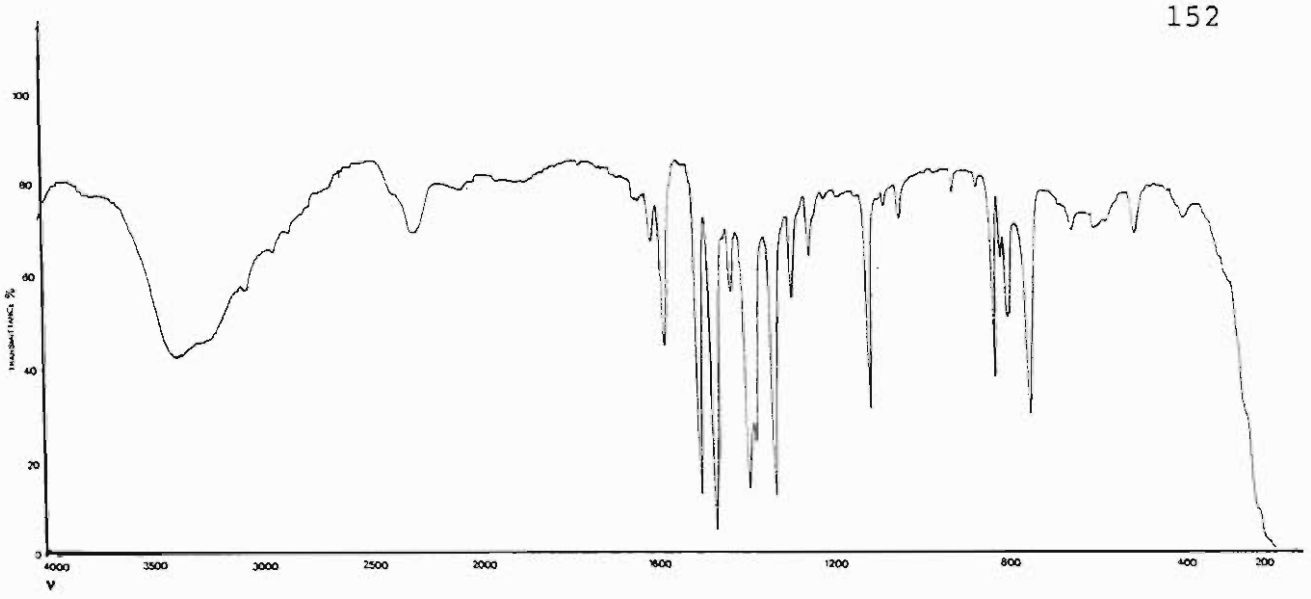

Figure 5.9(a) The infrared spectrum of the experimental precipitate obtained from the zinc-8-hydroxyquinoline system.

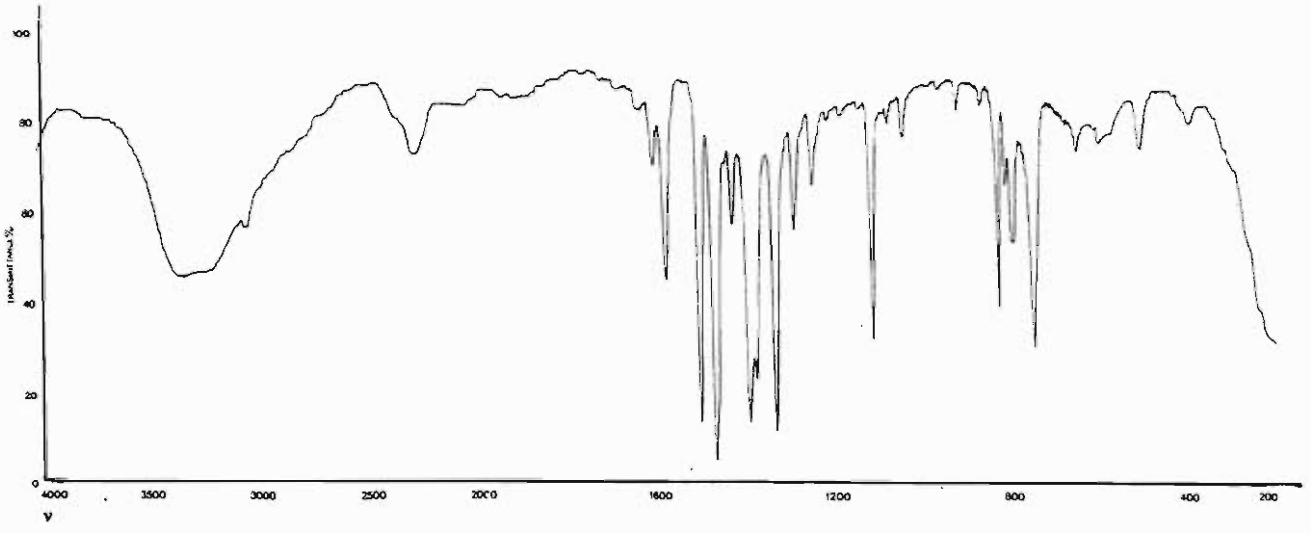

Figure 5.9(b) The infrared spectrum of the synthetic zinc 8-hydroxyquinolate precipitate.

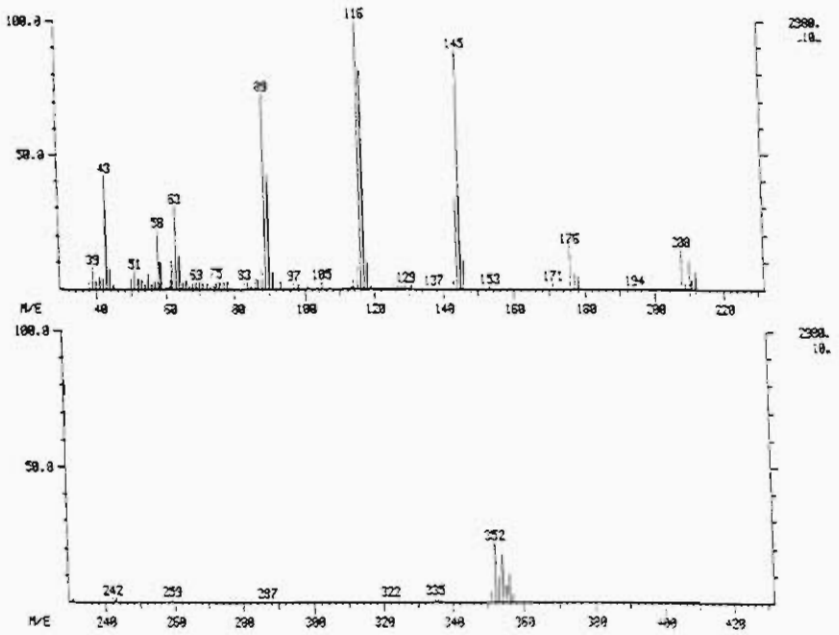

Figure 5.10(a) The mass spectrum of the experimental precipitate obtained from the zinc-8-hydroxyquinoline system.

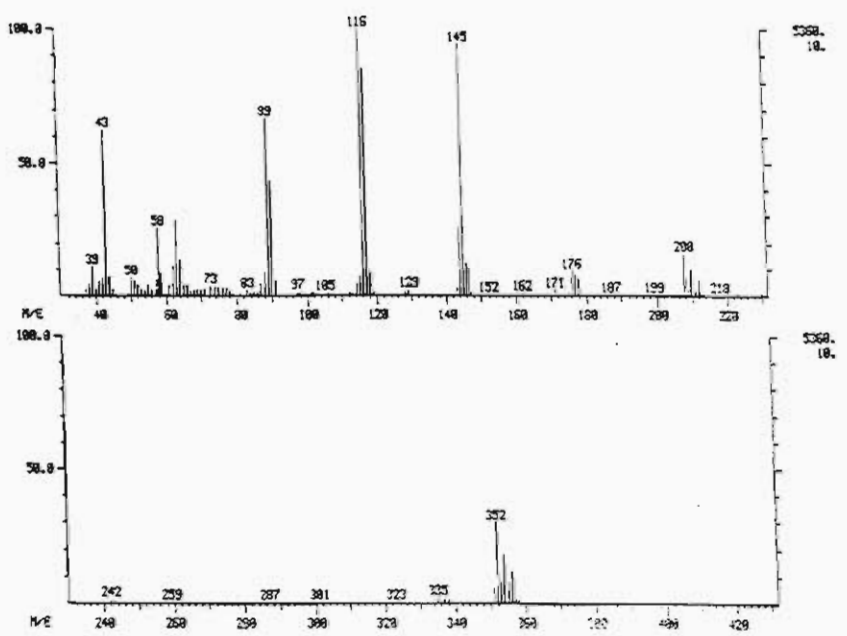

Figure 5.10(b) The mass spectrum of the synthetic zinc 8-hydroxyquinolate precipitate.

The similarity of the above mentioned comparisons proves that the precipitate obtained from the potentiometric titrations is in fact zinc 8-hydroxyquinolate. The crystal structure of zinc 8-hydroxyquinolate dihydrate is reported in the literature [115, 116]. According to Palenik [116] the oxine groups are planar whilst the zinc atom is displaced from this plane. The d^2sp^3 hybridisation of the zinc atom does not explain the deviation from the expected planar configuration. The reported crystal structure of zinc 8-hydroxyquinoline dihydrate is shown in Figure 5.11.

5.4 COMPLEXATION OF GERMANIUM WITH 8-HYDROXYQUINOLINE

The formation curves for this system are illustrated in Figure 5.12. The various germanium:8-hydroxyquinoline ratios gave non-superimposable curves with a definite trend of increasing $\overline{Z}$ values for the increasing ratios of oxine:germanium.

The formation curves of this system revealed rare features, viz. peaks at p[H] < 6.5, end-point regions in the range 6.5 < p[H] < 9.7 and steep rises at p[H] > 9.7. Similar peak features were reported previously [3,118], and in one case was attributed to the presence of a protonated species [118]. On approaching the end-point region, the EMF readings were highly unstable for more than 45 min., and no data was collected in the end-point region even though small increments of the titrant were added before recording EMF values. Nazarenko [70] reported that in

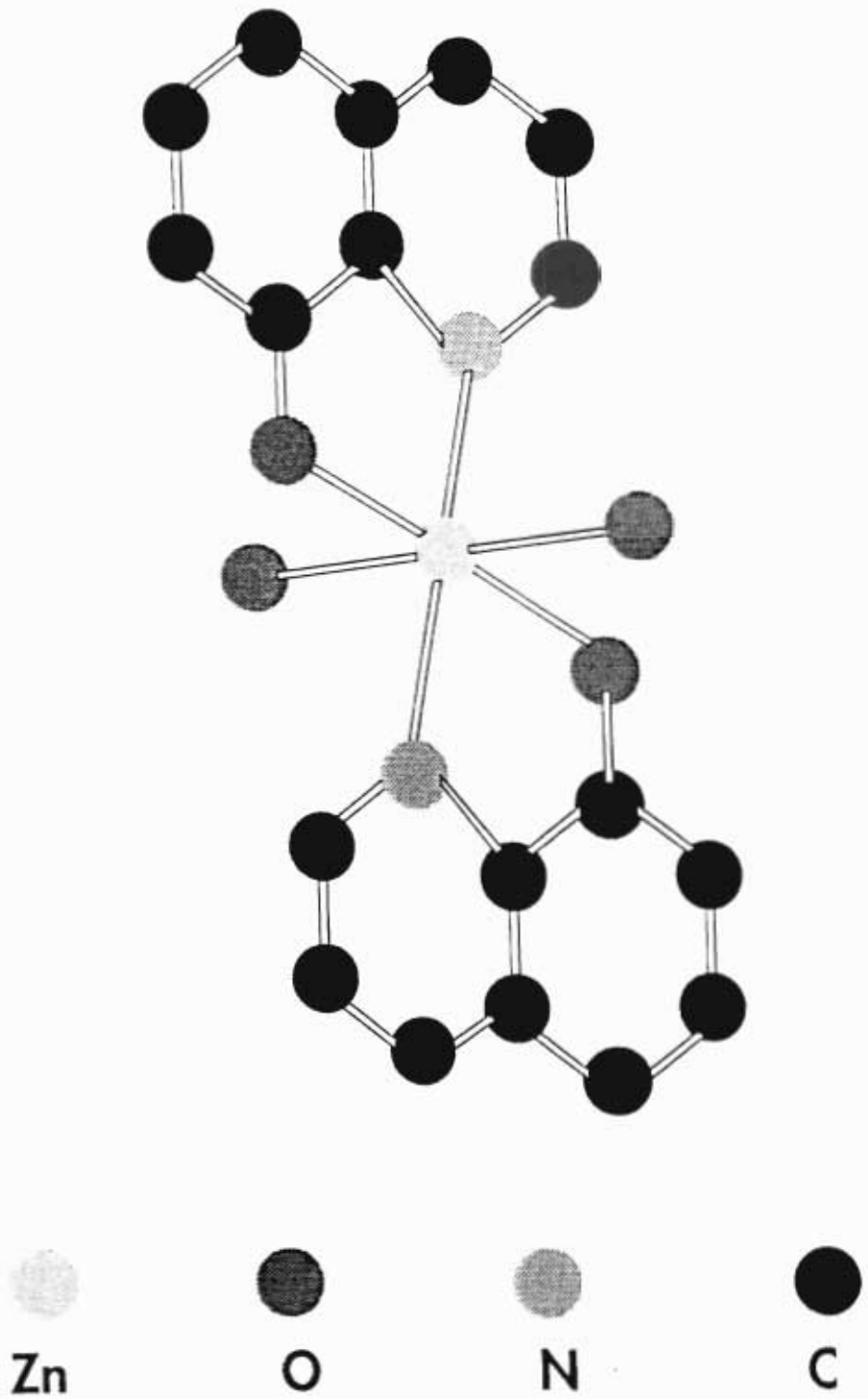

Figure 5.11 Diagram representing the reported crystal structure of zinc 8-hydroxyquinolate dihydrate [116].

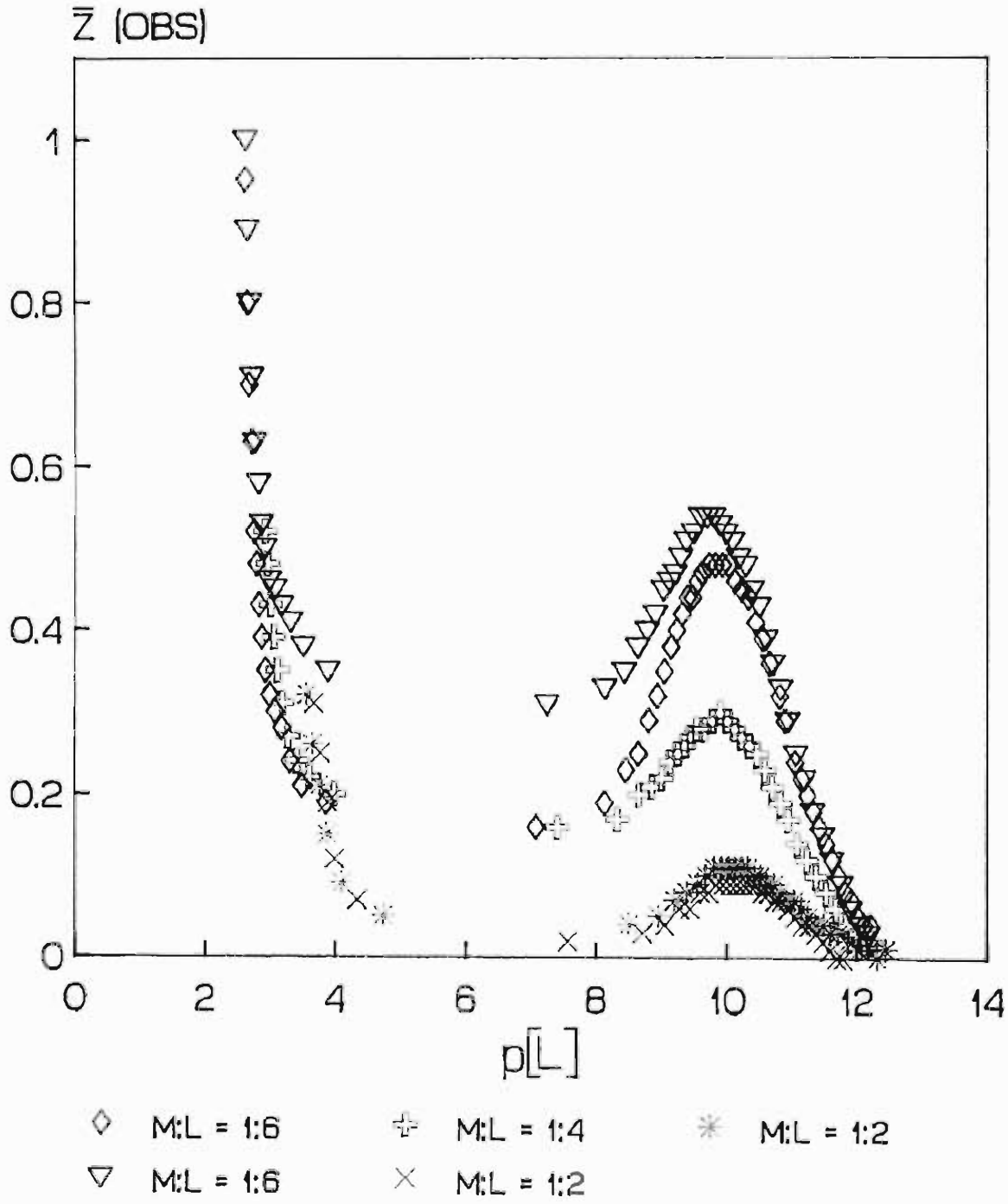

FIGURE 5.12 Formation curves for the germanium-8-hydroxyquinoline system.

the pH range ~ 6.9-9.4 and at a GeO_2 concentration greater than 0.01 mol dm^{-3}, only ions of pentagermanic acid, $Ge_5O^{2-}_{11}$, exist in solution, but below and above these p[H] values, metagermanic acid is formed by the following depolymerisation:

$$Ge_5O_{11}^{2-} + 4H_2O \rightleftharpoons 2HGeO_3^- + 3H_2GeO_3$$

In this study the germanium concentration was not as high as 0.01 mol dm^{-3}.

Reproducibility of the titrations was checked by repeating titrations 1 and 2. The repeat titrations (nos 4 & 5) gave superimposable formation curves, which differed near the end-point region. However it is known that EMF readings are less reliable at end-point regions because of poor buffering. Hence the titrations were considered to be reproducible.

The solution standardisations were checked by performing the repeat titration 4, with fresh stock solutions (including the germanium solution). The fact that the formation curve for this titration superimposed completely with that obtained for titration 1 showed that the preparation and standardisations of the stock solutions were reproducible. (As pointed out by an examiner this does not preclude the possibility of systematic errors in the way the solutions were standardized.)

To ensure that complexation rather than a dilution factor was being observed, uv spectra of the individual components and the complexes in this system

were examined. The variations in the wavelengths at which absorbance occurred when comparing the uv spectra of the components, viz. singly protonated, doubly protonated and doubly deprotonated 8-hydroxyquinoline, to those obtained on addition of the germanium solution, which incidentally does not absorb in the uv-visible range of the spectrum, confirmed the occurrence of germanium-8-hydroxyquinoline complexation.

The peaks observed in the formation curves were reported [118] to be sensitive to the cell constant (E^{o}_{cell}). In this study the cell was calibrated, *in situ*, by a strong acid - strong base titration before every complexometric titration. The calibration curves thus obtained were linear in agreement with the Nernst equation. The accumulated error derived from the standardisation and dispensing of the solutions and the calculation of E^{o}_{cell} was found to be approximately 0.83%. Figure 5.13 shows the variation in the peak $\overline{Z}$ values when the E^{o}_{cell} value was varied by such an amount. Titration 2 was chosen for this purpose. From Figure 5.13 it is obvious that the peak feature persists even when the extreme errors are taken into account, hence it can be deduced that the peaks are real and not an artifact of faulty calibration.

The fact that the peaks did not superimpose at various germanium:8-hydroxyquinoline ratios (see Figure 5.12) could perhaps suggest the presence of polynuclear species. This is usually confirmed by conducting experiments where the metal concentration is kept

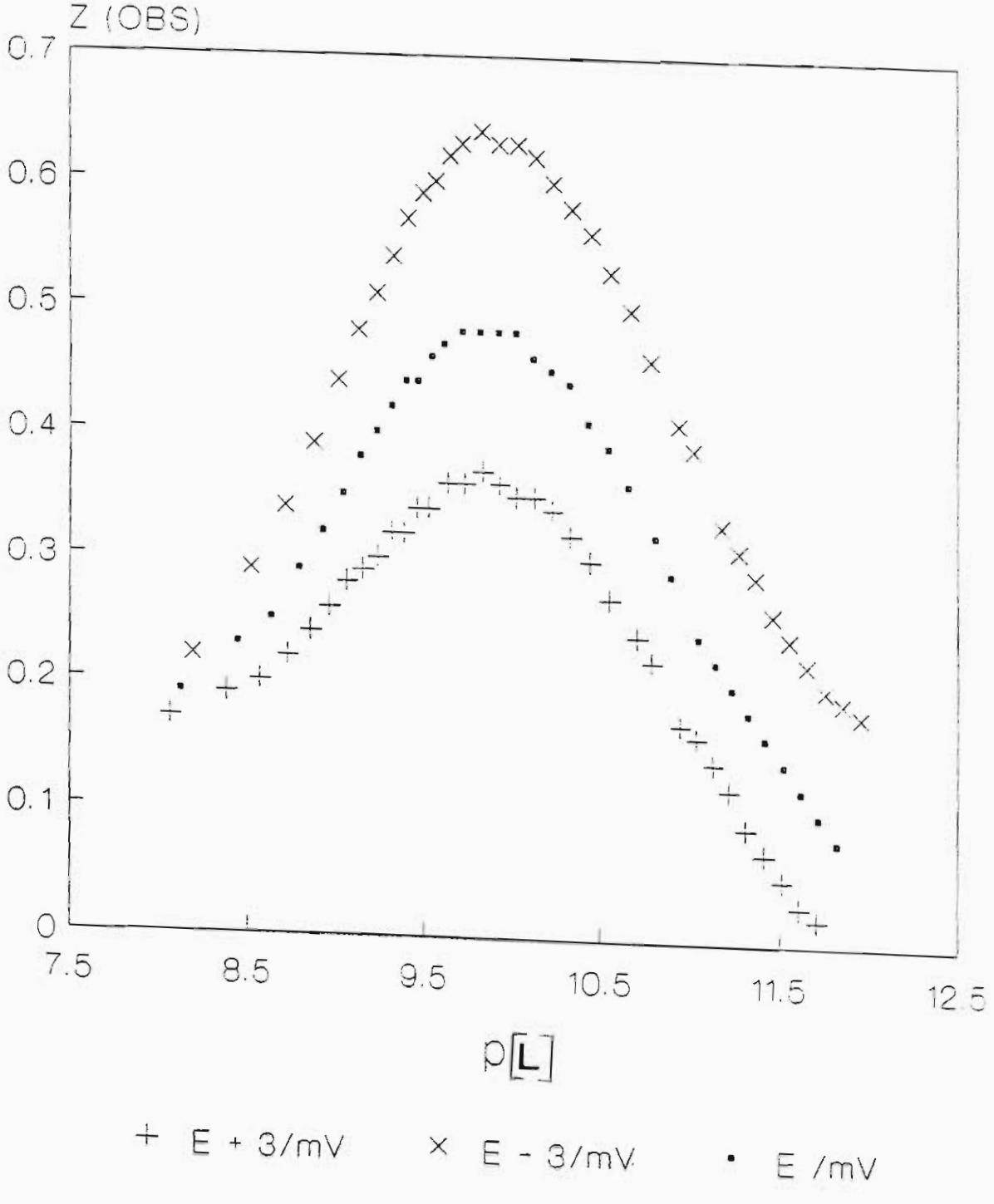

Figure 5.13 Plots illustrating the sensitivity of the peak feature to variations in E^{o} values.

constant throughout the titration. The design of such an experiment seemed impractical for this system mainly because of volume constraints incurred by the partially aqueous medium, i.e. every 0.40 cm^3 (smallest volume dispensed so as to eliminate proportionate errors) of titrant solution required an additional 0.60 cm^3 of dioxane in order to maintain a constant solvent composition.

Once the author was convinced that the unusual results obtained for the germanium-8-hydroxyquinoline system were real, modelling of this system with the aid of the computer program ESTA commenced. Fixed values were used for the stability constants of the species H_2O, $Ge(OH)^{3+}$, $Ge(OH)_2^{2+}$, $Ge(OH)_3^{+}$, $Ge(OH)_4$, $GeO(OH)_3^{-}$, $GeO_2(OH)_2^{2-}$ (see Table 5.1). The unusual features displayed on the formation curves enhanced the complexity of species selection.

Various models were tried on the entire data but none converged. Subsequently the data was divided into two sets, that below p[H] 6.5 and that above p[H] 9.7. This division was made on the basis of the formation curves which showed a peak below p[H] 6.5 and a steep rise above p[H] 9.7. Similar peak features in formation curves previously reported [118] were attributed to the presence of protonated species. Considering the low p[H] range involved, this is a reasonable assumption which can plausibly be extended to the germanium-oxine system.

According to the method used by Little [118], the

formation curves for this system are presented in two forms. Setting the number of dissociable protons on 8-hydroxyquinoline equal to two (NDP2) will focus on the formation of the GeL-type complex. Alternatively, setting the number of dissociable protons equal to one (NDP1) will focus on the formation of the GeLH-type complex. This difference is highlighted in Figure 5.14 where the two $\bar{Z}$ functions are plotted against p[H] for comparison purposes. Titration 3 was selected for this purpose. The fact that the protonated species inherent in the NDP1 curve gives a 'usual' curve seems to justify further that the peak in the NDP2 curve is due to protonated species. However attempts to include such a species in the model failed. (Just this complex was tried and then other doubles, triples etc. were included.)

The data displaying the peak feature was further sectioned at the crest of the peak, i.e. p[H] $\approx$ 4.0. This sectioning was resorted to since the formation curves for the region p[H] < 4.0 represented the shape of 'usual' formation curves. Again none of the various models converged.

Complexation of germanic acid with mandelic acid, has been investigated in aqueous solution between pH 2 and 7 by Clark [119]. The structure of mandelic acid is comparable to that of 8-hydroxyquinoline. Both are bidentate with the chelating atoms orientated in the β-position relative to each other. Two oxygen atoms constitute the chelating atoms of mandelic acid, whereas a nitrogen atom and an oxygen atom constitute

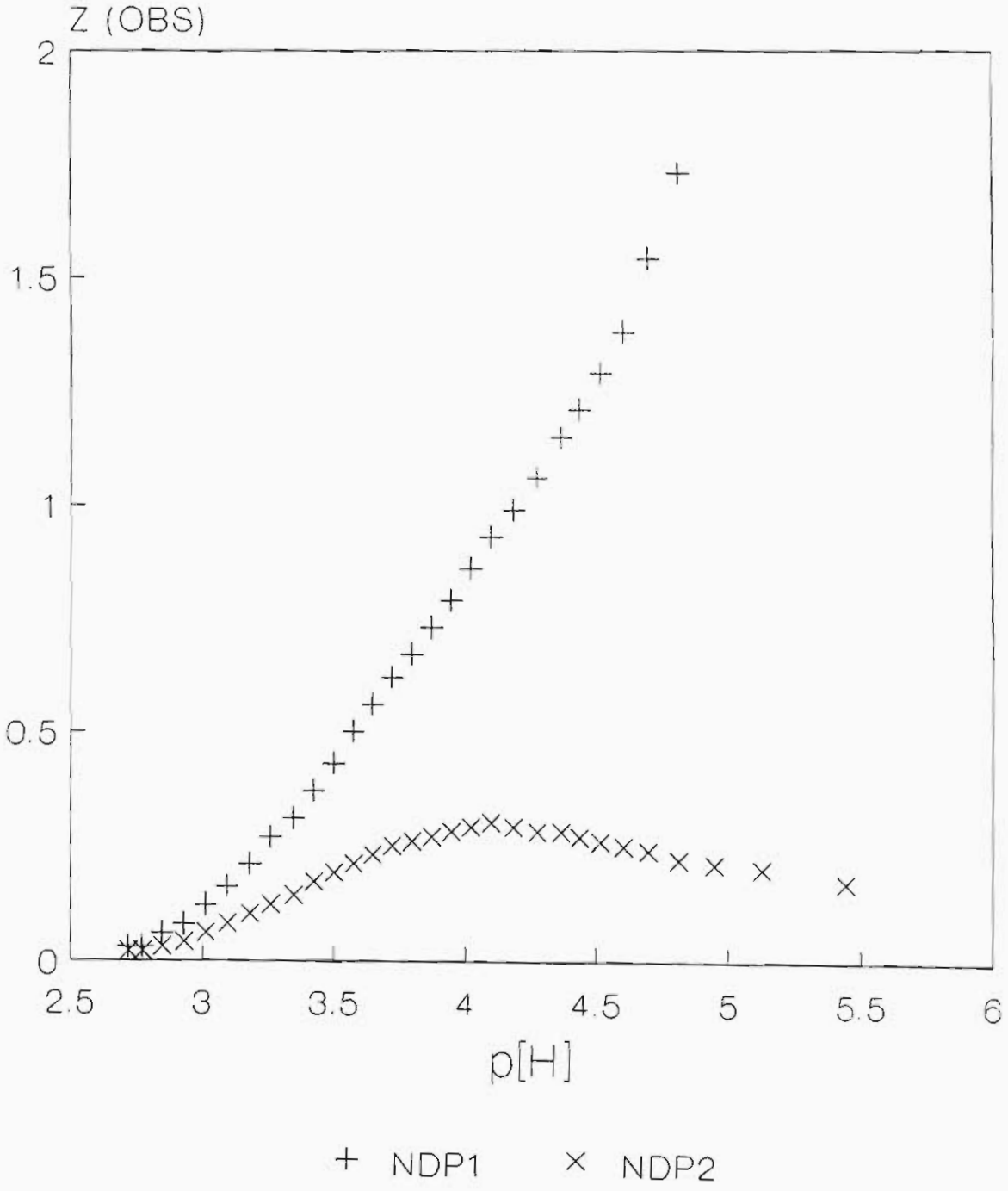

Figure 5.14 Plots highlighting the $\overline{Z}$ functions as the number of dissociable protons on 8-hydroxyquinoline are changed from one (NDP1) to two (NDP2).

the chelating atoms of oxine. The nitrogen atom of oxine and the equivalent oxygen atom (*O) in mandelic acid have similar pK_a values, viz. 3.97 [23] and 3.02 [120] respectively. This suggests comparable behaviour of oxine and mandelic acid, even though they have differing chelating atoms.

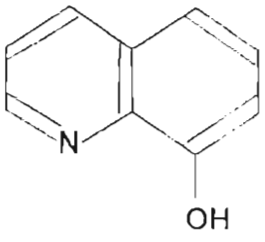

OXINE

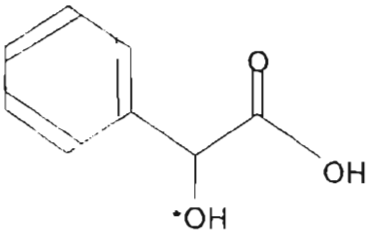

MANDELIC ACID

According to Clark [119] potentiometric titrations showed that the complex acid, viz. $Ge(HL)_2L$, behaved as a dibasic acid with the values of $pK_1 = 2.53$ and $pK_2 = 3.83$, for the following equilibria:

$$GeL_3^{2-} + H^+ \rightleftharpoons GeL_2(HL)^-$$

$$H^+ + GeL_2(HL)^- \rightleftharpoons GeL(HL)_2.$$

Because of the similarity of the ligands, these species were included in the model (for the data at p[H] < 6.5) but with no success.

Tetravalent germanium compounds are known to readily undergo hydrolysis [28]. The distribution of the

different monomeric forms of germanium at a germanium dioxide concentration less than and equal to 0.01 mol dm^{-3} as a function of p[H] [121], suggests that all germanium is present as the germanic acid species, $Ge(OH)_4$, at p[H] ≈ 2.4. Germanic acids are also reported to be weak acids [70]. The GeO_2 solutions used in this work were prepared at high alkalinity (see Section 2.6.2), which implies that germanium was present as $Ge(OH)_6^{2-}$ according to the literature [70]. Hence the hydrolysed species, viz. $Ge(OH)_4L$ and $Ge(OH)_2L_2$, were also considered when modelling the system but with no success.

Only one germanium-8-hydroxyquinoline complex is reported in the literature [30], viz. $Ge(OH)_2L_2$, with a stability constant of 6.61 at an ionic strength of 0.5 mol dm^{-3} NaCl. The presence of this complex and its corresponding stability constant was determined from distribution measurements. The value of log β_{11-4} for $Ge(OH)_4L$ was reported to be negligible.

Much computation was carried out on the data collected in this work, using the above mentioned species and modifications. Table 5.5 lists the species used to model the germanium-8-hydroxyquinoline system. Various combinations of these species were tried but unfortunately the problem of non-convergence was always evident. Hence no successful refinement of the stability constants were obtained.

The existence of complex germanium species in aqueous

media (see Section 1.1) and the limited investigation (never via potentiometric techniques) of the germanium-8-hydroxyquinoline system reported in the literature does not offer much direction in resolving the speciation of this system. However, a preliminary step could be a more complete understanding of the hydrolysis of germanium in the partially aqueous medium used in this study.

TABLE 5.5

The species used to model the germanium-8-hydroxyquinoline system. (These species are listed in no particular order.)

GeL	GeL_2	GeL_3
$Ge(LH)$	$Ge(LH)_2$	$Ge(LH)_3$
$GeL(LH)$	$GeL_2(LH)$	$GeL(LH)_2$
$GeL(OH)$	$GeL(OH)_2$	$GeL(OH)_3$
$GeL(OH)_4$	$GeL(OH)_5$	$GeL_2(OH)$
$GeL_2(OH)_2$	$GeL_2(OH)_3$	$GeL_2(OH)_4$
$GeL_3(OH)$	$GeL_3(OH)_2$	$GeL_3(OH)_3$
Ge_2L	Ge_2L_2	Ge_2L_3
$Ge_2L(LH)$	$Ge_2L_2(LH)$	$Ge_2L(LH)_2$
$Ge_2L(OH)_6$	$Ge_2L(OH)_5$	$Ge_2L(OH)_4$
$Ge_2L(OH)_3$	$Ge_2L(OH)_2$	$Ge_2L(OH)$
$Ge_2L_2(OH)_4$	$Ge_2L_2(OH)_3$	$Ge_2L_2(OH)_2$
$Ge_2L_2(OH)$	$Ge_2L_3(OH)_2$	$Ge_2L_3(OH)$

REFERENCES

1. D.F. Boltz, Rec. Chem. Prog. **24** (1963) 167.
2. R.G.W. Hollingshead, 'Oxine and Its Derivatives', **Vols. I-IV**, Butterworths Scientific Publications, London, 1954.
3. A. Albert and A. Hampton, J. Chem. Soc. (1954) 505.
4. L.E. Maley and D.P. Mellor, Austral. J. Sci. Res. **2A** (1949) 92.
5. S.J. Foster, Ph.D. Thesis, Univ. of Natal, Durban, 1990.
6. M.V. Pellow-Jarman, M.Sc. Thesis, Univ. of Natal, Durban, 1990.
7. B. Marchon, G. Cote and D.Bauer, J. Inorg. Nucl. Chem. **41** (1979) 1353.
8. J.D. Burton, F. Culkin and J.P. Riley, Geochimica et Cosmochimica Acta **16** (1959) 151.
9. G. Cote and D. Bauer, Hydromet. 5 (1980) 149.
10. *op. cit.*, Ref. 4, p. 579.
11. A.I. Vogel, 'A Text-book of Quantitative Inorganic Analysis Including Elementary Instrumental Analysis', 3rd Ed., Longman, London, 1961, p. 387.
12. J.J. Fox, J. Chem. Soc. (1910) 1119.
13. Kolthoff, Chem. Weekblad **24** (1927) 606, from Ref. 16.
14. S. Lacroix, Anal. Chim. Acta 1 (1947) 260.
15. K.G. Stone and L. Friedman, J. Am. Chem. Soc. **69** (1947) 209.
16. H. Irving, J.A.D. Edwart and J.T. Wilson, J. Chem. Soc. (1949) 2672.
17. E.B. Sandell and D.C. Spindler, J. Am. Chem. Soc. **71** (1949) 3806.
18. W.D. Johnston and H. Freiser, J. Am. Chem. Soc. **74**

(1952) 5239.

19. H. Irving and H.S. Rossotti, J. Chem. Soc. (1954) 2910.
20. L.G. Van Uitert and W.C. Fernelius, J. Am. Chem. Soc. **76** (1954) 375.
21. J.G. Jones *et al.*, J. Chem. Soc. (1958) 2001.
22. J.C. Tomkinson and R.J.P. Williams, J. Chem. Soc. (1958) 2010.
23. H.F. Steger and A. Corsini, J. Inorg. Nucl. Chem. **35** (1973) 1621.
24. J. Stary, Anal. Chim. Acta **28** (1963) 132.
25. D.A. Everest and J.E. Salmon, J. Chem. Soc. (1954) 2438.
26. D.A. Everest and J.C. Harrison, J. Chem. Soc. (1959) 2178.
27. N. Ingri, Acta Chem. Scand. **17** (1963) 597.
28. V.A. Nazarenko, 'Analytical Chemistry of Germanium', John Wiley & Sons, New York, 1974, p. 25.
29. C.F Baes and R.E. Mesmer, 'The Hydrolysis of Cations', John Wiley & Sons, New York, 1976, p. 348.
30. J. Tsau *et al.*, Bull. Soc. Chim. Fr. (1967) 1039.
31. H.S. Rossotti, 'The Study of Ionic Equilibria, An Introduction', Longman, London, 1978, p. 83.
32. F.J.C. Rossotti and H. Rossotti,'The Determination of Stability Constants', McGraw-Hill, New York, 1961.
33. M.T. Beck, Pure Appl. Chem. **49** (1977) 127.
34. H.S. Rossotti, 'The Study of Ionic Equilibria, An Introduction', Longman, London, 1978.
35. M.T. Beck, 'Chemistry of Complex Equilibria', Van Nostrand Reinhold, London, 1970.
36. H.S. Rossotti, Talanta **21** (1974) 809.
37. A. Albert and E.P. Serjeant, 'The Determination of

Ionistation Constants', Chapman and Hall, New York, 1984.

38. E.P. Serjeant,' Potentiometry and Potentiometric Titrations', **Vol. 69**, John Wiley & Sons, New York, 1984.
39. P.W. Linder *et al.*, 'Analysis Using Glass Electrodes', Open University Educational Enterprises, London, 1984.
40. J. Kielland, J. Am. Chem. Soc. **59** (1937) 1675.
41. I.N. Levine,'Physical Chemistry', 2nd Ed., McGraw-Hill, New York, 1983, pp. 265-271.
42. *op. cit.*, Ref 35, p. 27.
43. H.S. Harned and B.B. Owen, 'The Physical Chemistry of Electrolytic Solutions', Reinhold Publ. Corp., New York, 1950, p. 548.
44. H.F. Steger, Ph.D. Thesis, McMaster Univ., 1969, p. 34.
45. E. Högfeldt, 'IUPAC Stability Constants of Metal-Ion Complexes, Part A: Inorganic Ligands', Pergamon Press, Oxford, 1982, p. 34.
46. E. M. Woolley, D.G. Hurkot and L.G. Hepler, J. Phys. Chem. **74** (1970) 3908.
47. A.I. Vogel, 'A Text-book of Practical Organic Chemistry Including Qualitative Organic Analysis', 3rd Ed., Longman, London, 1956, p. 177.
48. 'American Society for Testing and Materials', 1978, method D1364.
49. *op. cit.*, Ref. 11, p. 712.
50. *ibid.*, p. 238.
51. *ibid.*, p. 243.
52. *ibid.*, p. 249.
53. *ibid.*, p. 139.
54. D.J. Keller, 'The Sigma Library of FT-IR Spectra', 1st

Ed., **Vol. 2**, Sigma Chemical Company, Inc., St Louis, 1986, p. 152 A.

55. B.C. Baker and D.T. Sawyer, Anal. Chem. **40** (1968) 1945.
56. *op. cit.*, Ref. 11, p. 433.
57. J.W. Mellor, 'A Comprehensive Treatise on Inorganic and Theoretical Chemistry', **Vol. III**, Longmans, London, 1927, p.266.
58. A. Navrotsky, J. Inorg. Nucl. Chem. **33** (1971) 1119.
59. J.H. Müller and H.R. Blank, J. Am. Chem. Soc. **46** (1924) 2358.
60. *op. cit.*, Ref. 28, p. 14.
61. M.C. Sneed and R.C. Brasted, 'Comprehensive Inorganic Chemistry, **Vol. VII**: The Elements and Compounds of Group IV A', Van Nostrand, 1958, p. 203.
62. A.W. Laubengayer and D.S. Morton, J. Am. Chem. Soc. **54** (1932) 2303.
63. J.H. Müller and M.S. Iszard, J. Am. Med. Sci. **163** (1922) 364.
64. W.J. Pugh, J. Chem. Soc. (1929) 1537.
65. A.J. de la Cuadra Blanco and A. de la Cuadra Herrera, Rev. Metal. Madrid **23** (1989) 157.
66. N. Ingri, Acta Chem. Scand. **17** (1963) 590.
67. A. de la Cuadra, An. Quim. **86** (1990) 221.
68. *op. cit.*, Ref. 28, p. 15.
69. *ibid.*, p. 127.
70. *ibid.*, p. 23.
71. D.T. Sawyer and J.L. Roberts, 'Experimental Electrochemistry for Chemistry', John Wiley & Sons, New York, 1974, p. 36.
72. D.P. Shoemaker and C.W. Garland, 'Experiments in Physical Chemistry', 2nd Ed., McGraw-Hill, New York,

1967, p. 465.

73. *op. cit.*, Ref. 37, p. 20.

74. G.W.C. Kaye and T.H. Laby, 'Tables of Physical and Chemical Constants', 14th Ed., Longman, London, 1973, pp. 19 & 29.

75. J.A. Riddick *et al.*, 'Techniques of Chemistry, **Vol. II**: Organic Solvents', 4th Ed., John Wiley & Sons, New York, 1986, p. 312.

76. G. Biedermann and L.G. Sillén, Arkiv. Kemi. 5 (1953) 425.

77. *op. cit.*, Ref. 32, p. 145.

78. G. Mattock, 'pH Measurement and Titration', Heywood, London, 1961, p. 95.

79. Metrohm, 'pH Glass Electrodes', maintenance pamphlet.

80. R.G. Bates, 'Determination of pH: Theory and Practice', John Wiley & Sons, New York, 1964, p. 324.

81. I.M. Kolthoff and M.K. Chantooni, J. Am. Chem. Soc. **87** (1965) 4430.

82. J.J. Lagowski *et al.*, 'The Chemistry of Nonaqueous Solvents, **Vol. VA**: Principles and Basic Solvents', Academic Press Inc., New York, 1978, p. 164.

83. A.G. Mitshell and W.F.K. Wynne-Jones, Trans. Faraday Soc. **51** (1955) 1690.

84. *op. cit.*, Ref. 82, p. 150.

85. Z. Boksay and B. Csákváry, Acta Chim. Acad. Sci. Hung. **67** (1971) 157.

86. G. Eisenman, 'Glass Electrodes for Hydrogen and Other Cations', Marcel Dekker Inc., New York, 1967, p. 106.

87. E.L. Purlee and E. Grunwald, J. Am. Chem. Soc. **79** (1957) 1366.

88. *op. cit.*, Ref. 78, p. 101.

89. Radiometer Manual, 'Check of Electrodes', p. 3.

90. 'CRC Handbook of Chemistry and Physics', 62nd Ed., CRC Press Inc., Boca Raton, 1981, p. D-126.

91. E. John, Polish J. Chem. **64** (1990) 63.

92. P.M. May and D.R. Williams, Talanta **29** (1982) 249.

93. A. M. Corrie and D.R. Williams, Annali di Chimica **68** (1978) 821.

94. E. Bottari *et al.*, Annali di Chimica **68** (1978) 813.

95. M. Mascini, Ion-Selective Electrode Rev. **2** (1980) 17.

96. J. Fries and H. Getrost, 'Organic Reagents for Trace Analysis', E. Merck Darmstadt, 1977, p. 415.

97. *op. cit.*, Ref. 11, p. 390.

98. *ibid.*, p. 388.

99. G. Gran, Acta Chem. Scand. **4** (1950) 559.

100. G. Gran, Analyst **77** (1952) 661.

101. *op. cit.*, Ref. 34, p. 80.

102. F.J.C. Rossotti and H. Rossotti, J. Chem. Ed. **42** (1965), 375.

103. N. Ingri , W. Kakolowicz, L. G. Sillen and B. Warnqvist, Talanta **14** (1967) 1261.

104. B.S Martincigh, Ph.D. Thesis, Univ. of Natal, Durban, 1987, p. 132.

105. P.M May, K. Murray and D.R. Williams, Talanta **32** (1985), 483.

106. K. Murray and P.M. May, 'Esta User's Manual Version 1.0', Department of Applied Chemistry, University of Wales Institute of Science and Technology, College of Cardiff, Wales, 1984.

107. S.C Edwards, M.Sc. Thesis, Univ. of Natal, Durban, 1991.

108. Statistical Graphics Corporation, 'STATGRAPHICS User's Guide-System', 1988.

109. R.M. Smith and A.E Martell, 'Critical Stability Constants, **Vol. 4:** Inorganic Complexes', Plenum Press, New York, 1976, p. 9.

110. C.W. Davies, 'Ion Association', Butterworth, London, 1962, pp. 39-43.

111. C.W. Childs and D.D. Perrin, J. Chem. Soc. (1969) 1039.

112. D.C. Atkins and C.S. Garner, J. Am. Chem. Soc. **74** (1952) 3527.

113. *op. cit.*, Ref. 44, p. 47.

114. F.W. Wehrli and T. Wirthlin, 'Interpretation of Carbon-13 NMR Spectra', Heyden & Son Ltd., London, 1978, chart inside back cover.

115. J.C. Bailar, H.J. Emeleus, R. Nyholm and A.F. Trotman-Dickenson, 'Comprehensive Inorganic Chemistry', **Vol** III, Pergamon Press, Oxford, 1973, p. 195.

116. L.L. Merritt, R.T.Cady and B.W. Mundy, Acta Cryst. **7** (1954) 473.

117. G.J. Palenik, Acta Cryst. **17** (1964) 696.

118. J. Little, M.Sc. Thesis, Univ. of Cape Town, 1984, p. 48.

119. E.R. Clark, J. Inorg. Nucl. Chem. **24** (1962) 81.

120. *op. cit.*, Ref. 28, p. 22.

121. S. Ramamoorthy and P.G. Manning, J. Inorg. Nucl. Chem. **35** (1973) 1571.